COLLINS

engineering report

Dallas Division | *Collins Radio Company, Dallas, Texas*

COLLINS

engineering report

Design Analysis - Unified S-Band System
for Apollo Network
Volume 3, Part V (Cont.)

table of contents

table of contents (cont)

table of contents (cont)

list of illustrations

Figure

list of illustrations (cont)

list of illustrations (cont)

list of tables

TERM	DEFINITION	PAGE
A	Peak Amplitude of Telemetry Subcarrier	g-6-3
a	One-Sided Baseband Noise Bandwidth	g-7-14
A_C	Peak Voltage Amplitude of Carrier	g-2-1
A_O	Peak Amplitude of Telemetry Demodulator Reference Signal	g-6-3
B_1	Telemetry IF Bandwidth	g-6-11
$b_{1,2}$	Polynomial Expansion Coefficients	g-4-15
B_2	Notation for Expression of Loop Transfer Function (See Equations g-8-7 and g-8-8).	g-8-4
B_C	Carrier Loop Noise Bandwidth	g-2-2
B_f	Filter Bandwidth	g-3-13
$2B_I$	IF Noise Bandwidth	g-8-11
B_L	One-Sided Loop Noise Bandwidth	g-3-13
B_{L_O}	One-Sided Loop Noise Bandwidth at Threshold	
$B_N = 2B_{L_O}$	Loop Noise Bandwidth (Two-Sided)	g-7-11
B_r	Telemetry Demodulator Reference Signal Filter Bandwidth	g-6-10
B_{TM}	Telemetry Demodulator Input Noise Bandwidth	g-2-2
B_{TV}	Upper Cutoff Frequency of Television (Video) Bandpass Filter	g-2-16
B_V	Voice Demodulator Loop Noise Bandwidth	g-2-2
BW	Bandwidth	g-1-8
C	Loop Filter Capacitor	g-8-6
D	Percent Distortion	g-3-11
d	Second-Order Coefficient in Phase Non-linearity Expansion	g-4-16
e_d	Total Harmonic Distortion Voltage	g-3-11
e_{dp}	Peak Harmonic Distortion Voltage	g-4-13

TERM	DEFINITION	PAGE
e_o	Output Voltage	g-3-10
$E(P^N)$	N^{th} Moment of the Function P	g-5-7
E_T^2	Transient Error Power Equivalent	g-8-2
e_{TV}	Television Signal Voltage	g-4-15
f_m	Maximum Modulation Frequency	g-2-15
f_n	Filter or Loop Natural Frequency	g-5-6
$F(s)$	Filter Transfer Function	g-4-12
$F_2(s)$	Laplace Transform of Optimum Second-Order Loop Filter Transfer Function	g-8-13
f_t	Voice Test Tone Frequency	g-7-13
g	(See equations g-4-9 through g-4-12)	g-4-13
$G = G_1$	Open-Loop Gain	g-3-10
G_o	Threshold Open-Loop Gain	g-8-6
$H(s)$	Loop Transfer Function	g-4-12
$J_n(X)$	n^{th}-Order Bessel Function of X	g-2-2
K_2	ω_n / ω_m	g-4-9
k_d	Discriminator Constant	g-4-16
K_M	Phase Detector Constant	g-3-10
K_p	Probability Distribution Factor	g-5-7
K_V	Voltage Controlled Oscillator Constant	g-3-10
$M_{C, V, TM}$	(See equations g-2-3 through g-2-8)	g-2-2
$m(t)$	PCM Modulating Function	g-6-3

TERM	DEFINITION	PAGE
α	Signal Suppression Factor	g-3-8
α_0	Threshold Signal Suppression Factor	g-3-8
β	Modulation Index	g-2-15
β_k	Modulation Index of Biomedical Information on k^{th} Subcarrier	g-7-4
$\beta_{m,v}$	Modulation Index of mth Biomedical Subcarrier or Voice Signal on 1.25-Mc Subcarrier	g-7-8
$\beta_{SC_{m,n}}$	Modulation Index of nth (or m^{th}) Subcarrier on Carrier	g-2-15
β_{TM}	Modulation Index of Telemetry Subcarrier on Carrier	g-2-15
β_{TV}	Modulation Index of Television Signal on Carrier	g-2-17
β_V	Modulation Index of Voice Subcarrier on Carrier	g-2-15
γ	Transratio of a Bandpass Filter	g-6-18
δ	Unit Impulse Function	g-5-8
Δf	Frequency Offset or Deviation	g-3-10
Δf_{TV}	Peak Carrier Frequency Deviation by TV Signal	g-2-15
δ_0	Loop Overshoot Factor	g-8-23
$\Delta\theta$	Phase Offset	g-3-10
$\Delta\theta_R$	Peak Carrier Phase Deviation by Ranging	g-2-1
$\Delta\phi_{ss_{max}}$	Peak Loop Phase Error Contributed by a Subcarrier	g-4-9
$\Delta\theta_{TM}$	Peak Carrier Phase Deviation by Telemetry	g-2-1
$\Delta\theta_V$	Peak Carrier Phase Deviation by Voice	g-2-1
$\Delta\omega$	Peak Frequency Deviation	g-4-9
ϵ_m	Peak Phase Error in Loop Due to Modulation	g-4-3
ϵ_T	Total Peak Phase Error in Loop	g-4-3

general

g-1.1 INTRODUCTION.

This report contains the results of an analysis by Collins Radio Company of data demodulation equipment requirements for Apollo Unified S-Band ground tracking stations. The purpose of the analysis is to define optimum system parameters to be used in equipment specifications.

Basis for the analysis was the subsystem described in GSFC Specification TDS-RFS-226[1] for the signal data demodulation equipment. A functional block diagram of the subsystem involved is given in figure g-1-1. A more detailed block diagram for each subunit is given in the analysis section for that unit.

Factors affecting the interface between the GSFC specification and the present Apollo Command Module equipment specifications and changes in CM equipment, which are expected to occur and which would affect the ground system data demodulation equipment, are discussed in section g-10.

The results of this study were incorporated into a Collins specification[2] which describes the subsystem to be implemented for the Apollo program.

---

[1] National Aeronautics and Space Administration, Goddard Space Flight Center, Greenbelt, Maryland, "Specification for Signal Data Demodulator System," Specification No. GSFC-TDS-RFS-226, Revision I, December 1963.

[2] Collins Radio Company, Dallas Division, Richardson, Texas, "Subsystem Specification, Unified S-Band Signal Data Demodulator," Specification No. 126-0429-001, Revision C, 4 September 1964.
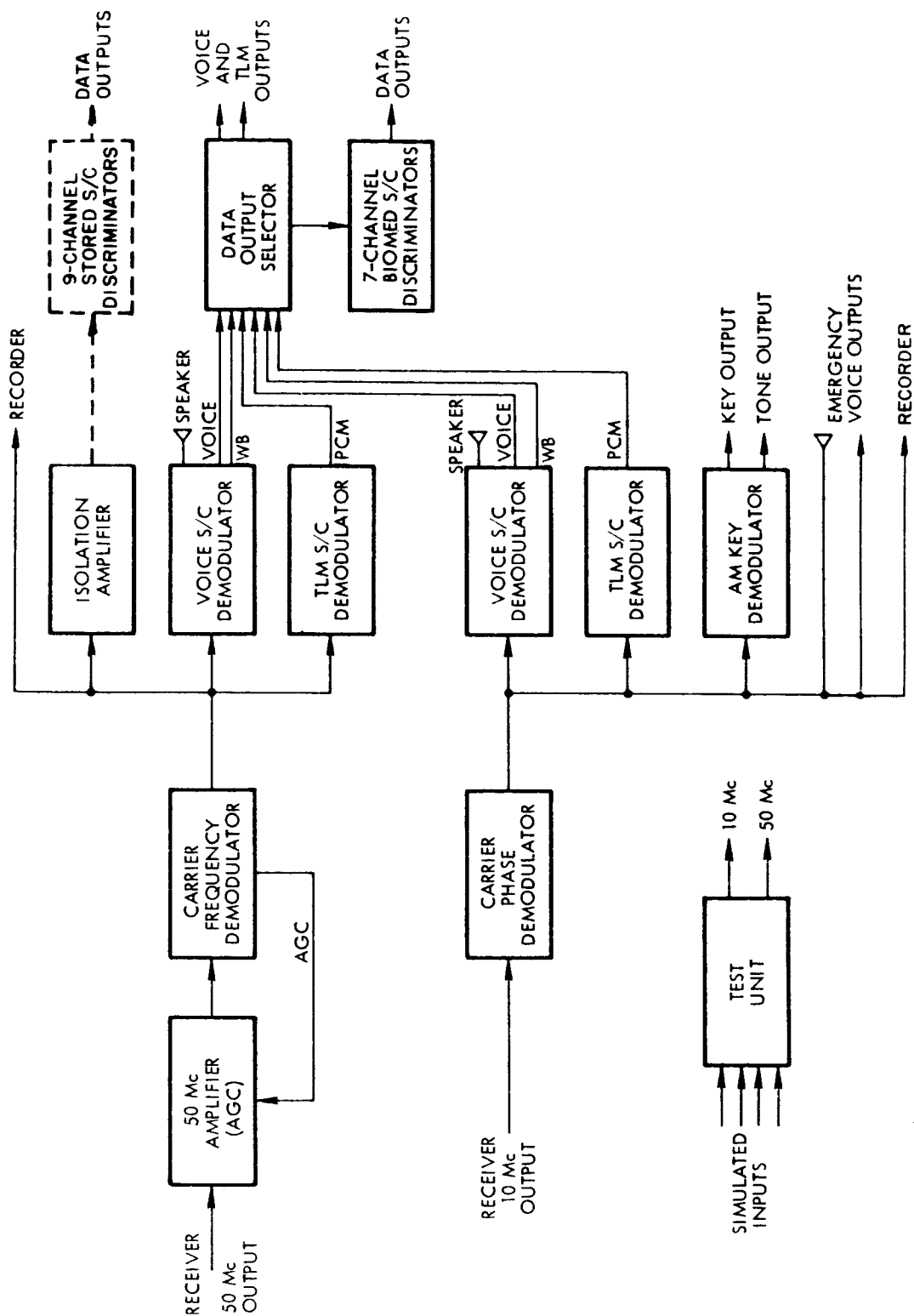
Figure g-1-1.   Signal Data Demodulator Subsystem Block Diagram

g-1.2   SPECIFIED APOLLO CIRCUIT PARAMETERS.

The various combinations of carriers, subcarriers, and modulation techniques used in the Apollo space-to-ground S-band circuits were given in GSFC-RFS-226 and are shown in tabular form in table g-1-1. The first four columns give Apollo modulation parameters. The last three columns give circuit quality parameters and therefore indicate some of the required performance characteristics for the signal data demodulator.

g-1.2.1   COLUMN I--MODE.

In the Apollo program, the transmission mode designation indicates the modulating signal involved, the modulation types, and the modulation indices. Sixteen modes are described in the table, with nineteen mode designations. The apparent duplication will be explained under mode B.

In modes D and E, the carrier is frequency modulated. In all other modes, the carrier is phase modulated.

In modes A, B, C, and D, "telemetry" indicates carrier modulation by a 1.024-mc subcarrier and "voice" indicates carrier modulation by a 1.25-mc subcarrier. Structure of these subcarriers are discussed under Column II, paragraph g-1.2.2. When television, PRN ranging, operational (analog) subcarriers, and the above voice and telemetry signals are shown in combination for a given mode, they have been linearly summed and phase- or frequency-modulated onto the rf carrier. The carrier is down-converted in the receiver and enters the demodulator system at if. frequencies of 10 and 50 mc.

Modes A and C are for voice and telemetry without ranging. Mode A is for high bit rate telemetry (51.2 kbps) and mode C is for low bit rate telemetry (1.6 kbps).

All modes prefixed with a B contain ranging modulation. All modes noted B-1 include ranging, voice, and telemetry, all modes noted B-2 include ranging and voice and B-3 modes contain ranging only. The second designation for each of the B modes identifies the up-link mode that is being transmitted at the same time as the indicated down-link mode. The up-link modulation affects the down-link signal because the spacecraft transponder performs a one-to-one turn around function on the up-link ranging signal mixed with the up-link voice and telemetry. That is, part of the modulation of the down-link carrier will be determined by the up-link mode. For example, in

TABLE g-1-1. MODULATION PARAMETERS
FOR APOLLO SPACECRAFT TO GROUND TRANSLUNAR COMMUNICATIONS

MODE	CHANNEL	CARRIER (a) ØM (b) FM		SUBCARRIER (a) ØM (b) FM		20 DB RF BANDWIDTH (kc)	DETECTION BANDWIDTH (kc)	S/N REQUIRED (db)
A	Telemetry	1.25	(a)	1.57	(a)		75.0	11.5
	Voice	0.91	(a)	2.50	(b)	4780	50.0	4.7
	Carrier	-		-			1.0	6.0
B-1:1-A	PRN Ranging	1.12	(a)	1.57	(a)		0.5	10.0
	Telemetry	1.25	(a)	1.57	(a)		75.0	11.5
	Voice	0.91	(a)	2.50	(b)	4780	50.0	4.7
	Carrier	-		-			1.0	6.0
B-1:1-D	PRN Ranging	0.60	(a)	1.57	(a)		0.5	10.0
B-1:1-E	Telemetry	1.25	(a)	1.57	(a)		75.0	11.5
	Voice	0.91	(a)	2.50	(b)	4780	50.0	4.7
	Carrier	-		-			1.0	6.0
B-1:1-F	PRN Ranging	0.45	(a)	1.57	(a)		0.5	10.0
	Telemetry	1.25	(a)	1.57	(a)		75.0	11.5
	Voice	0.91	(a)	2.50	(b)	4780	50.0	4.7
	Carrier	-		-			1.0	6.0
B-2:1-A	PRN Ranging	1.12	(a)	1.57	(a)		0.5	10.0
	Voice	0.91	(a)	2.50	(b)	4780	50.0	4.7
	Carrier	-		-			1.0	6.0

(a) Peak phase deviation.
(b) Modulation index.

TABLE g-1-1. MODULATION PARAMETERS
FOR APOLLO SPACECRAFT TO GROUND TRANSLUNAR COMMUNICATIONS (CONT)

MODE	CHANNEL	CARRIER (a) ΦM (b) FM		SUBCARRIER (a) ΦM (b) FM		20 DB RF BANDWIDTH (kc)	DETECTION BANDWIDTH (kc)	S/N REQUIRED (db)
B-2:1-D	PRN Ranging	0.60	(a)	1.57	(a)	4780	0.5	10.0
B-2:1-E	Voice	0.91	(a)	2.50	(b)		50.0	4.7
	Carrier	-		-			1.0	6.0
B-2:1-F	PRN Ranging	0.45	(a)	1.57	(a)	4780	0.5	10.0
	Voice	0.91	(a)	2.50	(b)		50.0	4.7
	Carrier	-		-			1.0	6.0
B-3:1-A	PRN Ranging	1.12	(a)	1.57	(a)	1840	0.5	10.0
	Carrier	-		-			1.0	6.0
B-3:1-D	PRN Ranging	0.60	(a)	1.57	(a)	1840	0.5	10.0
B-3:1-E	Carrier	-		-			1.0	6.0
B-3:1-F	PRN Ranging	0.45	(a)	1.57	(a)	1840	0.5	10.0
	Carrier	-		-			1.0	6.0
C	Telemetry	1.25	(a)	1.57	(a)	4780	3.0	11.5
	Voice	0.91	(a)	2.50	(b)		50.0	4.7
	Carrier	-		-			1.0	6.0
D-1	Telemetry	0.341	(b)	1.57	(a)		75.0	11.5
	Voice	0.320	(b)	2.50	(b)		50.0	4.7
	#1	6.900	(b)	2.50	(b)		3.0	10.0

(a) Peak phase deviation.
(b) Modulation index.

TABLE g-1-1. MODULATION PARAMETERS
FOR APOLLO SPACECRAFT TO GROUND TRANSLUNAR COMMUNICATIONS (CONT)

MODE	CHANNEL	CARRIER (a) ∅M (b) FM		SUBCARRIER (a) ∅M (b) FM		20 DB RF BANDWIDTH (kc)	DETECTION BANDWIDTH (kc)	S/N REQUIRED (db)
	#2	4.550	(b)	2.50	(b)		4.55	10.0
	#3	3.333	(b)	2.50	(b)		6.2	10.0
	#4	2.500	(b)	2.50	(b)		8.3	10.0
	#5	1.908	(b)	2.50	(b)		10.9	10.0
	#6	1.428	(b)	2.50	(b)		14.5	10.0
	#7	1.052	(b)	2.50	(b)		19.7	10.0
	#8	0.800	(b)	2.50	(b)		25.9	10.0
	#9	0.605	(b)	2.50	(b)		34.2	10.0
	Mode as whole					3300	3330.	3.0
D-2	Telemetry	0.341	(b)	1.57	(a)		75.2	11.5
	Voice	0.320	(b)	2.50	(b)		50.0	4.7
	Biomedical	Not Resolv.					Not res.	Not res.
	Mode as whole					3300	3330.	3.0
	Television	2.50	(b)	Not Appl.			400.	
E	Telemetry	0.341	(b)	1.57	(a)		75.	
	Voice	0.320	(b)	2.50	(b)		50.	4.4
	Mode as whole					3300	9000.	
F	Voice	1.00	(b)	Not Appl.		12.0	33.0	3.0
G	Key	1.25	(a)	100% (AM)		4600	1.0	10.0
	Carrier						1.0	6.0

(a) Peak phase deviation.
(b) Modulation index.

mode B-1:1-A, mode B-1 is being transmitted to earth, while an up-link mode (earth to spacecraft). denoted by A, is being transmitted. This A is not associated with down-link mode A. In up-link modes D and E, the carrier is phase deviated the same amount by the ranging signal and, therefore, modes B-1:1-D and B-1:1-E are identical for the down-link. The same is true of modes B-2:1-D and B-2:1-E, and of modes B-3:1-D and B-3:1-E.

In mode D-1, which has been deleted since the start of this program, one to nine analog fm telemetry subcarriers would have been linearly summed with the usual voice and telemetry subcarriers. Modulation parameters for these "stored analog" subcarriers is given as the second group in table g-1-2. The resulting composite would then have been used to frequency modulate the carrier. Mode D-2 is the FM mode for voice and telemetry only.

In mode E, a low-scan-rate television signal is subsituted for the fm telemetry subcarriers of mode D-1.

In mode F, the voice signal is phase modulated directly on the carrier (no subcarrier). This is the emergency voice mode.

In mode G, the carrier is phase modulated by a 512-kc subcarrier. The subcarrier is turned off and on (100% AM), for transmission of Morse Code signals. This is called the AM key mode.

g-1.2.2   COLUMN II--CHANNEL.

These are the components of the received signals. Telemetry indicates a 1.024-mc subcarrier phase modulated by a PCM signal at 1.6 kbps or 51.2 kbps. The modulation for the PCM signal is $\pm 90^\circ$ PSK, resulting in an ambiguity in the demodulated signal between plus and minus phase shift. This will be no problem in the Apollo program however, because the PCM code will be a type which is insensitive to plus or minus phase (such as NRZ-S on NRZ-M).

Voice in all modes, except F, indicates a 1.25-mc subcarrier, frequency modulated by a linear sum of the down-link voice and up to seven biomedical subcarriers. Information on the biomedical subcarriers is given in table g-1-2.

PRN ranging is a coded pulse pattern, the spectrum of which has a first null at approximately 1 mc. Demodulation of the PRN signal is not required of the signal data

TABLE g-1-2.   SIGNAL CHARACTERISTICS OF OPERATIONS DATA

DATA DESCRIPTION	DETECTED SIGNAL BW REQUIREMENTS (NOMINAL)
Real Time Biomedical Data, 7 channels:	
(1) SCO freq. 4 KC ±200 cps	2 cps
(2) SCO freq. 5.4 KC ±270 cps	2 cps
(3) SCO freq. 6.8 KC ±340 cps	2 cps
(4) SCO freq. 8.2 KC ±410 cps	2 cps
(5) SCO freq. 9.6 KC ±384 cps	2 cps
(6) SCO freq. 11 KC ±330 cps	2 cps
(7) SCO freq. 12.4 KC ±248 cps	30 cps
Stored Analog Channels:	
(1) SCO freq. 14.5 KC ±7.5%	435 cps
(2) SCO freq. 22 KC ±7.5%	660 cps
(3) SCO freq. 30 KC ±7.5%	900 cps
(4) SCO freq. 40 KC ±7.5%	1.2 KC
(5) SCO freq. 52.5 KC ±7.5%	1.575 KC
(6) SCO freq. 70 KC ±7.5%	2.10 KC
(7) SCO freq. 95 KC ±7.5%	2.85 KC
(8) SCO freq. 125 KC ±7.5%	3.75 KC
(9) SCO freq. 165 KC ±7.5%	4.95 KC

demodulator, but the PRN signal parameters must be known for analysis of system operation on other signals.

In mode D-1, the numbered channels are the analog fm telemetry subcarriers given in table g-1-2.

The above signals and television, where indicated in the respective modes, are linearly summed and used to modulate the carrier.

g-1.2.3   COLUMN III—"CARRIER".

This is the modulation produced on the carrier by the signals in Column II. For PM, the number represents the peak phase deviation of the carrier and for fm it represents the modulation index.

g-1.2.4   COLUMN IV—"SUB-CARRIER".

This is the modulation produced on the subcarrier by the signals in Column II. The numbers represent the phase deviation for PM and modulation index for fm, as in the carrier column.

g-1.2.5   COLUMN V—"20-db RF BANDWIDTH".

This number represents the spectrum of the RF signal and was given in RFS-226 as the "bandwidth measured between the -20 db points of the rf signal, assuming it is band limited with noise of upper cutoff frequency equal to the highest frequence in the channel with the largest product of modulation index and upper frequency cutoff."

g-1.2.6   COLUMN VI—DETECTION BANDWIDTH.

The numbers in this column represent the one-sided subcarrier detection bandwidth for telemetry, the two-sided noise bandwidth for the voice subcarrier, the one-sided loop noise bandwidth for the carrier tracking loop (PM), and the two-sided noise bandwidth for the fm carrier detector.

g-1.2.7   COLUMN VII—REQUIRED S/N.

This represents the channel signal-to-noise (S/N) ratio required out of the carrier demodulator. The S/N for each channel would be measured in the bandwidth of Column VI.

g-1.3 CARRIER DEMODULATOR PERFORMANCE TABLE.

In Collins subsystem specification 126-0429-001 for the Signal Data Demodulator, the Apollo circuit parameter table given in paragraph g-1.2 of this report was revised to more clearly define the operation of the carrier demodulators. The results of this revision are given in table g-1-3. The B-3 modes were removed, since they contain PRN ranging only, and the signal data demodulator is, therefore, not required to operate on them. Mode D-1 will be deleted in a forthcoming revision of the Collins Specification but will be left in for this report because the analysis may be of use in future projects. The first four columns were unchanged for the remaining modes.

g-1.3.1 COLUMN V—P_T/Φ_N.

This number is the input total-signal-power to noise-power-density ratio for which the first signal component (telemetry, voice, carrier, etc.) in the mode will threshold. Derivation of these numbers is described in section g-2 of this report.

g-1.3.2 COLUMN VI—BANDWIDTH.

These values are essentially the same as those in Column VI of the original table, except that, for conformity and ease of comparison, they are now given as two-sided noise bandwidths for all signal components. Voice was originally two-sided noise bandwidth and it, therefore, remains the same. Telemetry was originally given as a one-sided bandwidth of 75 kc and is now given as a two-sided bandwidth of 150 kc, which corresponds to the telemetry subcarrier demodulator if. bandwidth of the same value. The PM carrier demodulator is defined in the text of the specification as having a one-sided loop bandwidth of 100 cps; The original value of 1 kc in the table is, therefore considered to be in error. The 100-cps bandwidth is given in table g-1-3 as a two-sided bandwidth of 200 cps. In like manner, the other values are now all two-sided.

g-1.3.3 COLUMN VII—S/N IN COLUMN VI BANDWIDTH.

This column gives the signal-to-noise ratio (in the output noise bandwidth of Column VI) for the specified modulation mode and the input (P_T/Φ_N) of Column V. One of the components in each mode is the same as it was in the original table (decreased where necessary by 3 db for the change from one-sided to two-sided bandwidth). This component is the first to threshold in the mode and determines the value for Column V.

TABLE g-1-3.   APOLLO MODULATION PARAMETERS AND CARRIER DEMODULATOR PERFORMANCE

I	II	III MODULATION INDICES	IV MODULATION INDICES	V	VI	VII
MODE	CHANNEL	CARRIER	SUBCARRIER	P_T/Φ_N (db) (h)	BANDWIDTH (kc)	S/N (db) IN COLUMN VI BANDWIDTH (g)
A	Telemetry	1.25 (a)	1.57 (a)	65.0	150 (f)	8.5
	Voice (e)	0.91 (a)	2.50 (b)	65.0	50 (c)	9.4
	Carrier	-	-	65.0	0.2 (c)	36.3
B-1:1-A	PRN Ranging	1.12 (a)			-	-
	Telemetry	1.25 (a)	1.57 (a)	72.2	150 (f)	8.5
	Voice (e)	0.91 (a)	2.50 (b)	72.2	50 (c)	9.5
	Carrier	-	-	72.2	0.2 (c)	36.3
B-1:1-D	PRN Ranging	0.60 (a)			-	-
B-1:1-E	Telemetry	1.25 (a)	1.57 (a)	66.7	150 (f)	8.5
	Voice (e)	0.91 (a)	2.50 (b)	66.7	50 (c)	9.5
	Carrier	-	-	66.7	0.2 (c)	36.3
B-1:1-F	PRN Ranging	0.45 (a)			-	-
	Telemetry	1.25 (a)	1.57 (a)	65.9	150 (f)	8.5
	Voice (e)	0.91 (a)	2.50 (b)	65.9	50 (c)	9.5
	Carrier	-	-	65.9	0.2 (c)	36.3
B-2:1-A	PRN Ranging	1.12 (a)			-	-
	Voice	0.91 (a)	2.50 (b)	63.8 (65.5) (i)	50 (c)	4.7 (6.5) (i)
	Carrier	-	-	63.8 (65.5) (i)	0.2 (c)	31.7 (33.4) (i)

TABLE g-1-3.   APOLLO MODULATION PARAMETERS AND CARRIER DEMODULATOR PERFORMANCE (CONT)

I	II	III	IV	V	VI	VII
		MODULATION INDICES		$\dfrac{P_T}{\Phi_N}$ (db) (h)	BANDWIDTH (kc)	S/N (db) IN COLUMN VI BANDWIDTH (g)
MODE	CHANNEL	CARRIER	SUBCARRIER			
B-2:1-D	PRN Ranging	0.60 (a)			-	-
B-2:1-E	Voice (e)	0.91 (a)	2.50 (b)	58.1 (59.8) (i)	50 (c)	4.7 (6.5) (i)
	Carrier	-	-	58.1 (59.8) (i)	0.2 (c)	31.5 (33.2) (i)
B-2:1-F	PRN Ranging	0.45 (a)			-	-
	Voice (e)	0.91 (a)	2.50 (b)	57.3 (59.0) (i)	50 (c)	4.7 (6.5) (i)
	Carrier	-	-	57.3 (59.0) (i)	0.2 (c)	31.5 (33.2) (i)
C	Telemetry	1.25 (a)	1.57 (a)	60.2 (61.9) (i)	6 (f)	17.7 (19.4) (i)
	Voice (e)	0.91 (a)	2.50 (b)	60.2 (61.9) (i)	50 (c)	4.7 (6.5) (i)
	Carrier	-	-	60.2 (61.9) (i)	0.2 (c)	31.5 (33.2) (i)
D-1	Telemetry	0.341 (b)	1.57 (a)	74.8	150 (f)	10.7
	Voice (e)	0.320 (b)	2.50 (b)	74.8	50 (c)	14.9
	#1	6.900 (b)	2.50 (b)	74.8	3 (c)	53.8
	#2	4.550 (b)	2.50 (b)	74.8	4.55 (c)	48.4
	#3	3.333 (b)	2.50 (b)	74.8	6.2 (c)	44.3
	#4	2.500 (b)	2.50 (b)	74.8	8.3 (c)	40.5
	#5	1.908 (b)	2.50 (b)	74.8	10.9 (c)	37.0
	#6	1.428 (b)	2.50 (b)	74.8	14.5 (c)	33.2
	#7	1.052 (b)	2.50 (b)	74.8	19.7 (c)	29.3
	#8	0.800 (b)	2.50 (b)	74.8	25.9 (c)	25.7
	#9	0.605 (b)	2.50 (b)	74.8	34.2 (c)	22.1

TABLE g-1-3.   APOLLO MODULATION PARAMETERS AND CARRIER DEMODULATOR PERFORMANCE (CONT)

I	II	III MODULATION INDICES	IV	V	VI	VII
MODE	CHANNEL	CARRIER	SUBCARRIER	$\dfrac{P_T}{\Phi_N}$ (db) (h)	BANDWIDTH (kc)	S/N (db) IN COLUMN VI BANDWIDTH (g)
D-2	Telemetry	0.341 (b)	1.57 (a)	–	150 (f)	–
	Voice (e)	0.320 (b)	2.50 (b)	–	50 (c)	–
E	Television	2.50 (b)	Not Appl.	75.7	400 (d)	–
	Telemetry	0.341 (b)	1.57 (a)	75.7	150 (f)	11.6
	Voice (e)	0.320 (b)	2.50 (b)	75.7	50 (c)	16.0
F	Voice	1.25 (a)	Not Appl.	42.1	2.3 (d)	5.0
	Carrier	–	–	42.1	0.2 (c)	9.0
G	Key	1.25 (a)	100% (AM)	29.2	1.0 (j)	–3 (j)
	Carrier	–	–	29.2	0.06 (c)	8.9

NOTES:
(a) Peak phase deviation (carrier phase modulated).
(b) Modulation index (carrier frequency modulated).
(c) Two-sided Loopnoise Bandwidth.
(d) Baseband one-sided noise bandwidth.
(e) Seven Bio-Med Subcarriers may be linearly summed to voice and transmitted on this subcarrier. Modulation indexes are shown in Table g-1-2.
(f) Two-sided reference noise bandwidth at output of carrier demodulator.

(g) This column gives the required S/N in the indicated bandwidth at the specified value of P_T/Φ_N.
(h) Total input signal power-to-noise spectral density at input to carrier demodulator.
(i) First value for voice only. Second value for voice plus seven biomedical subcarriers.
(j) For 98% random-word intelligibility with a trained morse-code operator.

For example, in mode A, the telemetry S/N, (originally required to be 11.5 db in a 75-kc bandwidth), is required to be 8.5 in a 150-kc bandwidth. In section g-2, telemetry is found to threshold first in mode A, setting an input (P_T/Φ_N) of 65 db. For this input condition, the S/N for voice and the carrier are found to be 9.4 db and 36.3 db, respectively.

g-1.4 APOLLO RECEIVER CHARACTERISTICS.

The signal data demodulator system is required to operate with the Apollo Range and Range Rate (R & RR) receiver, a simplified block diagram of which is shown in figure g-1-2. In addition, the demodulator system is required to operate, with negligible reduction of performance, with interim tracking receivers. The output parameters of these receivers, which are considered to be partinent to this analysis, are as follows:

g-1.4.1 RANGE AND RANGE RATE (R & RR) RECEIVER OUTPUT CHARACTERISTICS.

g-1.4.1.1 50-MC OUTPUT. The 50-mc signal is derived in the R & RR receiver prior to any agc action. The gain and noise figure (1.7 db) of the preamplifier-receiver configuration are such that the noise power density at the input to the data demodulatior will be -109 dbm per cycle per second. The signal output level will vary from below the noise level to a maximum of +15 dbm.[*] The -3 db if. bandwidth at the data demodulator input will be 10 mc. It is estimated that frequency uncertainty of this signal, including that due to doppler, may be as great as ±150 kc.

g-1.4.1.2 10-MC OUTPUT. The 10-mc signal is derived in the R & RR receiver at a point within both the carrier tracking and the agc loops. Frequency uncertainty of the carrier will be restricted to ±4 cps; the level of the carrier component will be controlled to within ± 1 db, centered at about -70 dbm.[*] The data demodulator is required to operate with an input of -75 dbm[*] to permit equalizing several receiver outputs with attenuators. The level of signal components other than the carrier will vary with the modulation indices. The -3 db if. bandwidth at the data demodulatior input will be 3.3 mc. In the absence of an input signal, the receiver output noise level will be approximately 0 dbm.

[*] The receiver levels may differ from those given here. See section g-10.

Figure g-1-2. Range and Range Rate Receiver Block Diagram, Portion Applicable to Data Demodulator Signals
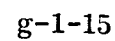
g-1.4.2 INTERIM TRACKING RECEIVER CHARACTERISTICS.

g-1.4.2.1 50 MC OUTPUT. When the tracking receiver is locked, the carrier component of the signal for input to the data demodulator will be controlled by the receiver to a fixed level of -10 dbm ± 3 db. The level of the signal components other than the carrier will vary with the modulation. When the tracking receiver is unlocked, the -10 dbm ± 3 db level applies to the total signal power. The -3 db if bandwidth at the data demodulator input will be 10 mc. Carrier frequency stability is not known but is assumed to be similar to that of the R & RR receiver.

g-1.4.2.2 10 MC OUTPUT. The 10-mc output is controlled in much the same manner as that of the 50-mc output, except the level is 0 dbm ± 3 db, instead of -10 dbm ± 3 db. The -3 db if bandwidth will be 5 mc and the stability is assumed to be the same as that for the R & RR receiver.

analysis of transmission modes from the Apollo Command Module

g-2.1 GENERAL.

An analysis of each of the transmission modes was made, to determine relative thresholds of different subchannels in the different transmission modes and to determine input signal-to-noise requirements of the carrier demodulators to meet the required output signal-to-noise ratios in the specified detection bandwidths for the subchannels.

In addition, an analysis of the spectrum of the input signal was made to determine what percent of the signal power would be passed by if, filters of various bandwidths centered at 50 mc and 10 mc. Unmodulated subcarriers were assumed and only modes A, C, and D-2 were analyzed because of the complexity of analysis for the other modes.

g-2.2 PM MODES.

The general form of the signal at the input to the carrier phase demodulator will be [3]:

$$v(t) = A_C \sin\left[\omega_C t \pm \Delta\theta_R + \Delta\theta_V \sin(\omega_V t + \phi_V(t)) + \Delta\theta_{TM} \sin(\omega_{TM} t + \phi_{TM}(t))\right], \quad (g\text{-}2\text{-}1)$$

where the symbols are as defined in the definition of terms list.

Denote the total power by:

$$P_T = A_c^2/2 \qquad (g\text{-}2\text{-}2)$$

---

* Signals transmitted from the Lunar Excursion Module (LEM) may differ from those specified here. See Section g-10.

(3) Stover, Harris A., "Second Interim Report on the Modulation Techniques Study for the Apollo C and D Subsystem," Report No. AR-151-2, Cedar Rapids, Iowa, Collins Radio Company, October 1962.

The signal-to-noise ratio in the carrier phase demodulator loop noise bandwidth, prior to carrier demodulation, may then be written as [3]:

$$(S/N)_C = \frac{1}{B_C} \left\{ \cos^2 (\Delta\theta_R) \, J_0^2 (\Delta\theta_V) \, J_0^2 (\Delta\theta_{TM}) \right\} P_T/\Phi_n, \qquad \text{(g-2-3)}$$

where Φ_N is the noise power spectral density (watts/cps) at the input to the carrier phase demodulator and P_T is the total signal power in the carrier pre-detection if. bandwidth. It is also shown that the signal-to-noise ratios at the output of the carrier phase demodulator in the voice and telemetry subcarrier bandwidths (Column VI, table g-1-3) may be written as:

$$(S/N)_V = \left(\frac{2}{B_V} \right) \left\{ \cos^2 \Delta\theta_R \, J_1^2 (\Delta\theta_V) \, J_0^2 (\Delta\theta_{TM}) \right\} P_T/\Phi_N \qquad \text{(g-2-4)}$$

$$(S/N)_{TM} = \left(\frac{2}{B_{TM}} \right) \left\{ \cos^2 \Delta\theta_R \, J_0^2 (\Delta\theta_V) \, J_1^2 (\Delta\theta_{TM}) \right\} P_T/\Phi_N \qquad \text{(g-2-5)}$$

Relationships of equations (g-2-3), (g-2-4), and (g-2-5), respectively, can be expressed as:

$$(S/N)_C = M_C \left\{ P_T/\Phi_N \right\} \qquad \text{(g-2-6)}$$

$$(S/N)_V = M_V \left\{ P_T/\Phi_N \right\} \qquad \text{(g-2-7)}$$

$$(S/N)_{TM} = M_{TM} \left\{ P_T/\Phi_N \right\} \qquad \text{(g-2-8)}$$

Values for M_C, M_V and M_{TM} are calculated in table g-2-1 and equations (g-2-3), (g-2-4), and (g-2 5) are plotted for modes A through C in figures g-2-1 through g-2-8.

From equation (g-2-3), the percentage of total transmit power devoted to the carrier is found to be:

$$\frac{P_C}{P_T} = \cos^2 (\Delta\theta_R) \, J_0^2 (\Delta\theta_V) \, J_0^2 (\Delta\theta_{TM}) \qquad \text{(g-2-9)}$$

In like manner, it is found from equation (g-2-4) and equation (g-2-5):

$$\frac{P_V}{P_T} = \cos^2 (\Delta\theta_R) \, J_1^2 (\Delta\theta_V) \, J_0^2 (\Delta\theta_{TM}) \qquad \text{(g-2-10)}$$

---

(3)   Stover, Op. cit.
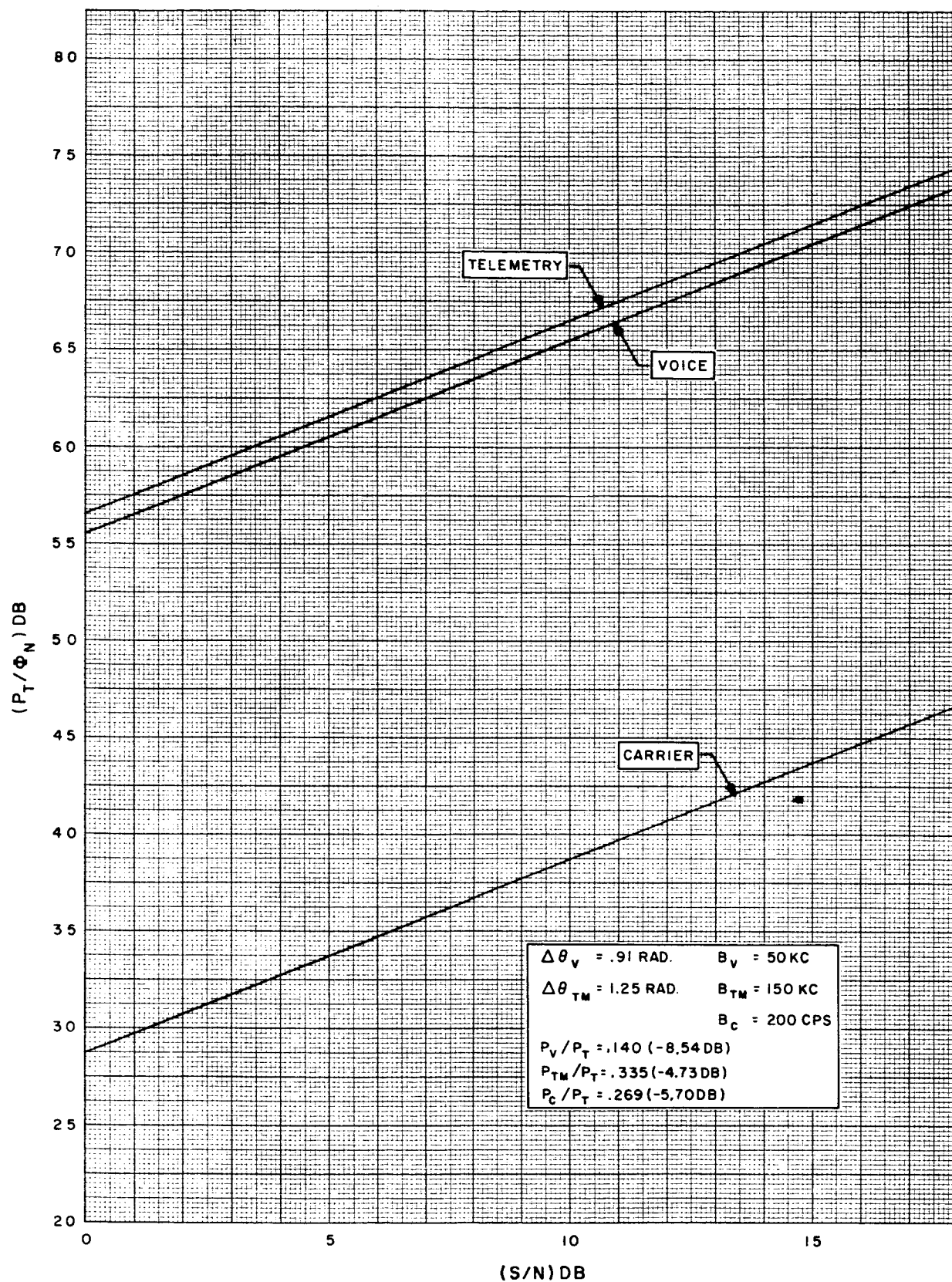
Figure g-2-1. Predetection Total Signal Power to Noise Density Ratio, Mode A
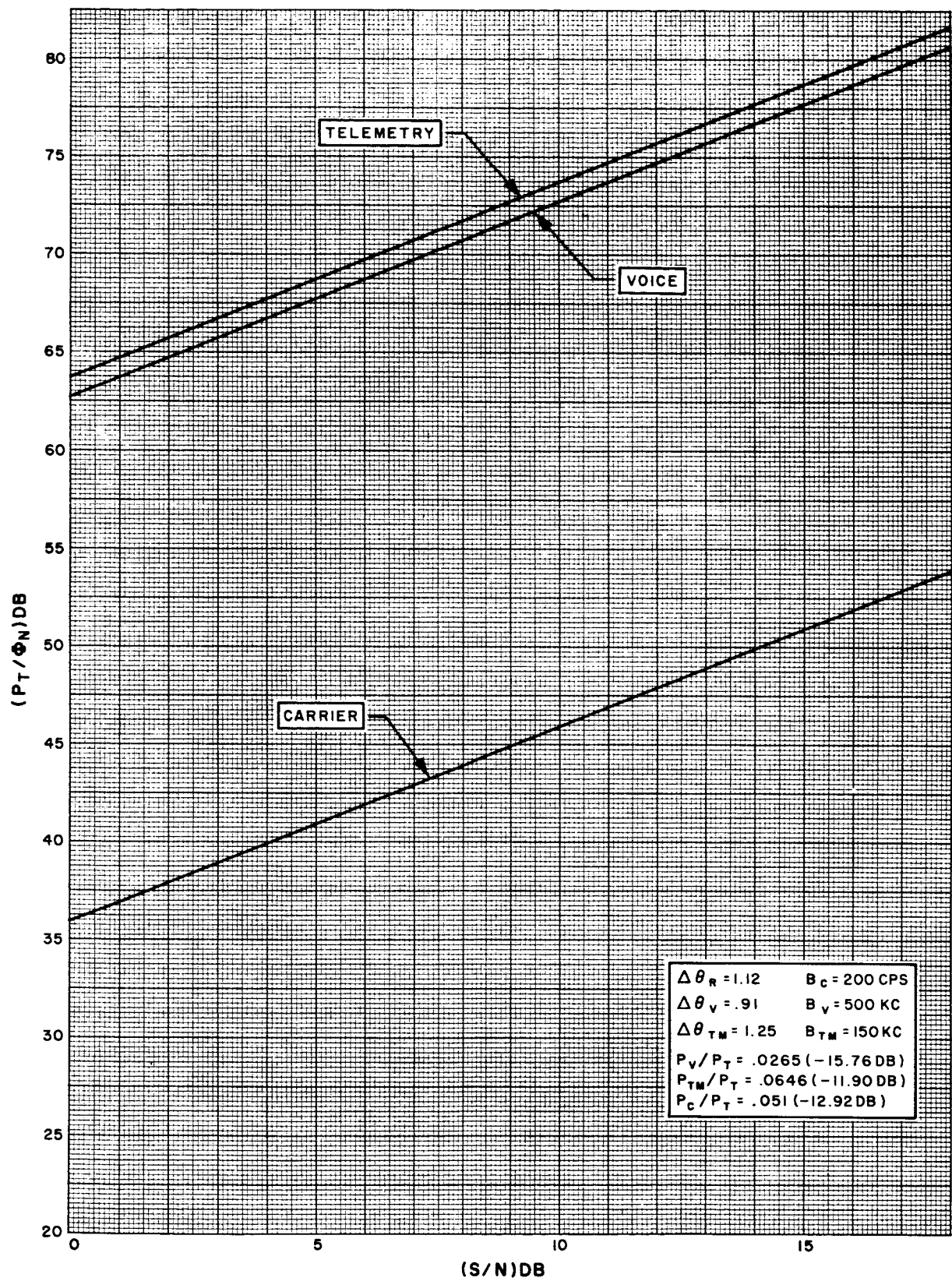
Figure g-2-2.   Predetection Total Signal Power to Noise Density Ratio, Mode B-1:1-A

Figure g-2-3. Predetection Total Power to Noise
Density Ratio, Mode B-1:1-D and B-1:1-3

Figure g-2-4.   Predetection Total Power to Noise Density Ratio, Mode B-1:1-F

Figure g-2-5.   Predetection Total Power to Noise Density Ratio, Mode B-2:1-A

Figure g-2-6.   Predetection Total Power to Noise Density
Ratio, Modes B-2:1-E and B-2:1-D

Figure g-2-7.   Predetection Total Power to Noise Density Ratio, Mode B-2:1-F

Figure g-2-8. Predetection Total Power to Noise Density Ratio, Mode C

$$\frac{P_{TM}}{P_T} = \cos^2(\Delta\theta_R) \; J_0^2(\Delta\theta_V) \; J_0^2(\Delta\theta_V) \; J_1^2(\Delta\theta_{TM}) \tag{g-2-11}$$

The ratios of P_V/P_C and P_{TM}/P_C may be found from these values and are given in table g-2-2.

TABLE g-2-1.   PM MODULATION ANALYSIS

MODE	$\Delta\theta_R$	$\Delta\theta_V$	$\Delta\theta_{TM}$	M_C	M_V	M_{TM}
A	-	0.91	1.25	-28.75	-55.53	-56.48
B-1:1-A	1.12	0.91	1.25	-35.92	-62.75	-63.71
B-1:1-D	0.60	0.91	1.25	-30.37	-57.19	-58.24
B-1:1-F	0.45	0.91	1.25	-29.61	-56.44	-59.39
B-2:1-A	1.12	0.91	-	-32.12	-59.08	-
B-2:1-D	0.60	0.91	-	-26.57	-53.40	-
B-2:1-F	0.45	0.91	-	-25.82	-52.64	-
B-3:1-A	1.12	-	-	-30.24	-	-
B-3:1-D	0.60	-	-	-24.67	-	-
B-3:1-F	0.45	-	-	-23.91	-	-
C	-	0.91	1.25	-28.7	-55.53	-42.5

For all modes: $B_C = 200$ cps

For all modes except B-3: $B_V = 5 \times 10^4$

For all mode B-1: $B_{TM} = 1.5 \times 10^5$

For mode C: $B_{TM} = 6 \times 10^3$

TABLE g-2-2.   RELATIVE LEVELS OF MAJOR SIGNAL
COMPONENTS FOR PM MODES

MODE	P_C/P_T(db)	P_V/P_T(db)	P_{TM}/P_T(db)	P_V/P_C(db)	P_{TM}/P_C(db)
A	-5.70	-8.54	-4.73	-2.84	+0.88
B-1:1-A	-12.92	-15.76	-11.90	-2.84	+0.88
B-1:1-D	-7.37	-10.20	-6.49	-2.84	+0.88
B-1:1-F	-6.61	-9.45	-5.54	-2.84	+0.88

TABLE g-2-2. RELATIVE LEVELS OF MAJOR SIGNAL
COMPONENTS FOR PM MODES (CONT)

B-2:1-A	-9.12	-11.96	-	-2.84	-
B-2:1-E	-3.57	-6.41	-	-2.84	-
B-2:1-F	-2.82	-5.65	-	-2.84	-
C	-5.7	-8.54	-4.73	-2.84	+0.88

From the curves given in figure g-2-1 through g-2-8, the relative thresholds of the
subchannels and carrier may be obtained and values for column VII of table g-1-3 may
be obtained for modes A through C. For each mode, the value of P_T/ϕ_N for which the
first threshold occurs for either the carrier, the voice subcarrier, or the telemetry
subcarrier can be determined. Threshold is defined for these signals as:

carrier: S/N = 8db in 200 cps

voice: S/N = 4.7 db in 50 kc

telemetry: S/N = 8.5db in 150 kc (6 kc for Mode C).

Having determined the critical value of P_T/ϕ_N, the corresponding signal-to-noise
ratios for the other subcarriers can be read directly. Modes A through C may be
summarized as follows:

Mode A:

From figure g-2-1:

P_T/ϕ_N for carrier S/N of 8db is 37.8 db

P_T/ϕ_N for voice S/N of 4.7 db is 60.2 db

P_T/ϕ_N for telemetry S/N of 8.5 db is 65.0 db

The first signal component to reach threshold is, therefore, telemetry, and it
will reach threshold when P_T/ϕ_N at the carrier demodulator input becomes 65 db.
For this carrier input condition, the voice signal at the voice subcarrier demodulator
input (measured in a 50 kc bandwidth) will be, from figure g-2-1, 9.4 db.

The carrier S/N for this condition does not fall within the range of figure g-2-1
and, therefore, must be calculated, using information from table g-2-2, as follows:

$P_C/P_T = 5.7db$

$$P_C/\Phi_N = 65.0-5.7 = 59.3 \text{db}$$

$$P_C/\Phi_N\Big|_{200cps} = 59.3-23=36.3 \text{ db}$$

Mode B-1:1-A

From figure g-2-2: the first component to reach threshold is telemetry at 8.5 db (in a 150-kc bandwidth).

(a) $P_T/\Phi_N = 72.2$ db

for this condition:

(b) $(S/N)_V = 9.5$ db (in 50 kc)

(c) $P_C/P_T = 12.92$ db

$\therefore$ $P_C/\Phi_N = 72.2-12.9=59.3$

and:

$$P_C/N\Big|_{200cps} = 59.3-23=36.3 \text{db}$$

Mode B-1: 1-D and B-1:1-E

From figure g-2-3: the first component to reach threshold is telemetry at 8.5 db, in 150 kc.

(a) $P_T/\Phi_N = 66.7$ db

(b) $(S/N)_V\Big|_{P_T/\Phi_N = 66.7} = 9.5$ in 50 kc

(c) $P_C/P_T = -7.37$ db

$\therefore$ $P_C/\Phi_N = 66.7-7.4 = 59.3$

and:

$$P_C/N\Big|_{200 cps} = 59.3-23 = 36.3 \text{ db}$$

Mode B-1:1-F

From figure g-2-4, the first component to reach threshold is telemetry at 8.5 db, in 150 kc bandwidth.

(a) $P_T/\Phi_N = 65.9$ db

(b) $(S/N)_V\Big|_{P_T/\Phi_N = 65.9 \text{ db}} = 9.5$ db in 50 kc

(c) $P_C/P_T = -6.61$

$\therefore P_C/\Phi_N = 65.9-6.6=59.3db$

$P_C/\Phi_N\Big|_{200\ cps} = 59.3-23 = 36.3\ db$

Mode B-2:1-A

From figure g-2-5, the first component to reach threshold is voice at 4.7 db, in 50 kc bandwidth.

(a) $P_T/\Phi_N = 63.8\ db$

(b) $P_C/P_T = 9.12\ db$

$P_C/\Phi_N = 63.8-9.1=54.7$

$P_C/N\Big|_{200\ cps} = 54.7-23=31.7db$

Mode B-2:1-D and B-2:1-E

From figure g-2-6, the first component to reach threshold is voice at 4.7 db, in 50 kc bandwidth.

(a) $P_T/\Phi_N = 58.1\ db$

(b) $P_C/P_T = -3.57db$

$P_C/\Phi_N = 58.1-3.6 = 54.5db$

$P_C/N\Big|_{200\ cps} = 54.5-23.0=31.5db$

Mode B-2:1-F

From figure g-2-7, the first component to reach threshold is voice at 4.7db, in 50 kc bandwidth.

(a) $P_T/\Phi_N = 57.3db$

(b) $P_C/P_T = -2.82\ db$

$P_C/\Phi_N = 57.3-2.8=54.5$

$P_C/\Phi_N\Big|_{200\ cps} = 50.5-23=31.5db$

Mode C

From figure g-2-8, the first component to reach threshold is voice at 4.7 db, in 50 kc bandwidth.

(a) $P_T/\Phi_N = 60.2\ db$

(b) $(S/N)_{TM}\Big|_{P_T/\Phi_N = 60.2} = 17.7$ db in 150 kc.

(c) $P_C/P_T = -5.7$ db

$P_C/\Phi_N = 60.2 - 5.7 = 54.5$ db

$P_C/\Phi_N\Big|_{200cps} = 54.5 - 23 = 31.5$ db –

g-2.3   FM MODES.

Modes D-1, D-2, and F will be considered. Mode D-1 has been deleted from the data demodulator requirements and it has been indicated (see section g-10) that Mode D-2 will be deleted also. These two modes will be analyzed, however, since they will be transmitted from the Block I vehicular equipment (near-earth missions).

The general form of the signal at the input to the carrier fm demodulator for mode D-1 will be [3]:

$$v(t) = A_C \sin\left[\omega_C t + \beta_V \sin\left(\omega_V t + \phi_V(t)\right) + \beta_{TM} \sin\left(\omega_{TM} t + \phi_{TM}(t)\right) + \sum_{n=1}^{9} \beta_{SC_n} \sin\left(\omega_{SC_n} t \phi_{SC_n}(t)\right)\right]$$ (g-2-12)

For mode E, the form will be:

$$v(t) = A_C \sin\left[\omega_C t + \frac{\Delta f_{TV}}{f_m} \phi_{TV}(t) + \beta_V \sin\left(\omega_V t + \phi_V(t)\right) + \beta_{TM} \sin\left(\omega_{TM}(t) + \phi_{TM}(t)\right)\right]$$ (g-2-13)

where:

$$\left|\phi_{TV}(t)\right| \leq 1$$

It can be shown [3] that the signal-to-noise ratio at the output of a frequency demodulator, measured in the bandpass of a subsequent subcarrier demodulator, may be written as:

$$S/N = (\beta^2/2B)\ (P_T/\Phi_N),$$ (g-2-14)

---

(3) Stover, Op. cit.

where P_T is the total signal power at the input to the carrier demodulator, β is the fm modulation index of the subcarrier on the carrier, Φ_N is the noise spectral density at the input to the carrier demodulator, and B is the subcarrier detection bandwidth.

This equation is true only when the demodulator is operating above threshold. Once the demodulator input signal-to-noise requirement for threshold is known and the loop bandwidth determined, there is a minimum input P_T/Φ_N, below which the conventional fm analysis (and the above equation) are no longer representative of the actual input-output relationships.

Equation (g-2-14) describes the relationship between the carrier demodulator input P_T/Φ_N and the resulting signal-to-noise ratio of the input to the voice and telemetry subcarrier demodulators in modes D-1, D-2, and E and the nine subcarriers of Mode D-1. Values of $\beta^2/2B$ for the signal components of mode D-1 are given in table g-2-3.

TABLE g-2-3. VALUES OF $\beta^2/2B$ FOR SIGNAL COMPONENTS OF MODE D-1

Component	β	B (kc)	$\dfrac{\beta^2}{2B}$	$10\log\left(\dfrac{\beta^2}{2B}\right)$
Voice	.320	50	1.024×10^{-6}	-59.88
PCM	.341	150	3.875×10^{-7}	-64.1
S. C. #1	6.90	3	7.94×10^{-3}	-21
#2	4.55	4.55	2.27×10^{-3}	-26.44
#3	3.33	6.2	8.94×10^{-4}	-30.48
#4	2.50	8.3	3.76×10^{-4}	-34.25
#5	1.908	10.9	1.67×10^{-4}	-37.77
#6	1.428	14.5	7.03×10^{-5}	-41.52
#7	1.052	19.7	2.83×10^{-5}	-45.48
#8	0.800	25.9	1.236×10^{-5}	-49.08
#9	0.605	34.2	5.37×10^{-6}	-52.7

It is also shown in reference (3) that the TV peak-signal to rms-noise ratio at the output of the carrier fm demodulator may be written in terms of the input P_T/Φ_N as:

$$(S/N)_{TV} = 12\left(\frac{0.7\Delta f_{TV}}{f_m}\right)^2 \frac{1}{f_m}(P_T/\Phi_N), \qquad \text{(g-2-15)}$$

(3) Stover, Op. cit.

where it is assumed that 70 percent of the total possible carrier deviation by the TV is used for picture information and 30 percent is used for synchronization. This assumption results in a 3-db reduction in signal power over that which would be available if a telemetry channel were used for synchronization purposes.

Equation (g-2-15), like equation (g-2-14), is only valid when the carrier demodulation loop is operating above threshold.

Equation (g-2-15) becomes:

$$(S/N)_{TV} = 12 \, (.7)^2 (2.50)^2 \left(\frac{10^{-3}}{400} \right)$$

$$= 9.14 \times 10^{-5} \text{ or } -40.39 \text{db,}$$

for

$$\beta_{TV} = (\Delta f_{TV} / f_m) = 2.50$$

$$f_m = 400 \text{ kc and}$$

$$B_{TV} = 400 \text{ kc}$$

Relationships of equations (g-2-14) and (g-2-15) are plotted in figures g-2-9, g-2-10, and g-2-11 for modes D-1, D-2 and E, respectively. In each of these figures, there is a value of P_T / ϕ_N below which the subcarrier and TV curves are broken. This is the minimum value of $P_T / \phi N$ for satisfactory carrier loop performance, derived in section g-4 for the fm modes. Above these values of P_T / ϕ_N equations (g-2-14) and (g-2-15) are applicable for the system under study and the curves of figures g-2-9, g-2-10 and g-2-11 are solid lines. For example, the loop bandwidth to be used for mode D-1, as determined in section g-4 is 11 mc, corresponding to $P_T / \phi_N = 74.8$ db. In figure g-2-9, the graph for mode D-1, it can be seen that the main carrier demodulator will threshold before any of the subcarriers. The same is true of modes D-2 and E.

The threshold S/N requirements for the subcarriers at the output of the carrier fm demodulator are:

$$(S/N)_V = 4.7 \text{ db in 50 kc}$$

$$(S/N)_{TM} = 8.5 \text{ db in 150 kc}$$

$$(S/N)_1 = 10 \text{ db in 3 kc}$$
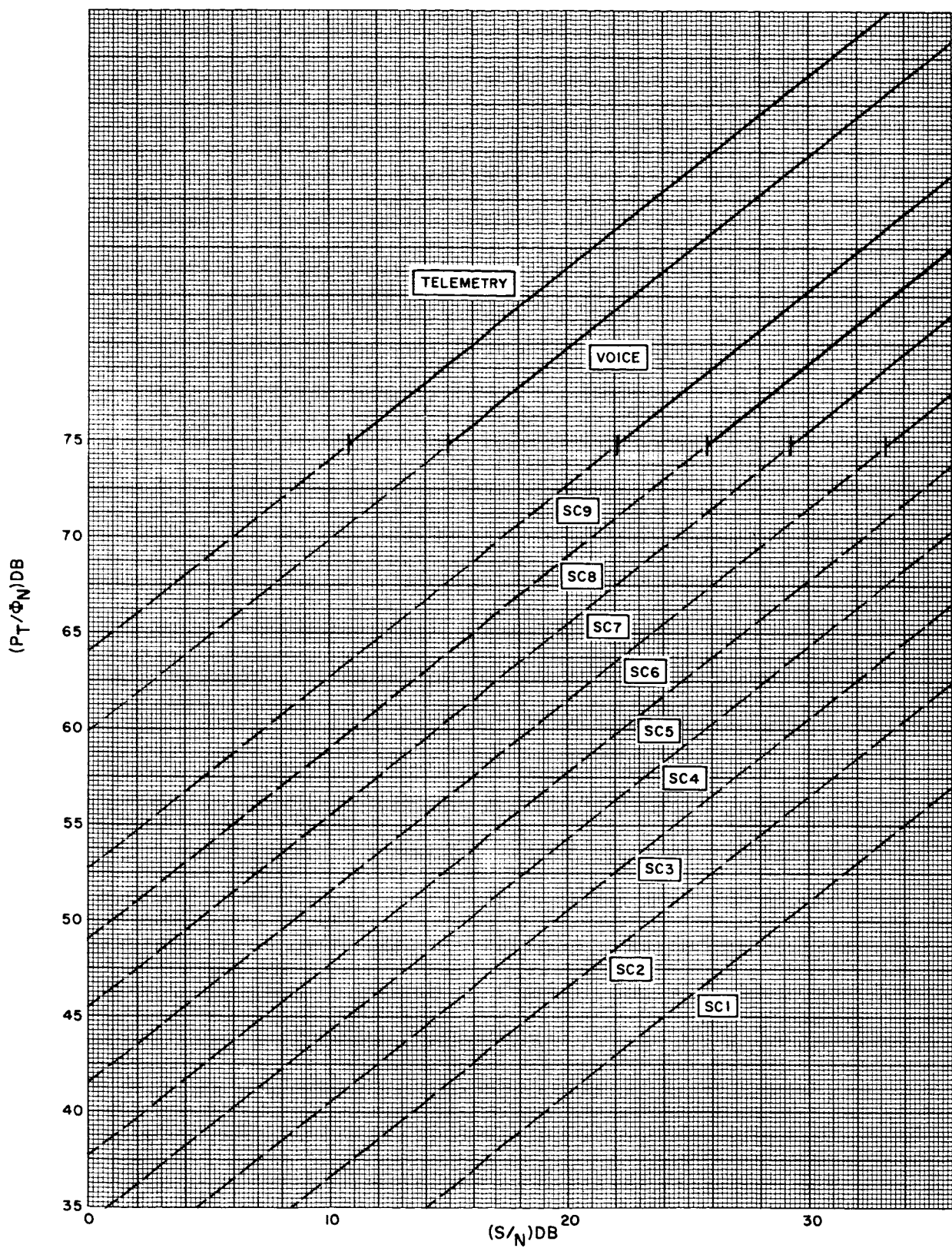
Figure g-2-9.   Predetection Total Power to Noise Density Ratio, Mode D-1
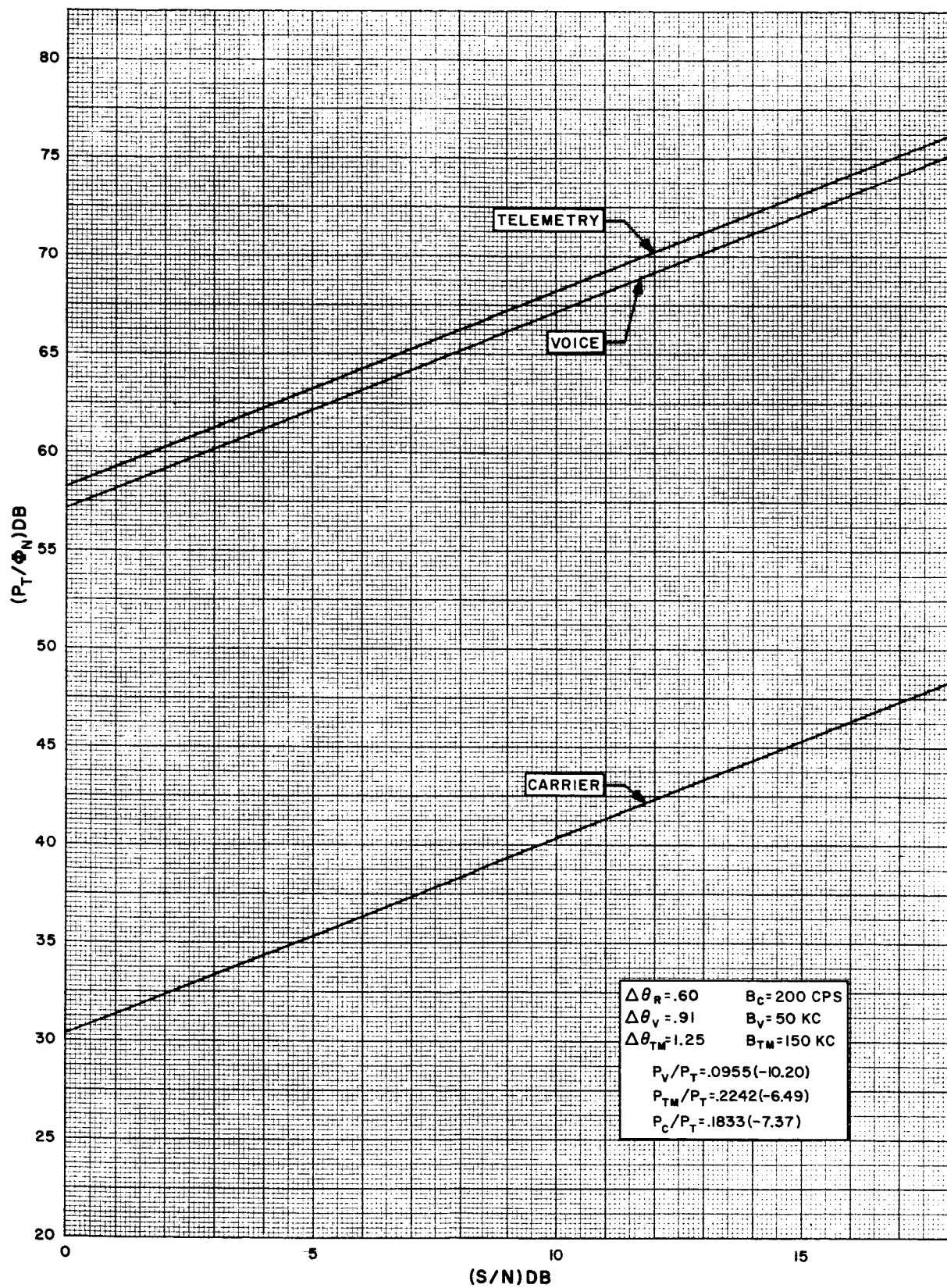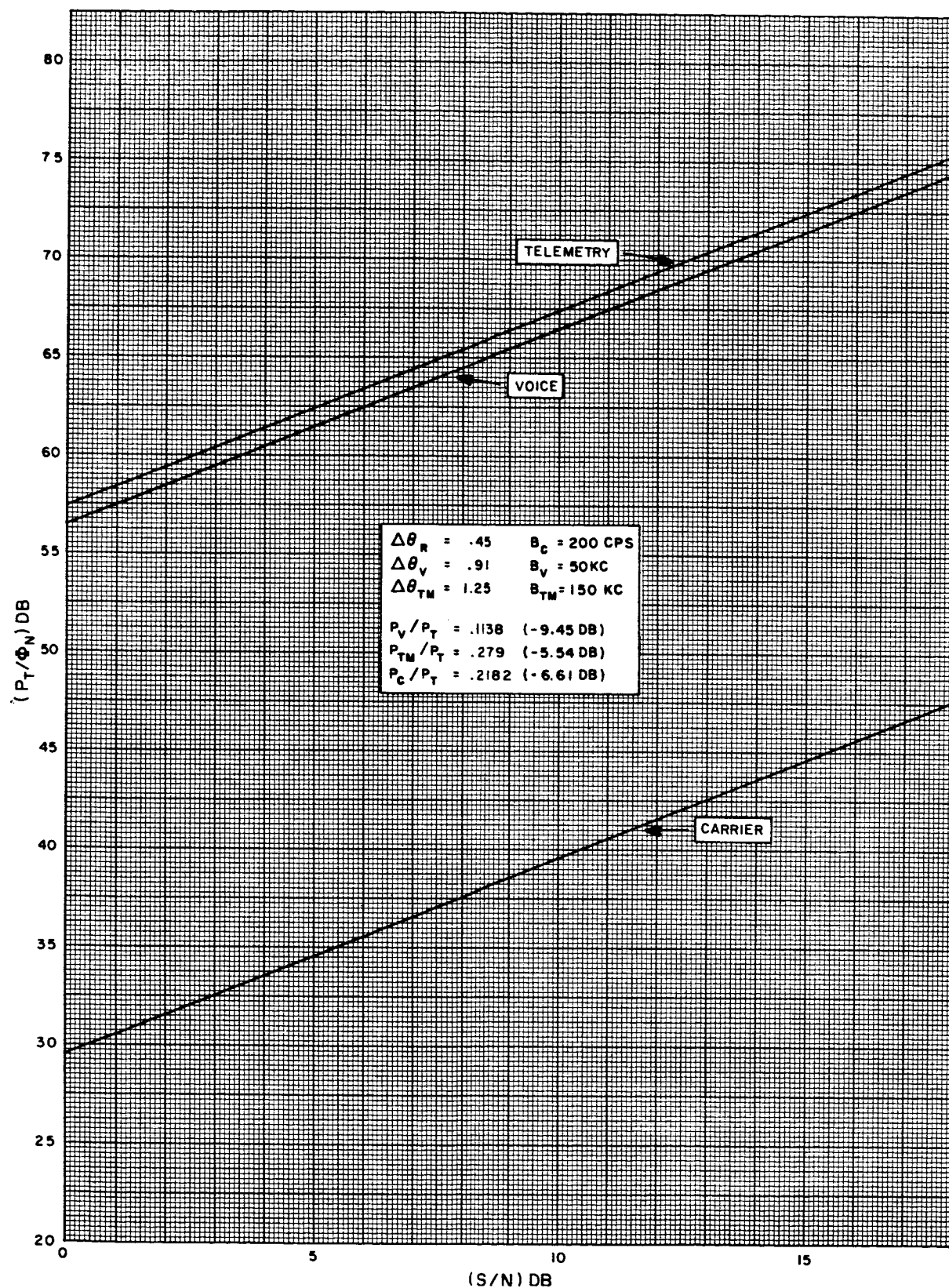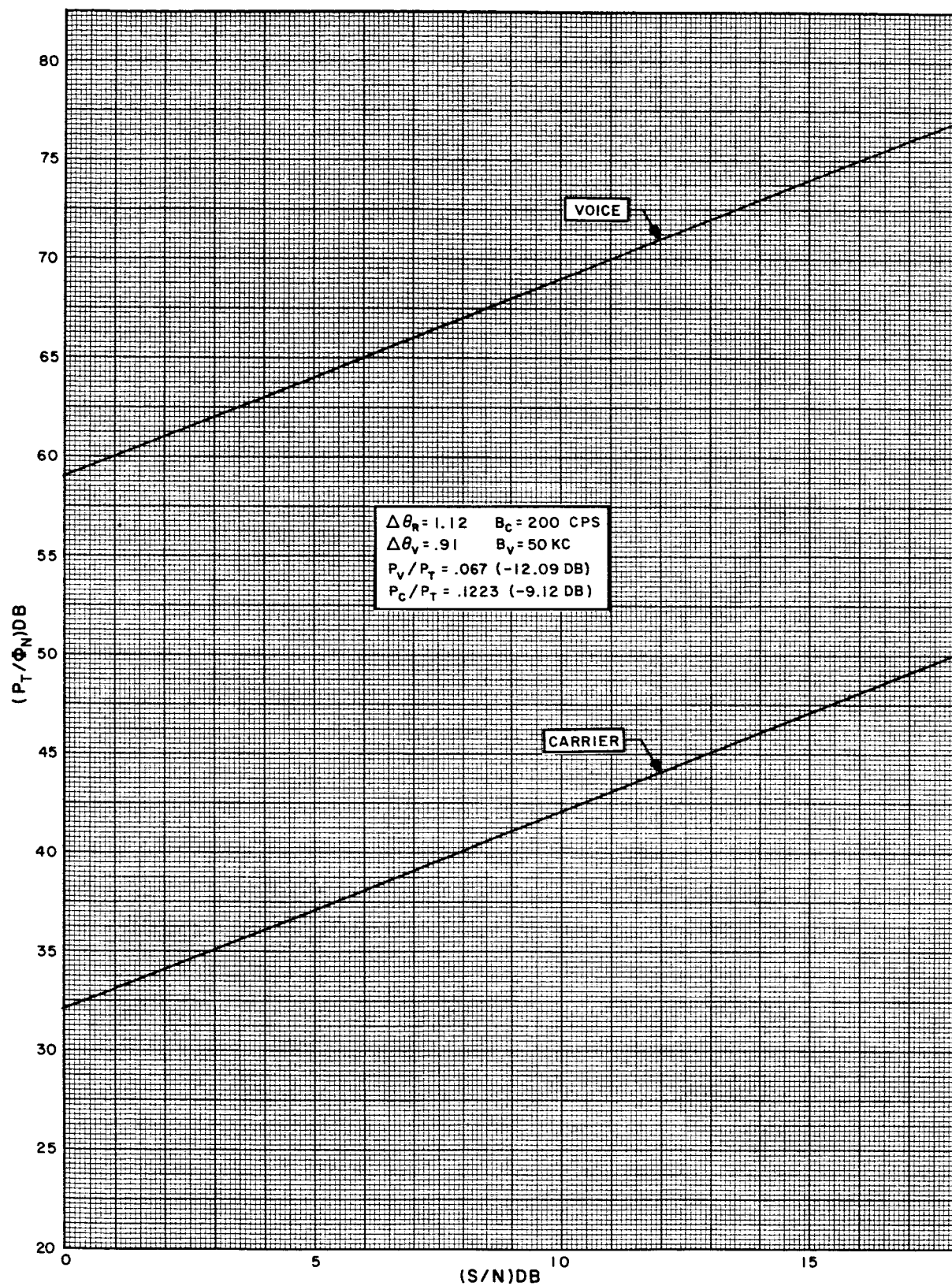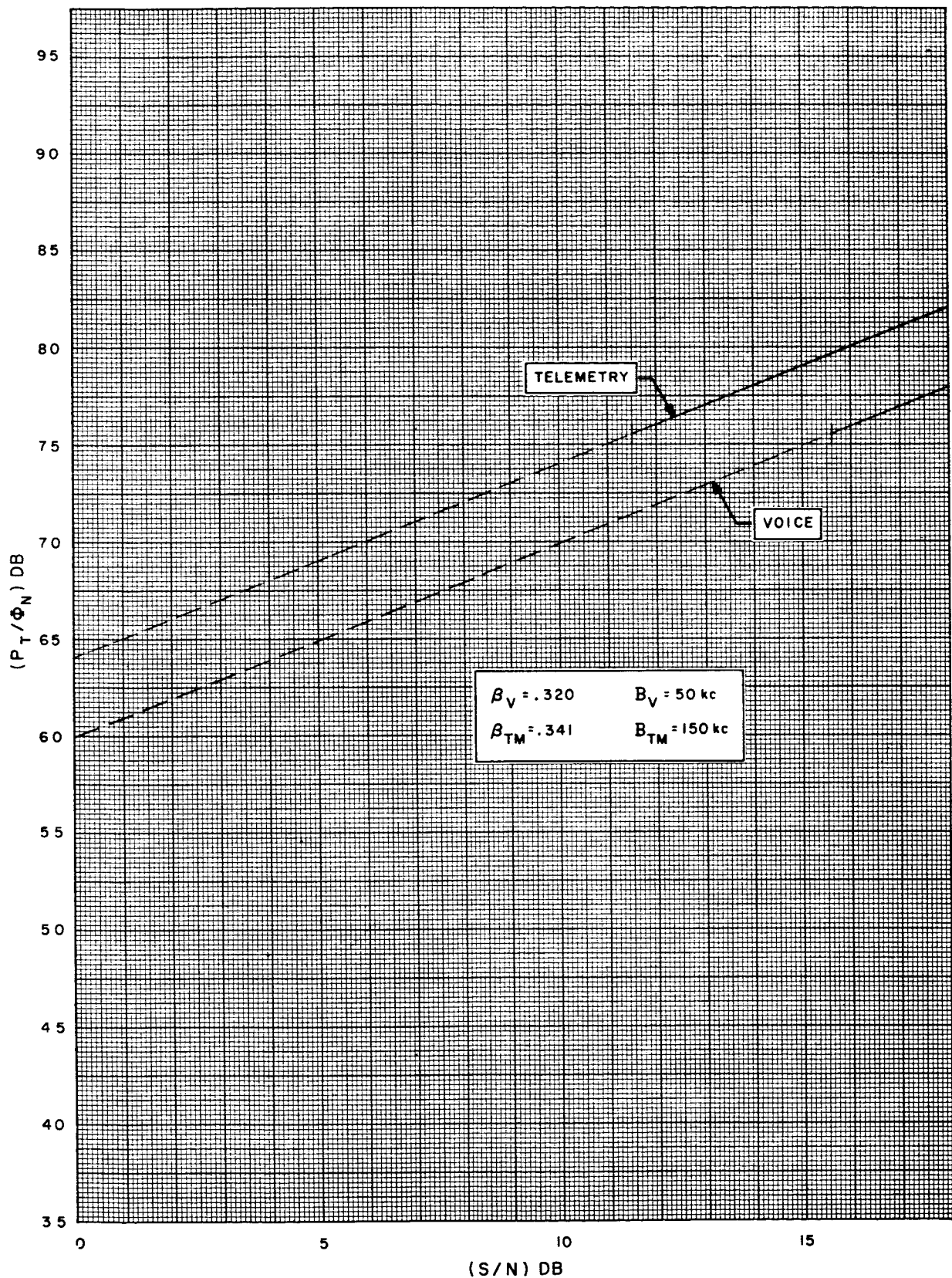
Figure g-2-10.   Predetection Total Power to Noise Density Ratio, Mode D-2

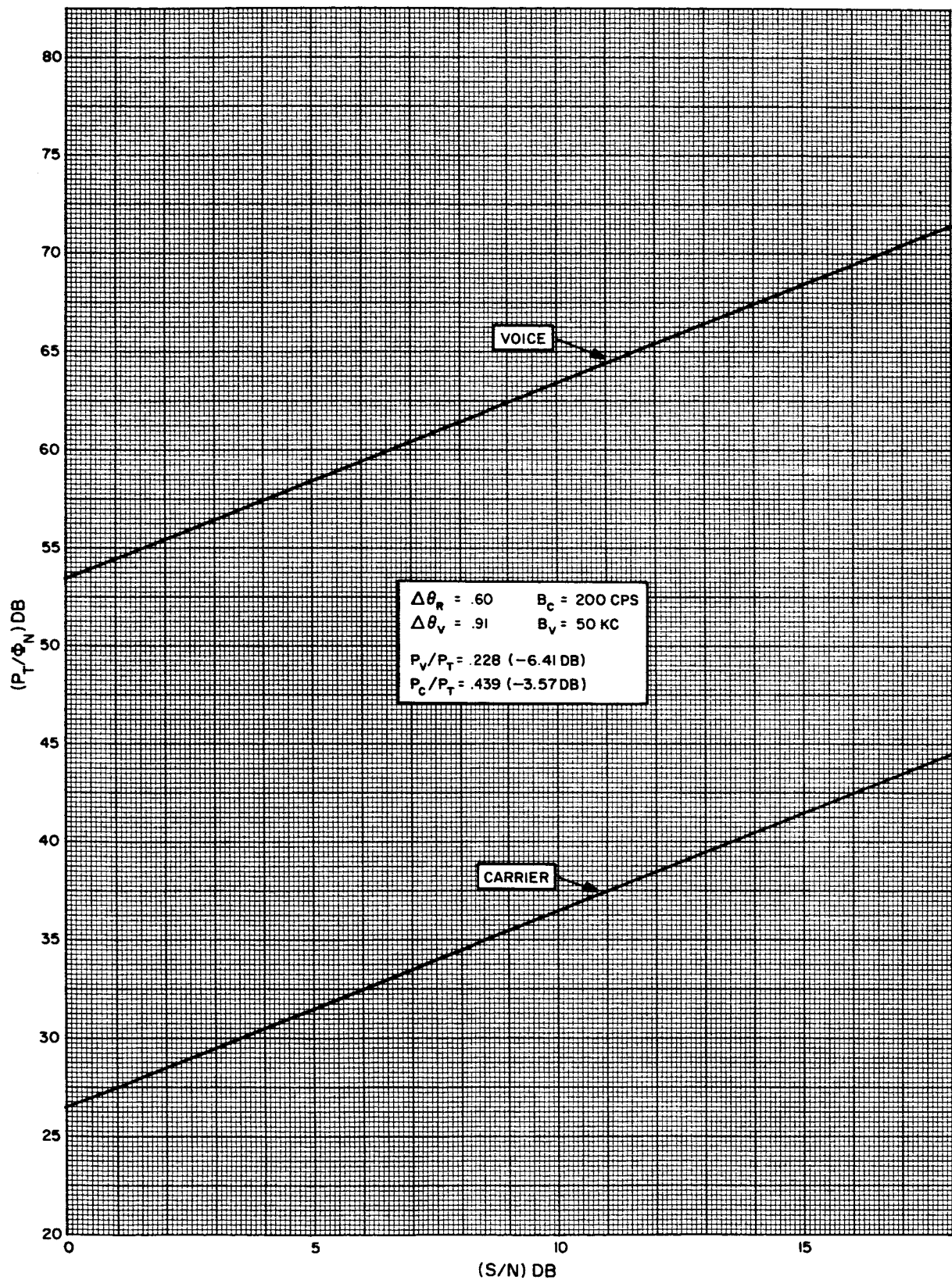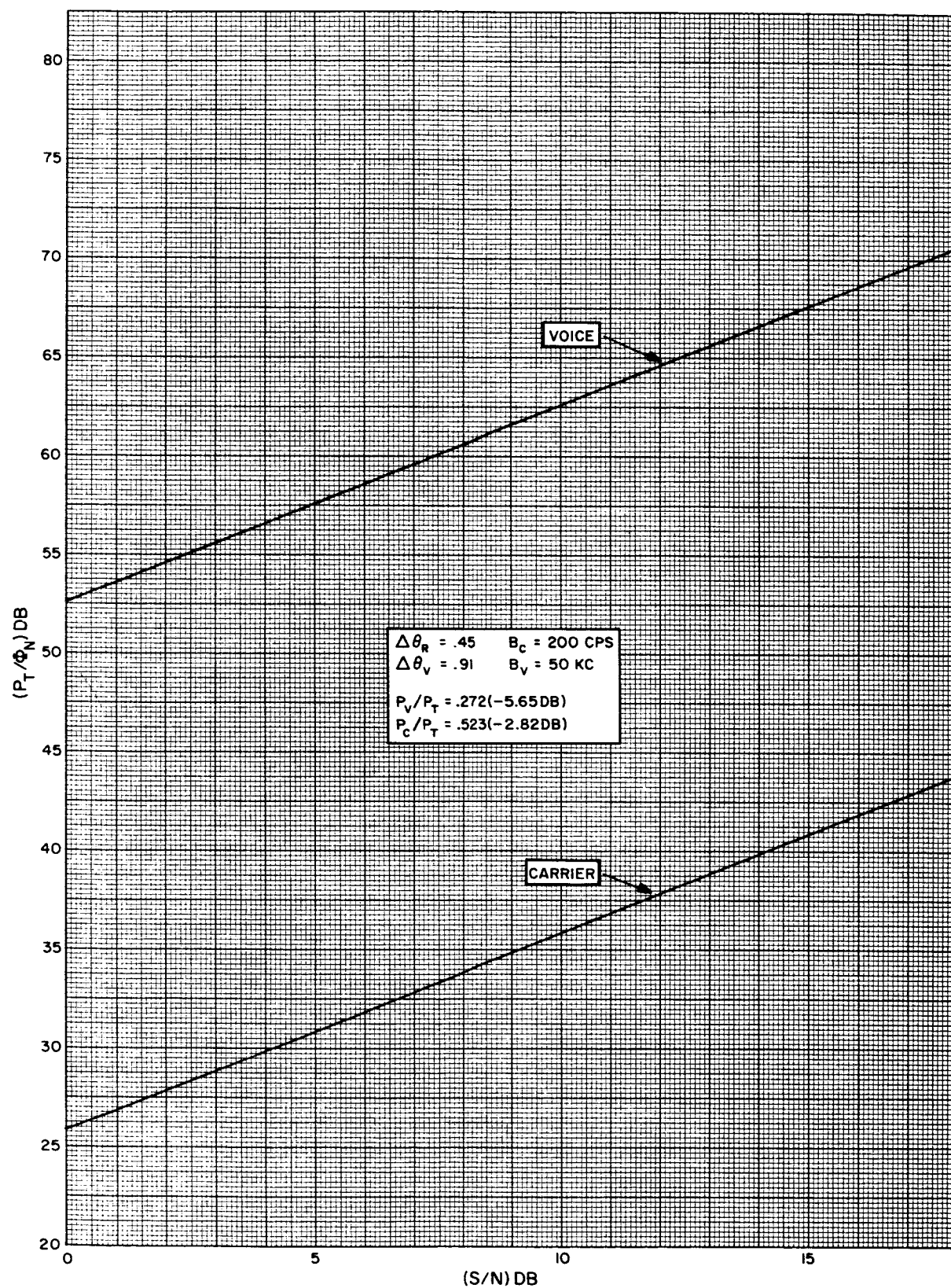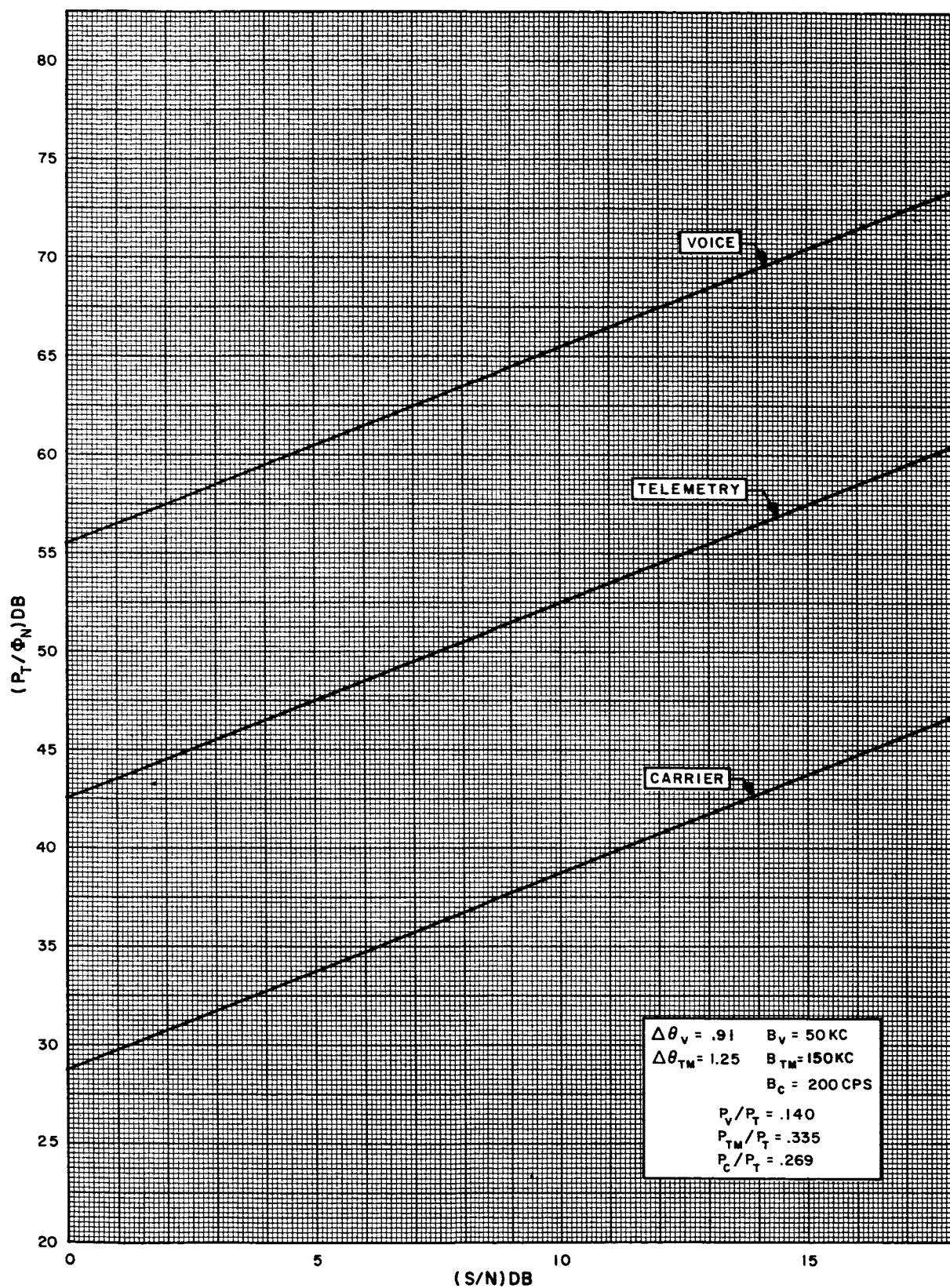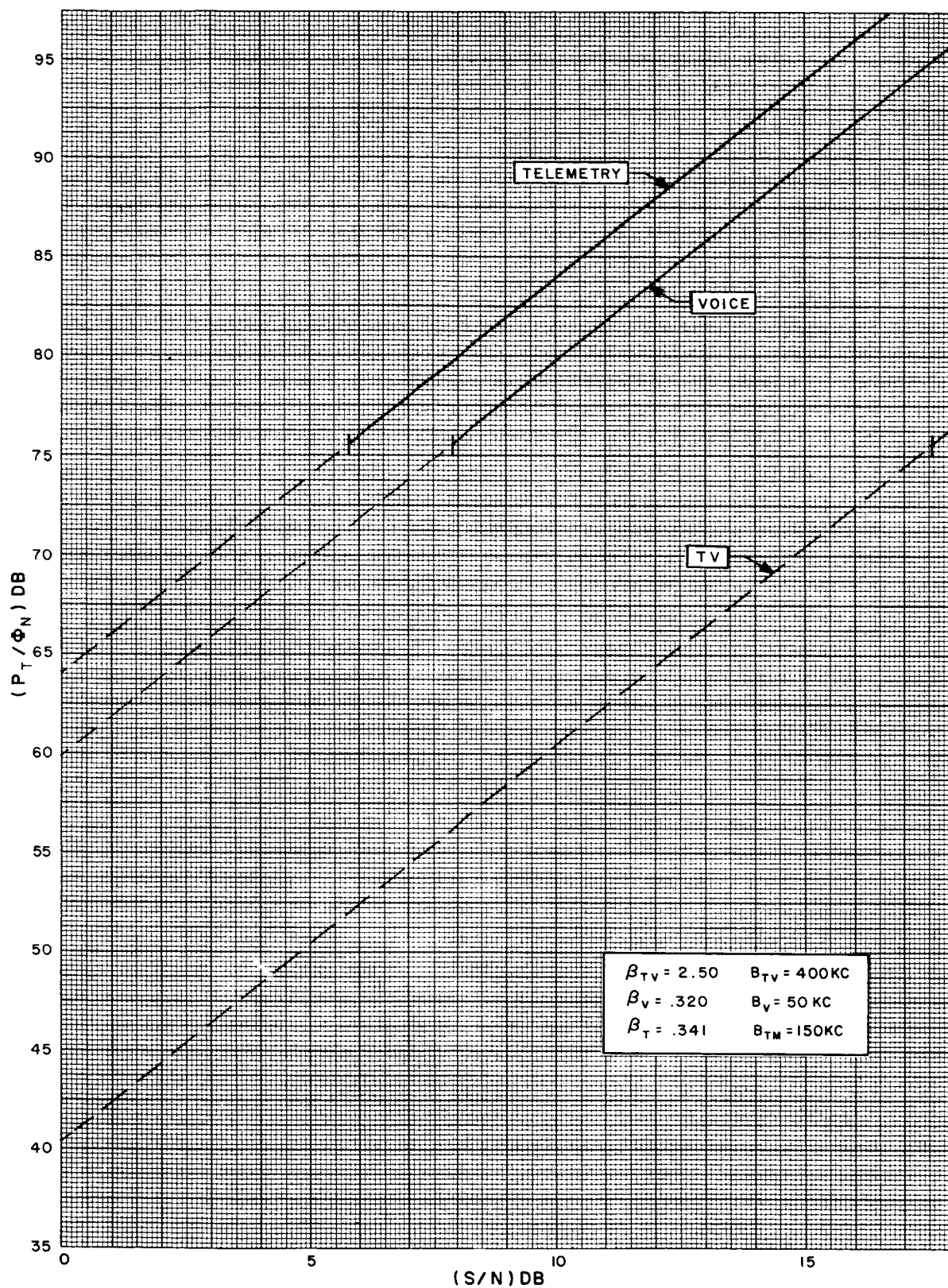Figure g-2-11.   Predetection Total Power to Noise Density Ratio, Mode E

$(S/N)_2 = 10$ db in 4.55 kc

$(S/N)_3 = 10$ db in 6.2 kc

$(S/N)_4 = 10$ db in 8.3 kc

$(S/N)_5 = 10$ db in 10.9 kc

$(S/N)_6 = 10$ db in 14.5 kc

$(S/N)_7 = 10$ db in 19.7 kc

$(S/N)_8 = 10$ db in 25.9 kc

$(S/N)_9 = 10$ db in 34.2 kc

As can be seen from the figures, the carrier threshold is the critical value of P_T/Φ_N for all three fm modes. At this critical value of P_T/Φ_N, the output signal-to-noise ratios for the subcarrier, as well as that for TV (peak signal-to-rms noise), may be read from the graphs. These are the values listed in Column VII of table g-1-3. Summaries of modes D-1 and E follow.

Mode D-1:

From section g-4, the carrier demodulator threshold is $P_T/\Phi_N = 74.8$db. From figure g-2-9, it can be seen that this is the first signal component to threshold and, for this value of P_T/Φ_N, the S/N of each subcarrier demodulator input in its respective bandwidth will be:

Signal	Bandwidth, (kc)	S/N, (db)
Voice	50.0	14.9
PCM	150.0	10.7
SC#1	3.0	53.8
SC#2	4.55	48.4
SC#3	6.2	44.3
SC#4	8.3	40.5
SC#5	10.9	37.0
SC#6	14.5	33.2
SC#7	19.7	29.3
SC#8	25.9	25.7
SC#9	34.2	22.1

<u>Mode E</u>:

From section g-4, the carrier demodulator threshold is $P_T/\Phi_N = 75.7$ db. It can be seen in figure g-2-11 that this is the first signal component in mode E to threshold and that, at this value of P_T/Φ_N, the S/N of the signal components in their respective bandwidths at the carrier demodulator output will be:

Signal	Bandwidth (kc)	S/N (db)
Voice	50	15.8
PCM	150	11.6
TV	400	35.3

g-2.4   APOLLO SIGNAL SPECTRUM ANALYSIS.

To determine the relative power spectrum of Apollo-like signals, a simplified signal may be assumed:[3]

$$v(t) = A_C \sin (\omega_C t + \Delta\theta_{TM} \sin \omega_{TM} t + \Delta\theta_V \sin \omega_V t) \qquad \text{(g-2-16)}$$

Where ω_{TM} and ω_V are the telemetry and voice subcarrier frequencies and $\Delta\theta_{TM}$ and $\Delta\theta_V$ are the telemetry and voice subcarrier modulation indices, respectively. It will be noted that the subcarriers are assumed to be unmodulated, to simplify the analysis, the computer program and the resulting spectra.

The effect of modulation on the subcarriers would have been to broaden each sideband into another, narrow spectrum. For the subcarrier modulation indices assumed (those given in table g-1-1), the spectra would not be greatly changed and the signal power contained in a given bandwidth would remain essentially the same. For these conditions, modes A and C may be considered to be identical. A second analysis was run, using the fm parameters, to determine the spectrum of mode D-2.

For the analysis, the signal of equation (g-2-16) may be represented in the form:

$$v(t) = A_C \sum_{n=-\infty}^{\infty} \sum_{n=-\infty}^{\infty} J_n(\Delta\theta_{TM}) \, J_m (\Delta\theta_V) \, \text{Sin} \, (\omega_C t + n\omega_{TM} t + m \omega_V t) \qquad \text{(g-2-17)}$$

A given sideband in this signal will then be:

$$V_{nm}(t) = A_C J_n (\Delta\theta_{TM}) \, J_m (\Delta\theta_V) \sin (\omega_C + n\omega_{TM} + m\omega_V)t \qquad \text{(g-2-18)}$$

and the normalized rms power of the sideband is:

$$\frac{P_{nm}}{A_C^2/2} = J_n^2 (\Delta\theta_{TM}) \, J_m^2 (\Delta\theta_V) \qquad \text{(g-2-19)}$$

<hr>

[3] Stover, Op. cit.

The signal components given in equation (9-2-19) were evaluated by digital computer program. Subcarriers which were more than 99 db below the total signal power were not recorded and those which were more than 5 mc from the carrier were not calculated.

The results are given in Tables g-2-4 and g-2-5 and are plotted in figures g-2-12 and g-2-13. The total power in the upper and lower sidebands is accumulated in column VI, but the positions and relative amplitudes of only the upper sideband of each pair, as given in column V, are plotted in the figures.

It will be noted that many of the sidebands found in the tables cannot be indicated in the figures because their magnitudes are too small.

From the tables, it can be seen that, for modes A and C (PM), 99.995 percent of the signal power would be passed by an if. channel 9.55-mc wide (provided, of course, that the signal is centered in the passband). For mode D-2 (fm), 99.998 percent of the signal power would be passed by a 5.0-mc if. channel. For the 3.3-mc and 10-mc bandwidths through which the PM and fm signals will be passed, approximately 84.8 percent of the PM signal and 100 percent of the fm signal would be available to the demodulators. The latter would indicate that, if the fm demodulator channel were linear, a carrier offset of 2.5 mc would cause an unsymmetrical loss of only 0.002 percent of the signal.

TABLE g-2-4. APOLLO SIGNAL SPECTRUM (SIMPLIFIED) MODES A AND C (PM)

I	II	III	IV	V	VI
		SUBCARRIER FREQUENCY MULTIPLIER (1)			
SIDEBAND NUMBER	BASEBAND FREQUENCY (MC)	TELEMETRY (2)	VOICE (3)	SIDEBAND LEVEL (db) (4)	ACCUMULATED POWER (%) (5)
Carrier	0	0	0	-5.697	26.931
1	0.226	1	-1	-13.593	35.675
2	0.346	-4	3	-81.151	35.675
3	0.452	2	-2	-35.640	35.731
4	0.572	-3	2	-48.972	35.733
5	0.678	3	-3	-65.201	35.733
6	0.798	-2	1	-23.090	36.715
7	0.904	4	-4	-99.941	36.715
8	1.024	-1	0	-7.739	70.377
9	1.250	0	-1	-11.552	84.369
10	1.370	-5	3	-99.098	84.369
11	1.476	1	-2	-26.143	84.855
12	1.596	-4	2	-64.922	84.855
13	1.702	2	-3	-51.870	84.857
14	1.822	-3	1	-36.422	84.901
15	1.928	3	-4	-83.991	84.901
16	2.048	-2	0	-17.236	88.681
17	2.274	-1	-1	-13.593	97.425
18	2.500	0	-2	-24.101	98.203
19	2.620	-5	2	-82.869	98.203
20	2.726	1	-3	-42.372	98.215
21	2.846	-4	1	-52.372	98.217
22	2.952	2	-4	-70.660	98.217
23	3.072	-3	0	-30.568	98.391
24	3.298	2	-1	-23.090	99.373
25	3.524	-1	-2	-26.143	99.859
26	3.750	0	-3	-40.331	99.877

27	3.870	-5	1	-70.319	99.877
28	4.076	1	-4	-61.162	99.879
29	4.096	-4	0	-46.518	99.883
30	4.202	2	-5	-91.418	99.883
31	4.322	-3	-1	-36.422	99.929
32	4.548	-2	-2	-35.640	99.983
33	4.774	-1	-3	-42.372	99.995
34	4.894	-6	1	-89.882	99.995
35	5.000	0	-4	-59.121	99.995

NOTES:

(1) Method by which the frequency of the sideband was derived.

(2) Number to be multiplied by 1.024 mc.

(3) Number to be multiplied by 1.25 mc.

(4) Level of each (upper and lower) sideband, relative to total signal level (Power or Voltage).

(5) Total Power of all components between and including the indicated sideband pair.

TABLE g-2-5.   APOLLO SIGNAL SPECTRUM (SIMPLIFIED) MODE D-2 (FM)

| SIDEBAND NUMBER | BASEBAND FREQUENCY (MC) | SUBCARRIER FREQUENCY MULTIPLIER (1) | | SIDEBAND LEVEL (4) (db) | ACCUMULATED POWER (5) (%) |
		TELEMETRY (2)	VOICE (3)		
Carrier	0	0	0	-0.478	89.574
1	0.226	-1	1	-31.521	89.714
2	0.452	-2	2	-74.766	89.714
3	0.572	3	-2	-99.653	89.714
4	0.798	2	-1	-52.865	89.716
5	1.024	1	0	-15.716	95.080
6	1.250	0	1	-16.283	99.786

7	1.476	-1	2	-53.422	99.786
8	1.822	3	-1	-77.752	99.786
9	2.048	2	0	-37.060	99.826
10	2.274	1	1	-31.521	99.966
11	2.500	0	2	-38.184	99.998
12	2.726	-1	3	-78.864	99.998
13	3.072	3	0	-61.947	99.998
14	3.298	2	1	-52.865	99.998
15	3.524	1	2	-53.422	100.000*
16	3.750	0	3	-63.626	
17	4.096	4	0	-89.341	
18	4.322	3	1	-77.752	
19	4.548	2	2	-74.766	
20	4.774	1	3	-78.864	
21	5.000	0	4	-91.573	

NOTES:

(1)   Method by which the frequency of the sideband was derived.

(2)   Number to be multiplied by 1.024 mc.

(3)   Number to be multiplied by 1.25 mc.

(4)   Level of each (upper and lower) sideband, relative to total signal level (Power or Voltage).

(5)   Total Power of all components between and including the indicated sideband pair.

*100% of signal power is indicated at this point because of roundoff errors.
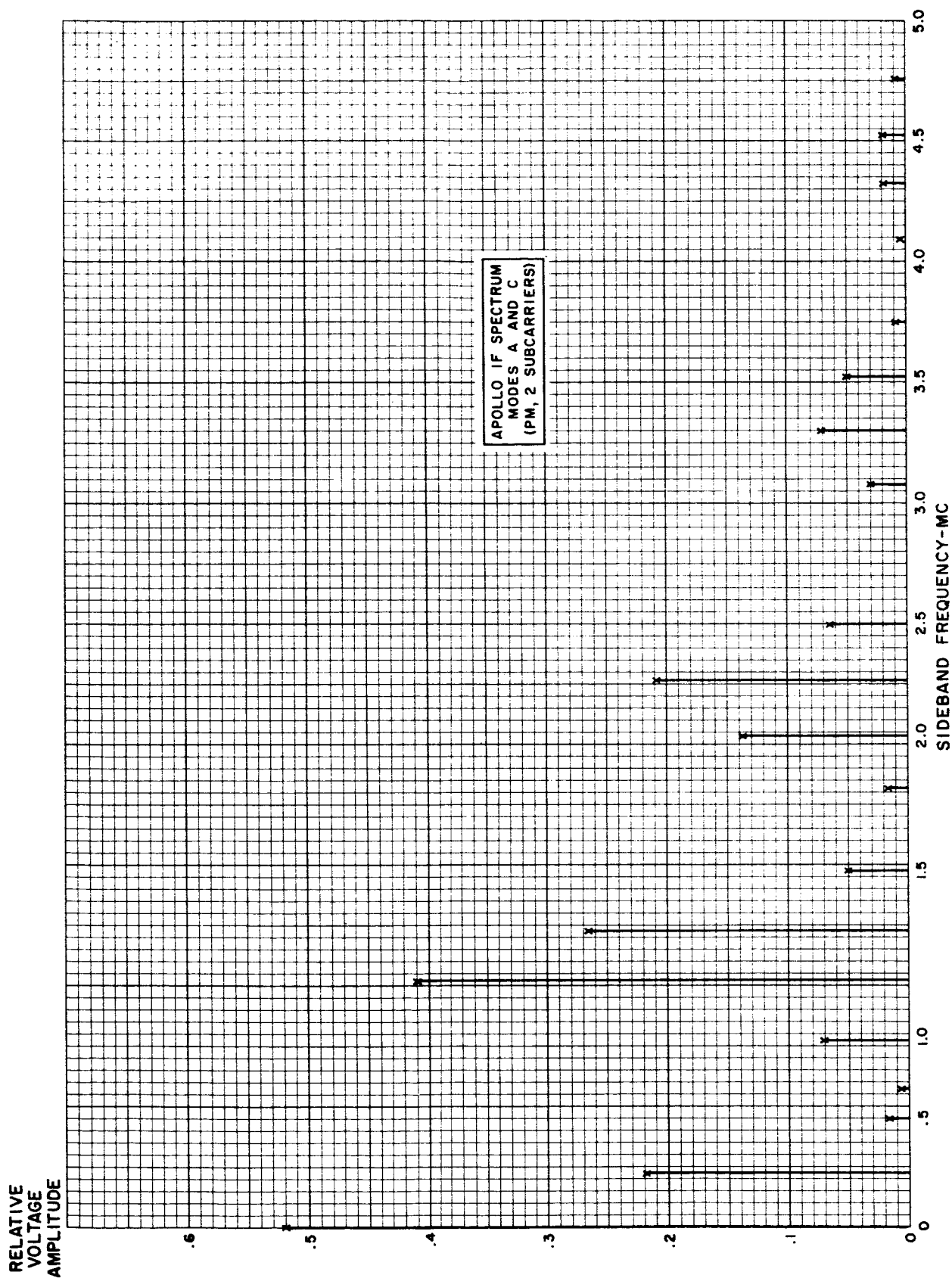
Figure g-2-12.   Apollo IF Spectrum Modes A and C (PM, 2 Subcarriers)
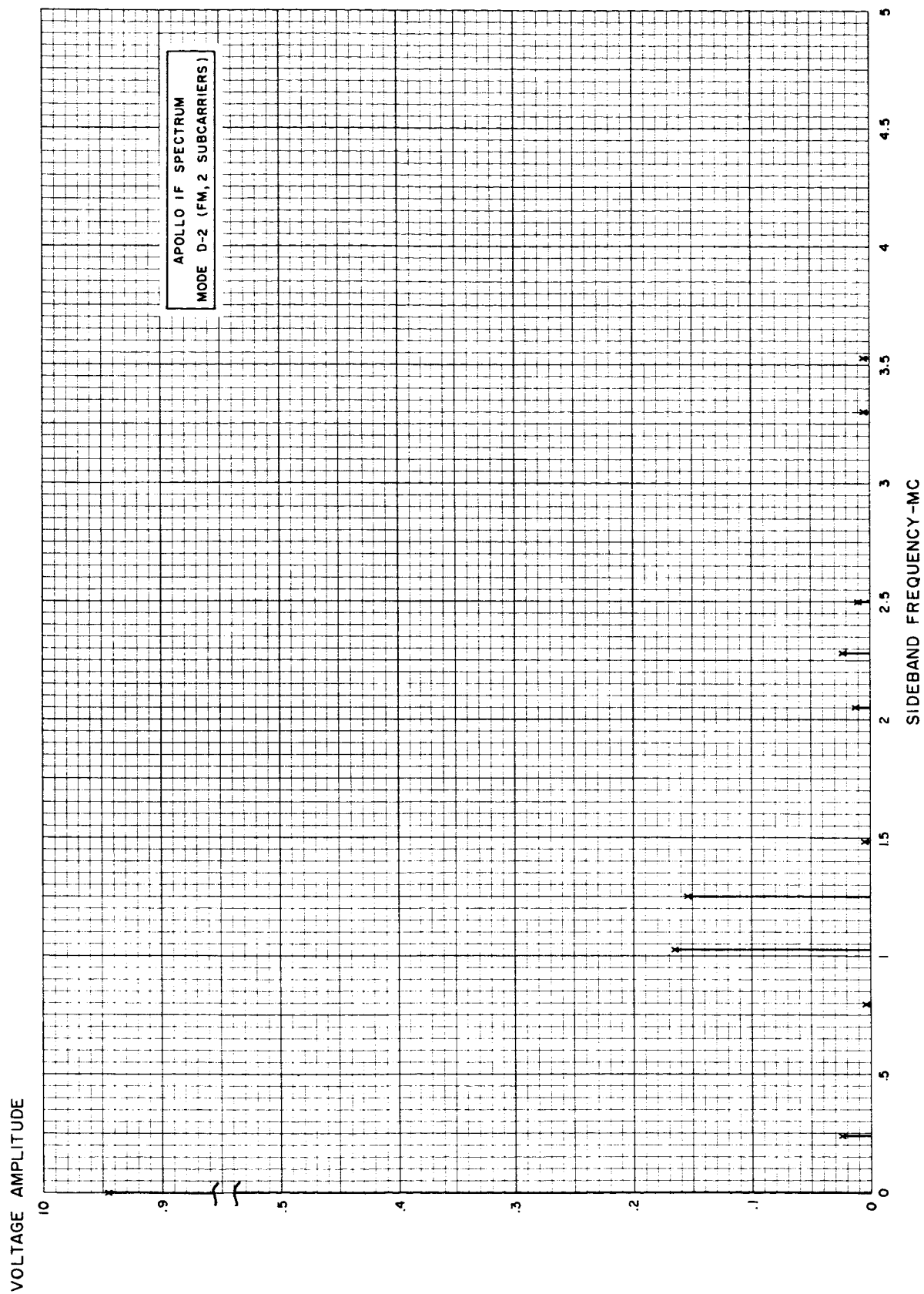
Figure g-2-13.   Apollo IF Spectrum Mode D-2 (FM, 2 Subcarriers)

analysis of carrier phase demodulator

g-3.1 GENERAL.

As indicated in section g-2, PM modulation is used in the Apollo program for emergency voice, as well as most of the normal operational data signals. A common PM demodulator, block diagram of which is shown in figure g-3-1, will be used for all of these signals.

The carrier phase lock loop is required to lock to the 10-mc if. signal from the R & RR tracking receiver. Two reference loop bandwidths are required and provided (30 cps and 100 cps) selected by changing the time constant of the loop tracking filter. The -3 db bandwidth of the signal channel of the tracking receiver is 3 mc.

The PM demodulator is only required to operate with the R & RR receiver when the tracking receiver is phase-locked to the carrier component of the incoming signal. Under these conditions, the level of the carrier component of the 10-mc output from the tracking receiver is maintained constant at -70 dbm.* Level variation between receivers was assumed to be ±5 db and the use of agc (shown in figure g-3-1) was given as optional.

Paragraphs g-3.2 through g-3.7 are concerned primarily with the operation of the PM demodulator on normal operational signals. Paragraph g-3.8 is a discussion of the problems of using the demodulator on the emergency voice signal (mode F).

---

*   This level will probably be -22 dbm. See section g-10.
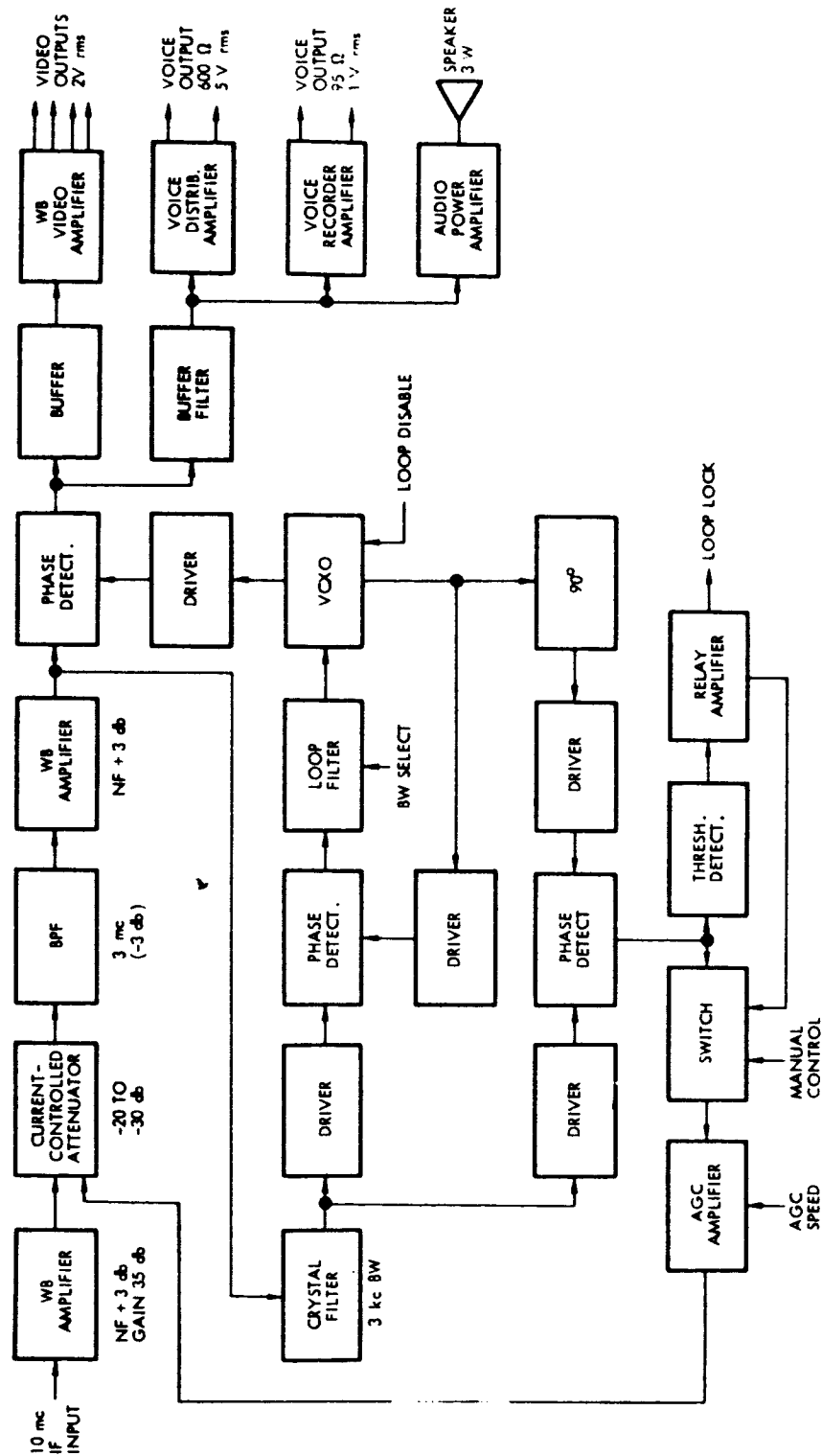
Figure g-3-1.   Carrier Phase Demodulator

g-3.2 THRESHOLD SIGNAL LEVEL.

The threshold signal level for the Apollo PM demodulator was defined[1] as the input carrier signal level at which the phase-loop jitter equals 0.35 radians rms. The GSFC specifications were calculated as follows:

Loop Bandwidth (B_{L_O})	100 cps	30 cps
Noise Density Level at 290°K	-174 dbm/cps	-174 dbm/cps
System Noise Figure**	2 db	2 db
$10 \log_{10}(2B_{L_O})$	23 db	17.8 db
S/N Margin $\approx \dfrac{1}{2\sigma_N^2} = \dfrac{1}{2(0.35)^2}$	6 db	6 db
Threshold Signal level	-143 dbm	-148.2 dbm
Allowable Margin	+2 dbm	+2 dbm
Input Signal for Specified Operation	-141 dbm	-146.2 dbm

Since the carrier signal level to the PM demodulator is maintained at a constant level, the input noise level to the demodulator increases as the receiver input signal level from the antenna decreases. Although it is convenient to specify the threshold sensitivity of the demodulator phase-lock loop in terms of the rf input carrier signal level, a test of loop threshold performance becomes a difficult task unless an R & RR receiver is available. In the Collins specification the loop threshold is defined as the power spectral density of the noise at the input to the demodulator for which the phase-loop jitter will be equal to or less that 0.35 radians rms. The noise is assumed to be

---

** Parametric amplifier noise figure was given[4] as 1.7 db. Overall system noise figure, however, is considered to be approximately 2.0 db.

[1] GSFC-TDS-RFS-226, Op. cit.

[4] National Aeronautics and Space Administration, Goddard Space Flight Center Greenbelt Maryland "2300-Mc Parametric Amplifier Performance Specification," Specification No. GSFC-553-PAR-1 (No date)

mixed with a steady-state -70 dbm signal. The two values for threshold noise density for the two loop bandwidths were determined as follows:

	100 cps	30 cps
Loop Bandwidth (B_{L_O})	100 cps	30 cps
Input Signal Level (constant)	-70 dbm	-70 dbm
Approximate Noise-to-Signal Ratio for σ_N equal to 0.35 radians rms	6 db	6 db
Noise Power Level for σ_N equal to 0.35 radians rms	-76 dbm	-76 dbm
$10 \log_{10} (2B_{L_O})$	+23 db	+17.6 db
Noise Density Per Cycle of Bandwidth	-99 dbm/cps	-93.6 dbm/cps
Allowable Margin	2 db	2 db
Threshold Noise Density	-101 dbm/cps	-95.6 dbm/cps
$10 \log_{10} (3 \times 10^6 \text{ cps})$	64.8 db	64.8 db
Noise Power in a 3-mc Noise Bandwidth at Threshold	-36.2 dbm	-30.8 dbm

It is shown in section g-8 that 0.35 radians rms phase jitter will result from a loop input signal-to-noise ratio of 6.3 db. This value can be found from the curve in figure g-8-7. The GSFC specification for the parametric amplifiers[4] lists the noise figure of the device as 1.7 db. From these two values, it can be seen that the signal level at threshold, with no allowable margin, is 8 db above the noise power as determined by $k \, T_o \, 2B_{L_O}$. The 8-db value used earlier in this section which was the sum sum of S/N = 6 db and NF = 2 db is, therefore, consistent with the value obtained from the more rigorous analysis.

It is also interesting to note that, for a given signal-to-noise ratio and input signal level to the demodulator, the operating conditions of the demodulator are independent of the noise figure of the preceding system components. To illustrate this fact, the following calculations of noise input to the system were made assuming noise figure of 0, 2, and 10 db, respectively.

---

[4] GSFC-553-PAR-1, Op. cit.

Loop Bandwidth (B_{L_O})	100 cps	100 cps	100 cps
Noise Density Level at 290°K	-174 dbm/cps	-174 dbm/cps	-174 dbm/cps
System Noise Figure	0 db	2 db	10 db
$10 \log_{10} (2B_{L_O})$	23 db	23 db	23 db
Signal-to-Noise Margin	6 db	6 db	6 db
Allowable Margin	2 db	2 db	2 db
Carrier Level for Threshold Operation	-143 dbm	-141 dbm	-133 dbm
Carrier Level to demodulator	-70 dbm	-70 dbm	-70 dbm
Gain required to raise carrier level to -70 dbm	+73 db	+71 db	+63 db
Noise Power at Threshold	-151 dbm	-149 dbm	-141 dbm
Gain value determined above	+73 db	+71 db	+63 db
Noise Power into Demodulator	-78 dbm	-78 dbm	-78 dbm
Spectral Density at input to Demodulator	-101 dbm/cps	-101 dbm/cps	-101 dbm/cps

g-3.3 LOOP OUTPUT LEVEL.

Since the tracking receiver gain in the PM modes is controlled only by the carrier component of the input signal, the signal (voice, telemetry, etc.) level at the output of the demodulator will be a function of both the modulation index used in the vehicle transmitter and the gain of the demodulator. Table g-2-2 summarizes the relative power distribution between the major signal components, including the modulated carrier. For the modulation indices which have been selected for Apollo, the telemetry-to-carrier power ratio (P_{TM}/P_C) is +0.88 db and the voice-to-carrier power ratio (P_V/P_C) is -2.84 db. For these modulation indices, if the output level from the demodulator is adjusted to a 1-volt rms value in accordance with the NASA Specification[1], the telemetry component of the output signal will be 0.83 volts rms and the voice component will be 0.56 volts rms.

---

[1] GSFC-TDS-RFS-226, Op. cit.

The exact agc characteristics of the tracking receiver have not been determined by Collins, but it is assumed that, with no signal suppression because of limiting on noise, the tracking receiver agc action will hold the 10-mc output level to a constant level within ±1 db. Since there is a possibility that the PM demodulator will be used on other projects after Apollo and since it is desirable to provide a 1-volt rms output when only the voice signal is present, it was decided to specify that an output level of 2 volts rms be attainable with a single tone modulating the input carrier at a modulation index of 1 radian rms.

It was assumed that the output carrier level variation between several tracking receivers could be as much as ±5 db and that the phase demodulator must accommodate these variations. Four solutions to this problem have been considered.

One way would be to adjust the output voltage to 2 volts rms with an input carrier level of -75 dbm and let the output voltage increase to 6.3 volts rms with an input carrier level of -65 dbm. This is permissible, provided that the following circuitry (subcarrier discriminators, tape recorder, etc.) can operate properly with this higher voltage impressed at their inputs. When the Collins specifications were written for the demodulator, it was not known whether the follow-up circuits would operate properly with a 6.3-volt rms input, but it was felt that the recorders would not.

Another approach would be to provide a manual gain control on the 10-mc if. amplifier in the demodulator, to be adjusted whenever the demodulator is connected to a different receiver. This approach is permissible, provided the change between receivers is an occasional one. However, if in normal usage the demodulator input is patched often or is switched back and forth between several tracking receivers, the manual gain control would be operationally undesirable.

The third solution to the receiver output variation problem would be to adjust the demodulator for proper operation with an input signal level of -75 dbm and provide individual attenuators on the outputs of all receivers so that receiver output levels can be adjusted to be the same.

The fourth solution is, of course, the use of agc to accommodate all input variations.

The choice of method was left to the equipment manufacturer so that cost and complexity could be minimized. The following restrictions were specified, however:

(1) An output signal level range of 2 to 6.3 volts rms is probably greater than that which is acceptable to the circuits following the PM demodulator.

(2) Each demodulator input must be rapidly patchable to the output of one of three receivers and manual gain control is not permissible.

(3) In the event that agc operation is necessary, a detailed specification for its operational characteristics is given.

It is expected that the third solution (equalizing receiver outputs with attenuator) will be the preferred one because of its simplicity.

g-3.4   FREQUENCY ACQUISITION OF PM CARRIER LOOP.

The GSFC specification requires that the carrier tracking loop be capable of automatically acquiring the signal within 100 milliseconds after the application of a jitter-free, steady-state, phase-coherent signal of threshold level or higher. A tracking range of ±10 cps is also specified. Assuming a maximum frequency offset from all causes (this includes oscillator drift in both the tracking receiver and the PM demodulator) of 10 cps and an optimum second order phase-lock loop with a loop bandwidth of 30 cps, the application of a steady-state, phase-coherent signal, free of any noise or phase jitter, gives an approximate acquisition time (equation g-8-45) of 15.4 milliseconds. It is believed that an 8-db input signal-to-noise ratio is sufficient to insure that the noise will not degrade the 15.4-ms value beyond the specified value of 100 ms.

For a loop bandwidth of 100 cps and all other conditions as above, the calculated acquisition time is 0.42 ms.

Under actual operating conditions, however, the action of the R & RR receiver will affect the acquisition of the carrier by the PM demodulator so that the acquisition time may be much longer than the specified 100 milliseconds. The tracking receiver has approximately the same phase-lock loop bandwidths as the PM demodulator and, during acquisition, both loops will be trying to acquire the carrier component of the signal simultaneously. The 10-mc intermediate frequency into the PM demodulator is determined by the tracking receiver vco (voltage controlled oscillator) and the

frequency of the tracking receiver vco will be varied at some rate during acquisition. The second-order phase-lock loop has, of course, a finite maximum tracking rate. For these reasons, the initial frequency error in the carrier reference loop of the PM demodulator may be several hundred cps when the receiver acquires lock. The resulting acquisition problem is difficult to analyze because of non-linearities but the acquisition time will increase.

The acquisition calculations assume no non-linearities other than those in the loop itself. If the if. amplifier or the phase detectors in the PM demodulator become saturated, the acquisition time estimates must include the recovery time of these components. As indicated in paragraph g-1.4.1.2, the receiver output noise level when the receiver is unlocked will be approximately 0 dbm. It is therefore possible that some of the PM demodulator circuits will be saturated prior to acquisition and the total acquisition time would be increased accordingly.

g-3.5 LOOP BANDWIDTH AS A FUNCTION OF SIGNAL-TO-NOISE RATIO.

As shown in figure g-8-8 and as expressed by equation (g-8-27), the loop noise bandwidth for a second-order loop that uses a limiter is a function of the limiter suppression factor, α . The limiter suppression factor in turn is a function of the input signal-to-noise ratio, ρ , as illustrated in figure g-8-7. Notice that ρ is the signal-to-noise ratio in the loop noise bandwidth.

The threshold noise bandwidths are 60 cps and 200 cps, respectively, and, as specified, they occur at ρ = 4.27 (or 6.3 db). To determine α_0 (the limiter suppression factor for these conditions), it is necessary to determine the signal-to-noise ratio into the limiter . Assuming that the noise bandwidth of the crystal filter preceding it is 3.0 kc, the signal-to-noise power ratio into the limiter at threshold (no margin) is 0.0852 for the 60-cps loop and 0.284 for the 200-cps loop. It can be seen from figure g-8-7 that the limiter suppression factor at threshold is 0.44 for the 200-cps loop. Because figure g-8-7 is difficult to read for ρ = .0852, equation (g-8-21) may be used and α_o for the 60-cps loop is found to be 0.251. These values of limiter suppression factor at threshold may then be used with equation (g-8-27) and figures g-8-7 and g-8-8 to determine the loop noise bandwidth for signal levels above threshold. Figure g-3-2 gives this information for the two threshold loop noise bandwidths.
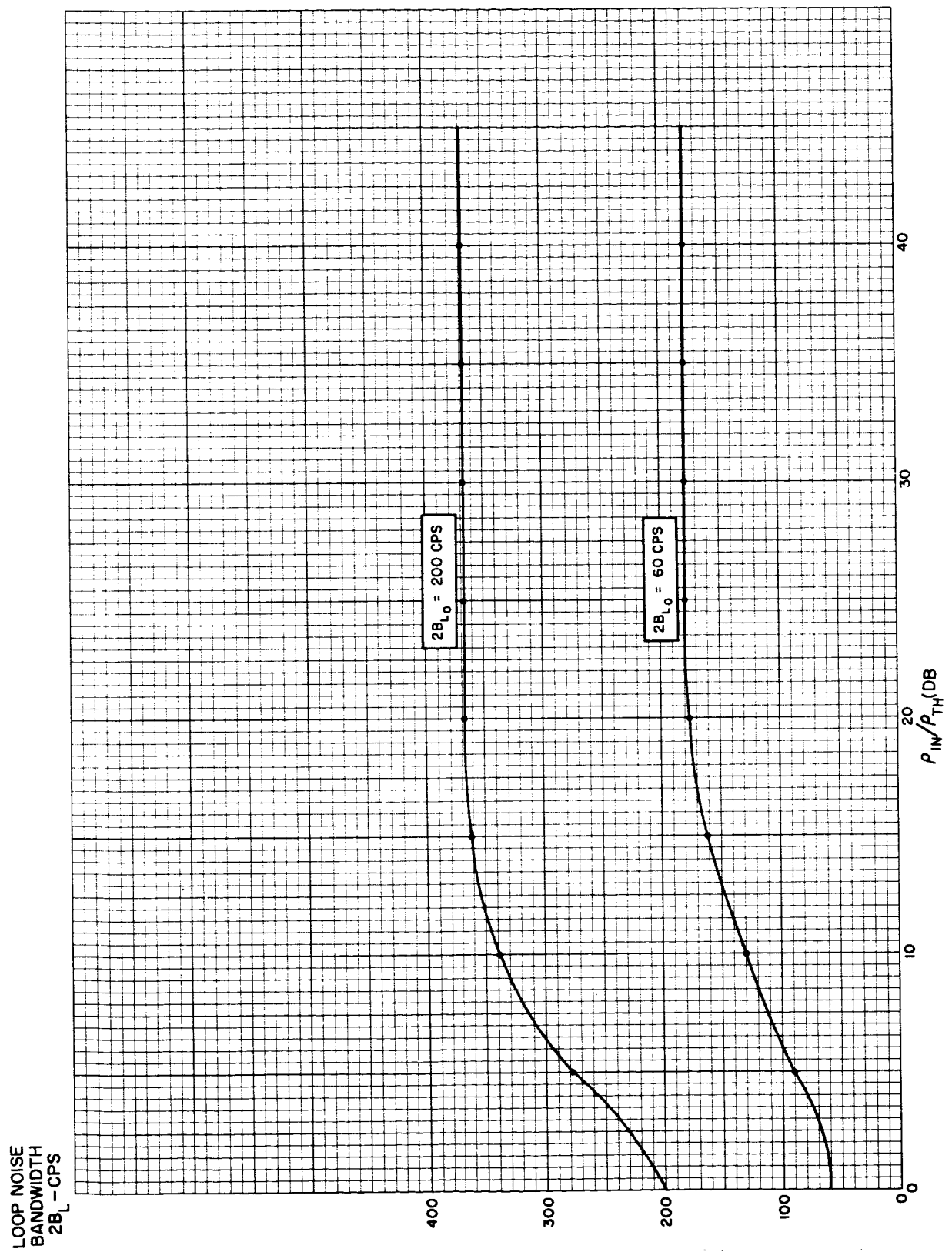
Figure g-3-2. Loop Noise Bandwidth as a Function of
Normalized Input Signal-to-Noise Ratio

g-3.6 STATIC PHASE ERROR DUE TO FREQUENCY OFFSET.

The theoretical static phase error due to a frequency offset (phase ramp) for the approximate second order phase-lock loop is given in equation (g-8-42):

$$\Delta\theta = \frac{360\,\Delta f}{G_1} \quad \text{degrees} \tag{g-3-1}$$

It can be seen that the static phase error can be made arbitrarily small as the open loop gain (G_1) is made arbitrarily large. The maximum frequency offset (Δf) that is to be expected because of drift in the tracking receiver is 4 cps and if, for example, it is desired to limit $\Delta\theta$ to 5° for this frequency offset, G_1 must be equal to or greater than 288. Therefore, if a limiter precedes the phase detector and if a maximum static phase error of 5° is allowed, then equation (g-8-24) can be written as:

$$K_M K_V = \frac{288}{\alpha} \tag{g-3-2}$$

In paragraph g-3.5, it was found that, with a limiter input noise bandwidth of 3 kc, the threshold suppression factor (α_o) is 0.251 for the 60-cps loop and 0.44 for the 200-cps loop. This would require that the product $K_M K_V$ at threshold have the respective values of 1.15×10^3 and 6.50×10^2 for the two threshold loop noise bandwidths.

g-3.7 DISTORTION.

The harmonic distortion which is produced when a sine-wave phase detector is used to demodulate a PM signal will be related to the modulation index of the signal. With a carrier, phase-modulated by a single tone to a peak phase deviation of $\Delta\theta$, the output of the sine-wave phase detector (peak value of output normalized to unity) will be:

$$e_o = \sin(\Delta\theta \sin\omega_m t), \tag{g-3-3}$$

which can be written as:

$$e_o = 2\sum_{\substack{n=1 \\ n\text{ odd}}}^{\infty} J_n(\Delta\theta)\,\sin n\omega_m t \tag{g-3-4}$$

The total harmonic distortion voltage is equal to the square root of the sum of the squares of the odd terms of the expansion of the Bessel function of the first kind or, in equation form:

$$e_d = 2 \sqrt{\sum_{\substack{n=3 \\ n\,odd}}^{\infty} J_n^2 (\Delta\theta)} \qquad\qquad (g\text{-}3\text{-}5)$$

The percent distortion is now expressed as:

$$D = \sqrt{\frac{\displaystyle\sum_{\substack{n=3 \\ n\,odd}}^{\infty} J_n^2 (\Delta\theta)}{J_1(\Delta\theta)}} \times 100 \text{ (percent)} \qquad\qquad (g\text{-}3\text{-}6)$$

A plot of distortion, as determined by this equation, is shown in figure g-3-3.

It can be seen that distortion of no less than 1.5 and 4.5 percent can be expected for phase deviations of 0.6 and 1.0 radians, respectively.

g-3.8   PM EMERGENCY VOICE DEMODULATION.

Several major problems associated with the demodulation of the emergency voice signal were eliminated or at least reduced with the transfer of the signal from the fm carrier to the PM carrier.

The signal acquisition problem of the fm demodulator has been minimized because most of the doppler is removed from the input signal in the range and range rate tracking receiver prior to the input of the PM demodulator. Recognition of the emergency voice signals is simplified because no other signals except ranging are present on the PM baseband. The backup conventional discriminator has been eliminated. All agc problems, including automatic selection of one of several agc detectors, is eliminated because of the coherent agc provided in the R & RR receiver for the PM signal.

The new specification now permits the main PM carrier loop demodulator to demodulate the emergency voice signal in addition to those previously defined.

The emergency voice signals will be in the frequency range of 300 cps to 2.3 kc and will be phase modulated onto the carrier with a peak deviation of 1.25 radians.
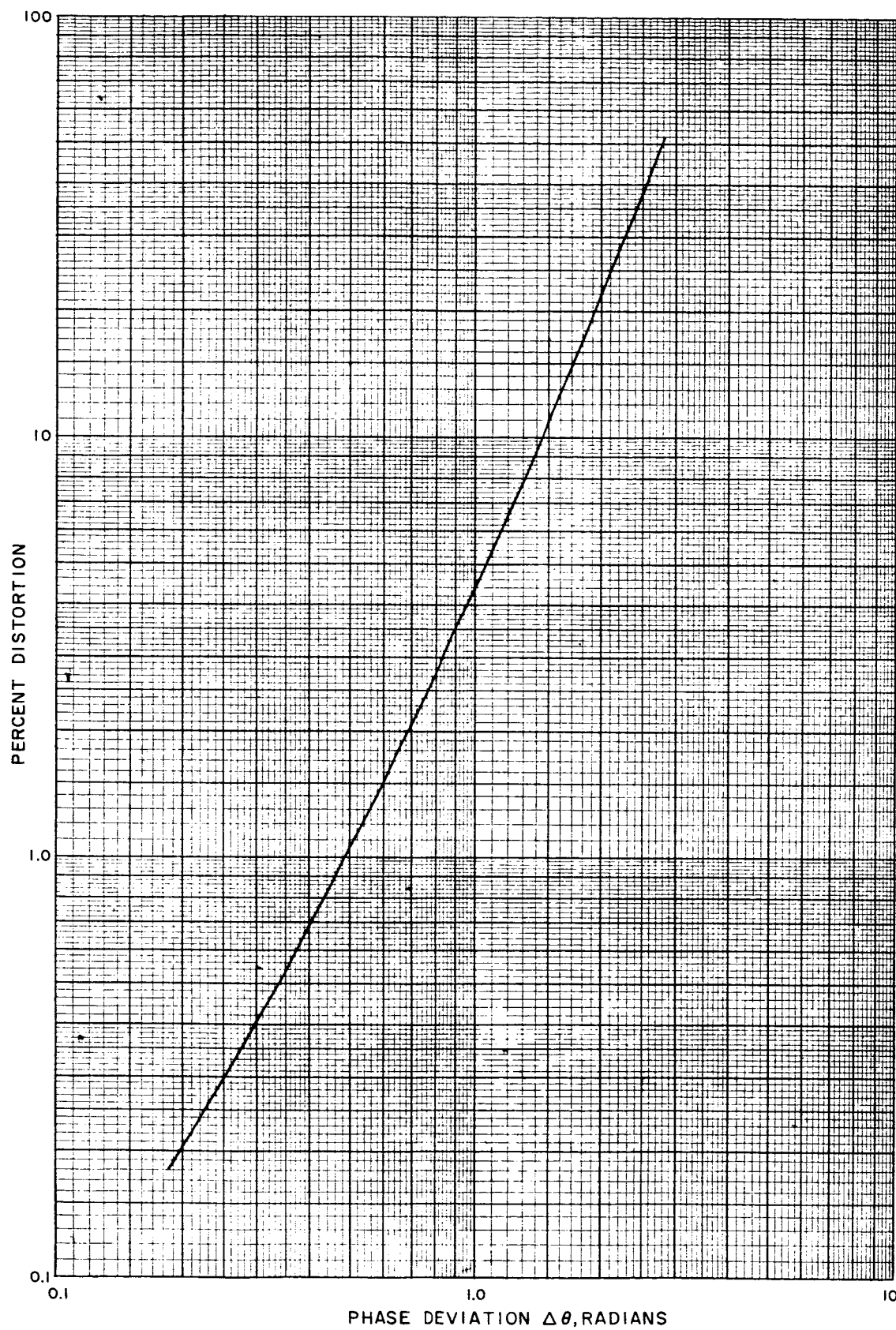
Figure g-3-3. Harmonic Distortion of a Phase Detector with Sine Wave Characteristics

It can be seen from figure g-3-2 that the PM carrier loop will track out the low-frequency components of the emergency voice signal for large input signal-to-noise ratios, if the threshold loop noise bandwidth, $2B_{L_O}$, is 200 cps and the bandpass filter preceding the phase detector is 3 kc. There are several ways to avoid this condition. The first way is to operate in the 60-cps loop position for emergency voice. This however, is not a desirable operational restriction for an emergency function. A second way is to eliminate the limiter so that loop gain (G) would remain constant and consequently the loop bandwidth would not increase with increasing input signal-to-noise ratios. A third way is to precede the phase detector with a bandpass filter which is narrower than 3 kc.

By preceding the phase detector and limiter with such a filter, one can assure that the carrier loop will still satisfy the original requirements plus the added emergency voice requirements. The maximum bandwidth for the filter can be determined by assuming that $2B_{L_O}$ is 200 cps and that $2B_L$ for strong signals is required to be no greater than 300 cps. Since α at strong signals is 1, α_o can be found from equation (g-8-27) to be 0.571. Then, using the curve in figure g-8-7, the signal-to-noise ratio in the filter at threshold (ρ_{f_o}) is found to be 0.52. Then, the filter bandwidth (B_f) is related to $2B_{L_O}$ by:

$$\frac{B_f}{2B_{L_O}} = \frac{\rho_{1_o}}{\rho_{f_o}} \qquad \text{(g-3-7)}$$

And the filter should, therefore, have a bandwidth of approximately 1.64 kc. As shown in figure g-3-1, the output of the wideband phase detector will be filtered for audio use, to remove the higher, unwanted noise components. It has been shown that, in coherent detection systems, post filtering is as effective as bandpass filtering, provided the desired signal has not been removed in the detection process or filtered out.

analysis of carrier fm demodulator

g-4.1 GENERAL.

A block diagram of the carrier fm demodulator is given in figure g-4-1. The circuit receives a 50-mc input from the range and range rate (R & RR) receiver. This signal is amplified and converted to 120 mc for demodulation in the wideband phase lock loop. Six wideband outputs from the phase lock loop are provided for extraction of subcarrier and/or baseband modulating signals. When the loop is locked, coherent agc is provided for the 50-mc signal from the quadrature phase detector. Non-coherent and manual agc are also provided. A loop lock detector automatically transfers from coherent to non-coherent agc when the loop is not locked.

In this section, the phase lock loop bandwidths, the agc gain range, the input and output signal levels, and the input noise levels are calculated.

g-4.2 CARRIER LOOP BANDWIDTH SELECTION.

g-4.2.1 CRITERION FOR OPTIMUM PERFORMANCE.

The criteria used for selection of optimum bandwidths for the carrier fm demodulation loop is that, for a given form of carrier modulation (Apollo mode) and white gaussian noise at the loop input, the loop threshold should occur at the minimum possible total-signal-power-to-noise-spectral-density ratio at the phase detector input. The bandwidths obtained with this criteria are considered to be optimum for the modulation characteristics assumed.
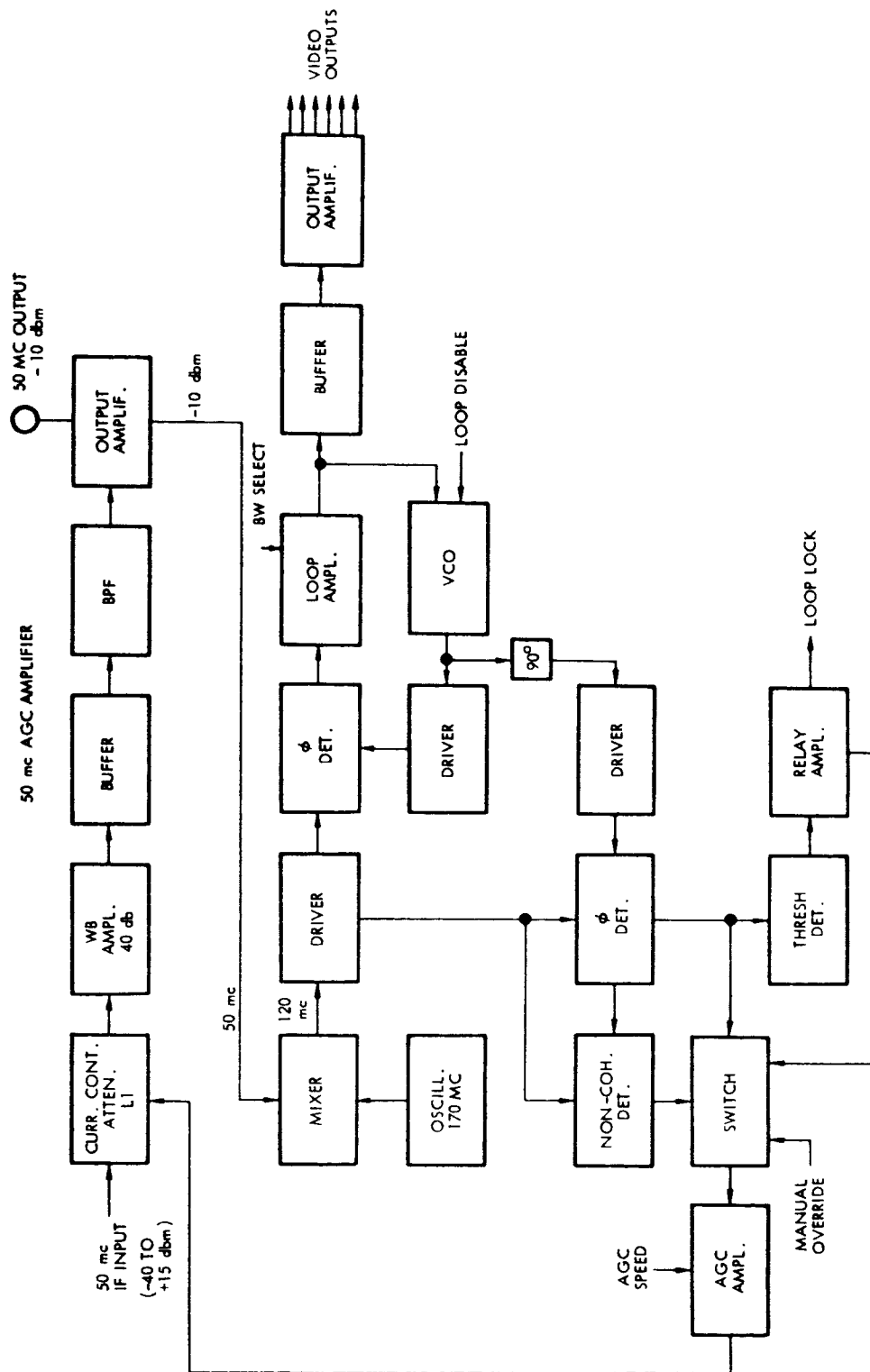
Figure g-4-1.   Carrier Frequency Demodulator

The total peak phase error in the wideband demodulator loop is the sum of the errors due to modulation and noise as follows:

$$\epsilon_T = \epsilon_m + \rho_N \sigma_N \qquad\qquad (g\text{-}4\text{-}1)$$

where:

ϵ_T = total loop peak phase error in radians

ϵ_m = total modulation tracking error in radians

σ_N = rms noise error in radians

ρ_N = weighting factor for noise error

The choice of value for ρ_N depends on the condition of loop error due to noise which will be considered to be acceptable. If $\rho_N = 1$, the allowable loop error due to noise will be equal to the rms noise error. The actual error will exceed this value approximately 16 percent of the time and the use of such a criteria would, therefore, be unacceptable. If $\rho_N = 3$, the loop error due to noise will exceed the allowable amount (three times the rms value) only 0.13 percent of the time, which would be an acceptable condition. These two values are used for comparison in the following section, where an optimum loop bandwidth is chosen for demodulation of the television mode, E.

g-4.2.2   PHASE ERROR ANALYSIS, APOLLO MODE E.

In mode E, the modulation consists of 400-kc bandwidth television at baseband, plus a voice subcarrier and a telemetry subcarrier. Thus the modulation tracking error (ϵ_m) is made up of three terms. Even though the subcarriers are modulated, they will be treated for purposes of simplifying this analysis as pure sine waves. For worst-case design, the three error terms will be added algebraically as follows:

$$\epsilon_m = \epsilon_{TV} + \epsilon_{TM} + \epsilon_V \qquad\qquad (g\text{-}4\text{-}2)$$

It has been shown[5] that the total peak phase error produced by such an FM signal in a phase-locked loop may be expressed as:

$$\epsilon_T = \frac{\dot{\omega}}{\omega_n^2} + \frac{\beta_{TM}}{\sqrt{1 + \left(\frac{\omega_n}{\omega_{TM}}\right)^4}} + \frac{\beta_V}{\sqrt{1 + \left(\frac{\omega_n}{\omega_V}\right)^4}} + 0.729 \, \rho_N \sqrt{\left(\frac{\Phi N}{P_T}\right)} \omega_n \qquad (g\text{-}4\text{-}3)$$

where:

$\beta_{TM, V}$ = FM modulation index of telemetry and voice subcarriers onto carrier

$\omega_{TM, V}$ = telemetry and voice subcarrier frequencies in radians/sec.

ω_n = loop natural frequency in radians/sec

$\dot{\omega}$ = maximum TV frequency ramp, radians/sec^2

The largest value for $\dot{\omega}$ will occur when there is a full black-to-white transition in the picture material. Assuming 70 percent of the peak-to-peak TV voltage is used by the picture and the rest by the synchronization information, it can be seen that:

$$\dot{\omega} = \frac{0.8 \left[0.7 \, (2\pi) \, \Delta f_{TV}\right]}{\tau_r} \qquad (g\text{-}4\text{-}4)$$

where:

Δf_{TV} = peak-to-peak carrier frequency deviation by the TV signal

τ_r = 10-to-90% rise time of a voltage transition in the bandwidth, f_m.

$f_{m_{TV}}$ = maximum modulating frequency of the TV signal.

Since $\tau_r = 0.35/f_{m_{TV}}$,[6] the phase error for the loop due to television with 70% picture is, therefore:

$$\epsilon_{TV} = 10 \Delta f_{TV} f_{m_{TV}} / \omega_n^2$$

[5] Martin, Benn D., "The Pioneer IV Lunar Probe: A Minimum-Power FM/PM System Design," Technical Report No. 32-215, Jet Propulsion Laboratory, Cal.Tech., Pasadena, California, March 1962.

[6] Termin, F.E., "Electronic and Radio Engineering", 4-th Edition, McGraw-Hill Book Company, 1955

The procedure for determining the optimum loop bandwidth is to first define a set of values for ϵ_T and ρ_N which will be considered as threshold conditions and then to determine the value of ω_n for which $\frac{P_T}{\Phi_N}$ is a minimum, using these values. This could be done mathematically, but it was decided to do it graphically, since the sensitivity of minimum $\frac{P_T}{\Phi_N}$ with changes in ω_n is more clearly seen.

Three sets of values for ϵ_T and ρ_N were used for comparison purposes:

$$\epsilon_T = 1, \ \rho_N = 3$$

$$\epsilon_T = 1, \ \rho_N = 1$$

$$\epsilon_T = \pi/2, \rho_N = 3$$

The first two sets represent extreme cases one might consider for defining threshold because $\epsilon_r = 1$ is a very low value for allowable error and $P_N = 1$ is a very noisy loop condition. The third set represents a more reasonable and common choice for determining optimum loop bandwidth. The plots of P_T/Φ_N versus ω_n for these three sets of criteria are shown in figure g-4-2. For $\epsilon_T = 1$, $\rho = 3$, and for $\epsilon_T = 1$, $\rho = 1$, the plots were made assuming 100 percent of the peak-to-peak carrier frequency deviation is used by the TV signal, synchronization being accomplished on the telemetry channel. For $\epsilon_T = \frac{\pi}{2}$ and $\rho = 3$, curves are shown for both 70 and 100 percent use of the peak-to-peak carrier frequency deviation by the TV signal. The other parameters of equation (g-4-3) were obtained from section g-1 as $\Delta f_{TV} = 2$ mc, $\beta_{TM} = 0.341$, $\beta_V = 0.320$, $f_V = 1.25$ mc, and $f_{TM} = 1.024$ mc.

Using the curve for $\epsilon_T = \frac{\pi}{2}$, $\rho = 3$ in figure g-4-2, it can be seen that the loop natural frequency that results in a minimum required P_T/Φ_N is 12×10^6 radians for the case where 70 percent of the TV voltage is used for picture information and 11×10^6 radians for the case where 100 percent of the TV voltage is used for the picture information. These correspond (using equation (g-8-10)) to loop bandwidths of 12.7 and 11.6 mc, respectively. It can be seen that, for the 70 percent case, the threshold is within 0.4 db of the minimum value over the natural frequency range of 10 mc
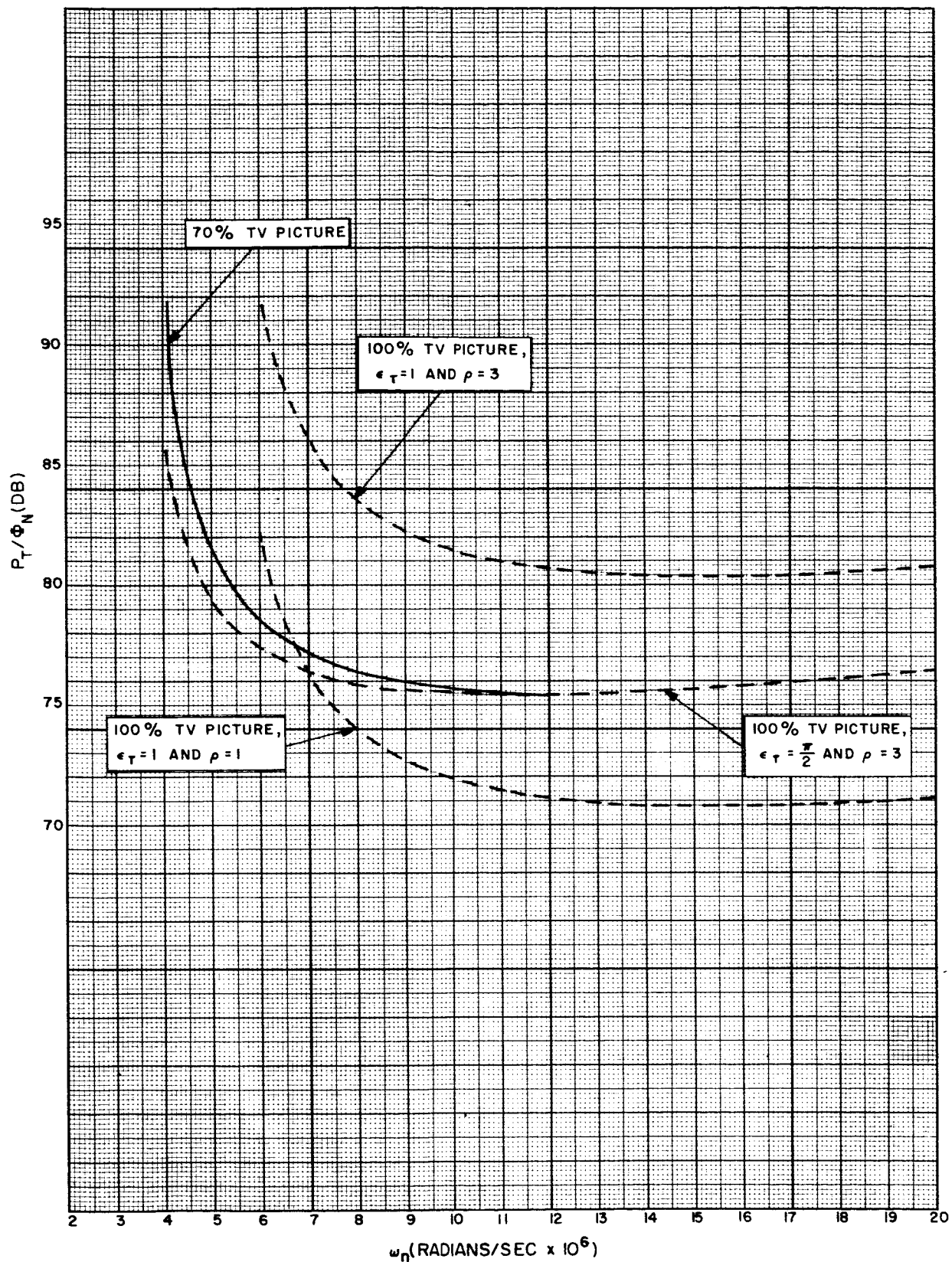
Figure g-4-2. Threshold as a Function of Loop Natural Frequency for Carrier Frequency Demodulator, Mode E

to 17 mc, while the same range for the 100-percent case is 8.5 mc to 17 mc. The passband preceding the demodulator is only 10 mc and it was felt that the percentage of TV voltage used for the picture would be between 70 and 100 percent. For these reasons, a compromise value of 11 mc for the loop bandwidth was selected.

g-4.2.3 PHASE ERROR ANALYSIS, APOLLO MODE D-1.

In mode D-1, the modulation as described in GSFC-TDS-RF-226 consists of the voice subcarrier, the telemetry subcarrier and nine analog channel subcarriers. As noted in paragraph g-2.3, this mode has been deleted from the Apollo transmission modes. However, an analysis is included here as being representative of other uses of the carrier fm demodulator. Here again, the subcarriers will be treated as pure sine waves. The total peak phase error in the loop will be[5].

$$\epsilon_T = \frac{\beta_V}{\sqrt{1 + \left(\frac{\omega_n}{\omega_V}\right)^4}} + \frac{\beta_{TM}}{\sqrt{1 + \left(\frac{\omega_n}{\omega_V}\right)^4}} + \sum_{n=1}^{9} \beta_{SC_m} \bigg/ \sqrt{1 + \left(\frac{\omega_n}{\omega_m}\right)^4}$$

$$+ \; 0.729 \; \rho_N \left[\Phi_N / P_T \right]^{1/2} \; \omega_n^{1/2} \qquad\qquad \text{(g-4-5)}$$

where:

β_{SC_m} = FM modulation index of mth subcarrier onto carrier,

ω_m = m^{th} subcarrier frequency in radians/sec, and the other quantities are as previously defined.

Using the same procedure as described above for Mode E and taking $\epsilon_T = \frac{\pi}{2}$ and $\rho = 3$, a curve of P_T / Φ_N vs. ω_n may be plotted. Parameter values for equation (g-4-5) were taken from tables g-1-1 and g-1-2. The resulting curve is shown in figure g-4-3. As can be seen from the figure, P_T / Φ_N is rather insensitive to ω_n beyond about 4×10^6 radians/sec. The two-sided loop noise bandwidth is $1.06 \, \omega_n$ and was chosen as 4 mc. This value is used as an alteranate bandwidth for the carrier fm demodulator.

---

[5] Martin, Op. cit.
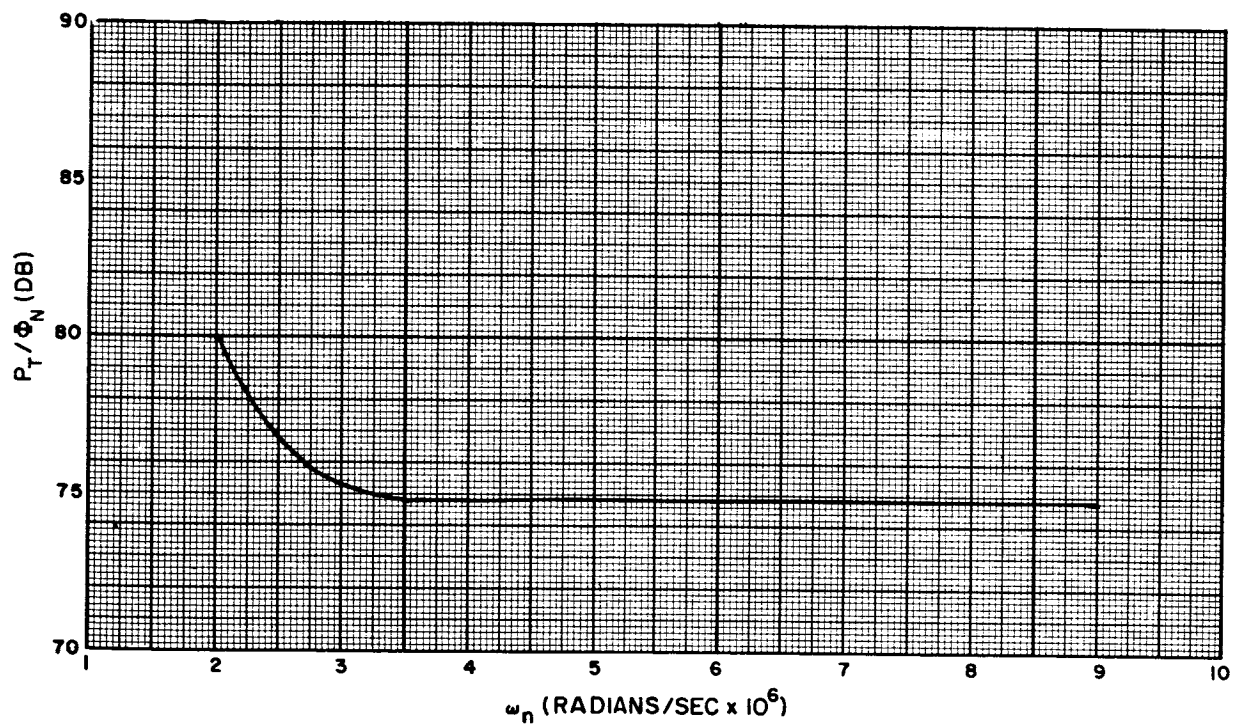
Figure g-4-3.   Threshold Level as a Function of ω_n for
Carrier Frequency Demodulator, Mode D-1

To facilitate the calculation involved in equation (g-4-5), the curves of figures g-4-4 and g-4-5 were plotted. These curves show the relationship between $K_2 = \omega_n/\omega_m$ and $1/\sqrt{1 + K_2^4}$. $\Delta\omega/\omega_m$ is equivalent to the β_{SC_m} of equation (g-4-5) and $\Delta\phi_{ss_{max}}$ is the error contribution by the particular subcarrier under consideration.

g-4.3 GAIN RANGE FOR CARRIER FM AGC SYSTEM.

The gain range for the carrier fm agc system must exceed the range of the input signal level from the R & RR receiver. The lower limit of this range can be calculated by determining the minimum acceptable signal level for modes E and D-1 for the loop bandwidths determined above. This input level may be found as follows:

Receiver input noise spectral density	-174 dbm
Noise figure [1]	2 db
Receiver gain [1]	65 db
Demodulator noise power spectral density	-107 dbm

Mode E:

Loop noise bandwidth (11×10^6)	70.4 db
Noise Power	-36.6 dbm
Required signal power to noise spectral density in 11 mc at threshold (figure g-4-2)	75.7 db/cps
Required signal-to-noise ratio in 11 mc	5.3 db
Signal Power out of range and range rate receiver at threshold	-31.3 dbm

---

[1] GSFC-TDS-RFS-226, Op. cit.

$$\Delta\Phi_{SSMAX}\Big/\frac{\Delta\omega}{\omega_m} = \frac{1}{\sqrt{1+K_2^4}}$$

$$\text{WHERE: } K_2 = \frac{\omega_n}{\omega_m}$$
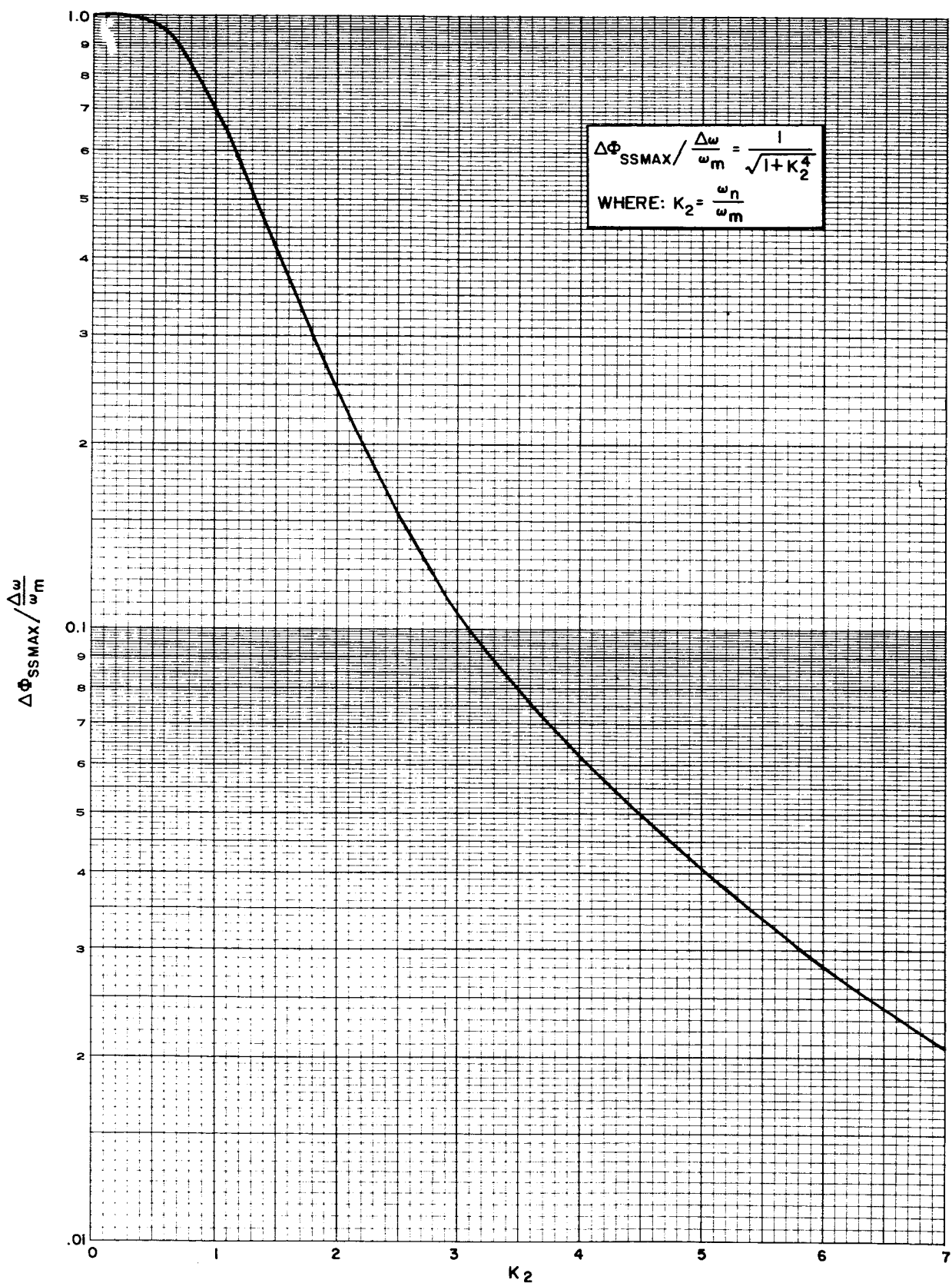
Figure g–4–4.   Ancillary Curve to Aid in Calculation of Loop Tracking Error Assigned to Mode D–1 Signal Components, Expanded Lower Range of K_2

$$\Delta\Phi_{SS\,MAX}\Big/\frac{\Delta\omega}{\omega_m} = \frac{1}{\sqrt{1+K_2^4}}$$

$$\text{WHERE: } K_2 = \frac{\omega_n}{\omega_m}$$
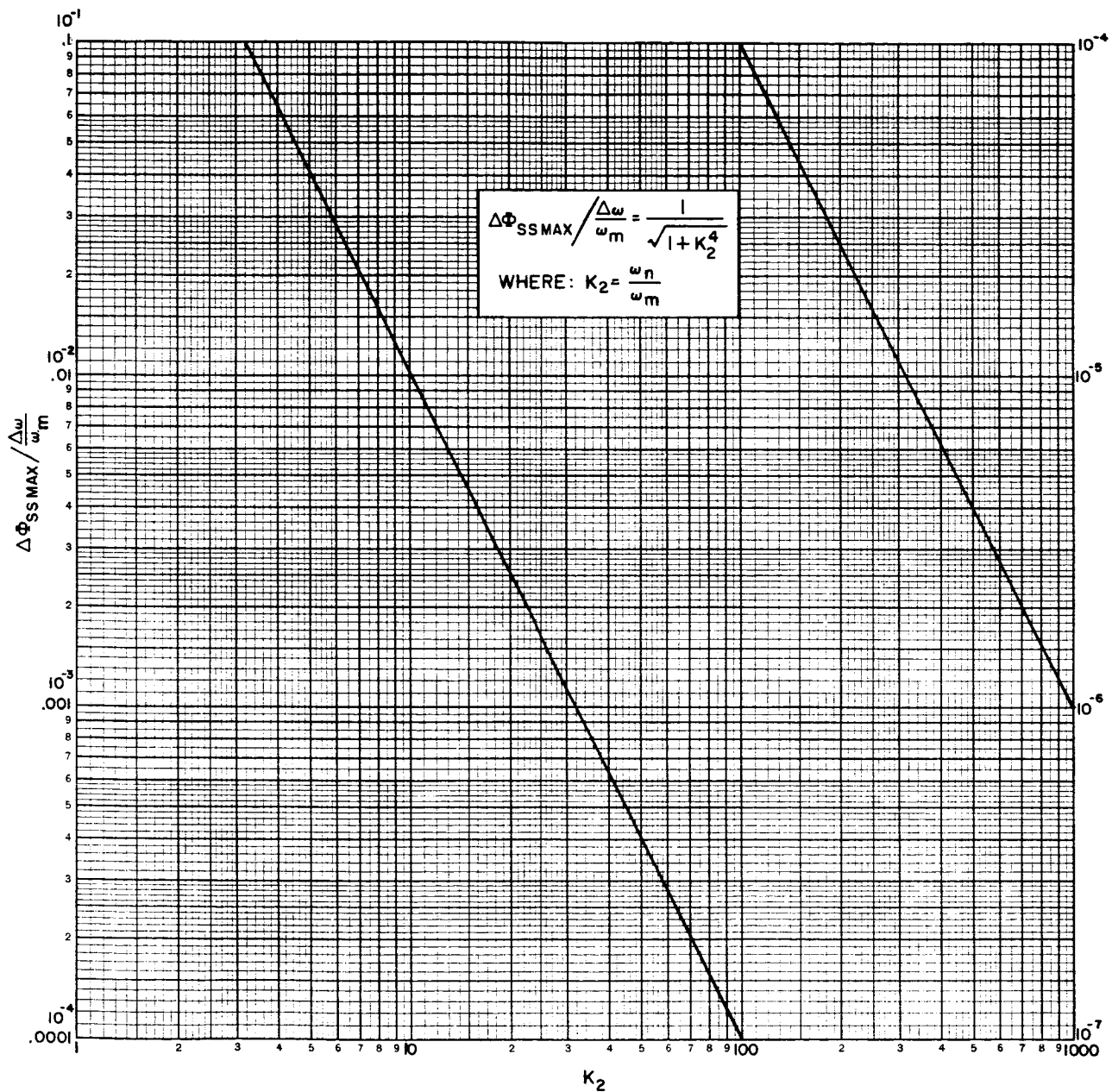
Figure g-4-5.   Ancillary Curve to Aid in Calculation of Loop Tracking Error Assigned
to Mode D-1 Signal Components, Extended Range of K_2

g-4-11

<u>Mode D-1</u>:

Loop noise bandwidth (4×10^6)	66 db
Noise Power	-41 dbm
Required signal power to noise spectral density in 4 mc at threshold (figure g-4-3)	74.8 db/cps
Required signal-to-noise ratio in 4 mc	8.8 db
Signal power out of range and range rate receiver at threshold	-32.2 dbm

The maximum signal level to be expected from the R & RR receiver may be determined from fixed receiver gain as follows:

Maximum receiver input[1]	-50 dbm
Receiver gain[1]	65 db
Maximum input signal level	+15 dbm

There is an indication that the receiver output may limit at approximately 0 dbm (see section g-10), but +15 dbm will be considered to be the maximum output for this analysis. From the above calculations, the lowest usable signal level is -32.2 dbm and, with a maximum signal level of +15 dbm the range of signal level over which the agc system must operate becomes: 15 + 32.2 = 47.2 dbm.

g-4.4 AGC LOOP TIME CONSTANTS.

The agc loop transfer function may be written as a function of agc loop gain, G,[7]:

$$H(s) = \frac{G \, F(s)}{1 + G \, F(s)} \qquad \text{(g-4-6)}$$

F (s) is the filter transfer function for a simple low-pass filter, with the form:

$$F(s) = \frac{1}{1 + \tau s} \qquad \text{(g-4-7)}$$

---

[1] GSFC-TDS-RFS-226, Op. cit.

[7] Brockman, M. and Victor, W., "The Application of Linear Servo Theory to the Design of AGC Loops," JPL External Publication No. 586, 22 December 1958.

Substituting equation (g-4-7) into equation (g-4-6),

$$H(s) = \frac{G/\tau}{s + \frac{1}{\tau}(1 + G)}$$ (g-4-8)

For a step input in voltage of magnitude 1, the Laplace transform of the output will be:

$$O(s) = \frac{G}{1 + G}\left[\frac{1}{s} - \frac{1}{s + g}\right]$$ (g-4-9)

Where:

$$g = \frac{1}{\tau}(1 + G)$$ (g-4-10)

The signal level to the demodulation circuits will, therefore, be:

$$P_S(t) = \frac{G}{1 + G}\left\{u(t) - e^{-gt}\right\}$$ (g-4-11)

The agc speeds are specified[1] as rise times (τ_o) or the time for $P_S(t)$ to reach 90 percent of $\frac{G}{1 + G}$. Thus the required value of g is given by:

$$g = -\frac{1}{\tau_o} \ln 0.1 = \frac{2.3}{\tau_o}$$ (g-4-12)

from equations (g-4-10) and g-4-12):

$$\tau = \frac{\tau_o(1 + G)}{2.3}$$ (g-4-13)

From equation (g-4-13), τ is plotted in figure g-4-6, as a function of G, for the four specified loop rise times.

g-4.5 DEMODULATOR OUTPUT SIGNAL LEVELS.

An output signal level of 1 volt rms is desired for recording purposes. Using equation (g-2-12), the power of the telemetry and voice subcarrier for mode D-2 modulation (see table g-1-1) is found to be:

$$P_{TM} = \frac{\beta_{TM}^2}{2} P_T = 0.058 P_T$$ (g-4-14)

[1] GSFC-TDS-RFS-266, Op. cit.
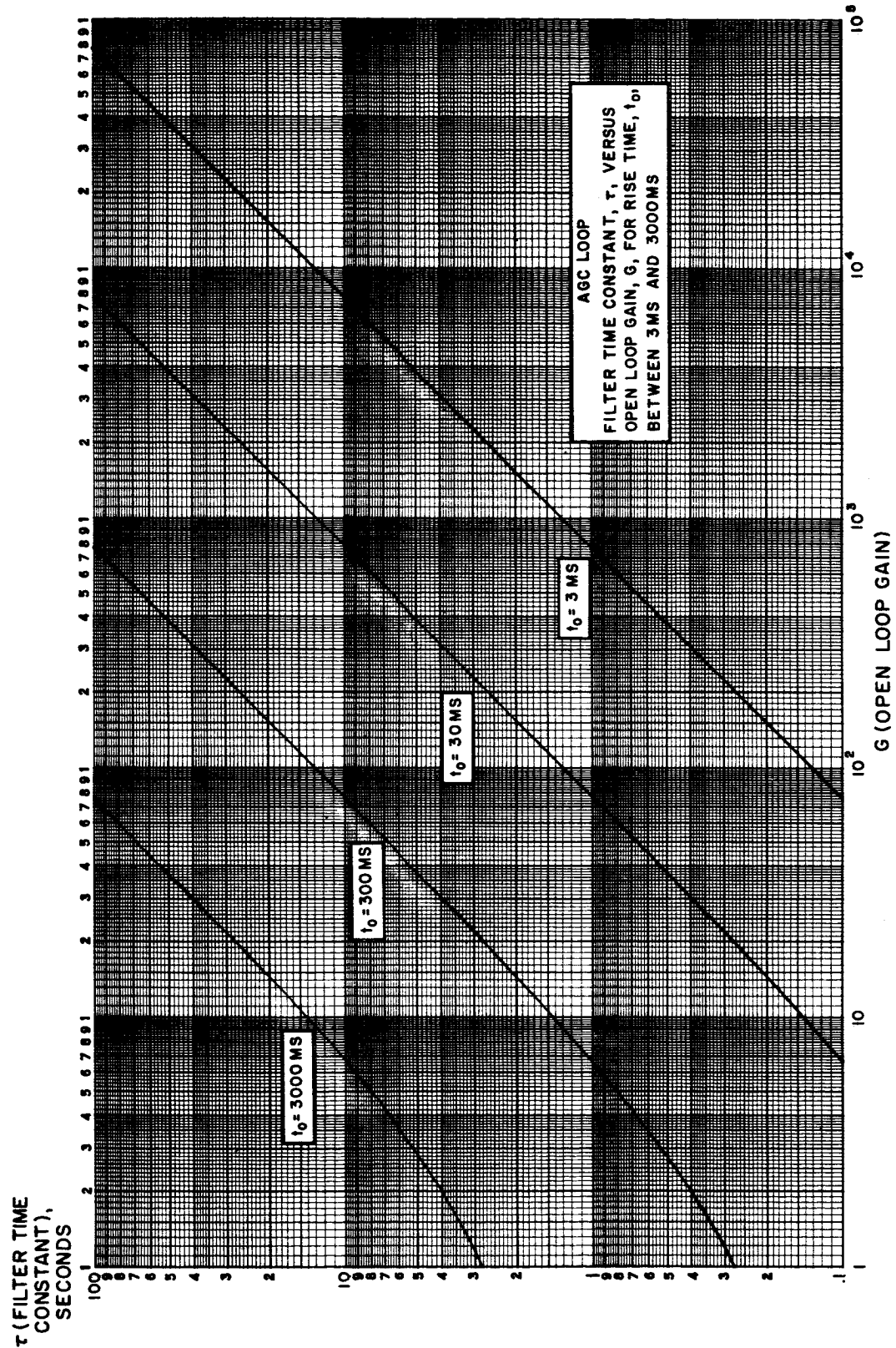
Figure g-4-6. AGC Loop Filter Time Constant, τ, versus Open Loop
Gain, G, for Rise Time, t_o, Between 3 ms and 3000 ms

$$P_V = \frac{\beta_V^2}{2} P_T = 0.0512 \, P_T \qquad \text{(g-4-15)}$$

Since the output levels are, therefore, approximately the same, 1-volt rms total output will yield about 0.7 volt rms per channel.

g-4.6 INTERMODULATION DISTORTION.

For mode E operation, the peak-to-peak amplitude of the difference frequency (226 kc) between the two subcarriers which appears in the baseband should be about 60 db below the peak-to-peak video picture signal. To determine if this is a reliazable value, the maximum allowable distortion for such a condition will be found. This is a second-order distortion product and will have two primary causes: a quadratic voltage characteristic in the baseband amplifier or vco and a linear delay characteristic in the if. amplifier. For analysis, 67 percent of the allowable distortion will be assigned to the first cause and the remaining 33 percent to the second cause. Noiseless input signals will be assumed.

The voltage nonlinearity may be written in terms of frequency deviation as:

$$e_o = b_1 \, (\Delta f) + b_2 \, (\Delta f)^2 \qquad \text{(g-4-16)}$$

From table g-1-1, Δf for television will be $\pm 1 \times 10^6$ cps, and the peak output voltage for television will be:

$$e_{TV} = b_1 \, (10^6) \qquad \text{(g-4-17)}$$

The distortion component at 226 kc will be:

$$e_d = b_2 \, (\beta_V f_V) \, (\beta_{TM} f_{TM}) \, \sin (\omega_V - \omega_{TM}) \qquad \text{(g-4-18)}$$

or a peak distortion of:

$$e_{dp} = b_2 \, (1.4 \times 10^{11})$$

Since the distortion power due to this cause must be 67 percent of $P_{TV} \times 10^{-6}$:

$$\frac{e_{TV}}{e_{dp}} = \frac{10^3}{\sqrt{.67}} = \frac{b_1 \, (10^6)}{b_2 \, (1.4 \times 10^{11})} \qquad \text{(g-4-19)}$$

and therefore:

$$\frac{b_1}{b_2} \geq 171 \times 10^6 \qquad \text{(g-4-20)}$$

In mode E, the peak deviation is 1.75 mc. If the total nonlinearity is assumed to be second-order, the percent linearity must be:

$$\% \text{ linearity } = \frac{b_2 \left(1.75 \times 10^6\right)^2}{b_1 \left(1.75 \times 10^6\right)} \times 100 \qquad \text{(g-4-21)}$$

$$= 1.0\%,$$

which the manufacturer indicates is realizable.

The distortion due to linear delay, or parabolic phase, can be expressed as[8]:

$$e_d = 2 k_d d \, V(t) \, \dot{V}(t) \qquad \text{(g-4-22)}$$

where:

d = second-order coefficient in expansion of the phase nonlinearity

$k_d V(t) = \Delta f(t)$ = instantaneous frequency deviation of the if. signal (r/s)

k_d = discriminator constant $\left(\dfrac{r/s}{volt}\right)$

In mode E, the instantaneous deviation due to the voice and telemetry subcarrier is:

$$\Delta f(t) = \beta_V \omega_V \sin \omega_V t + \beta_{TM} \omega_{TM} \sin \omega_{TM} t \qquad \text{(g-4-23)}$$

and, from equation (g-4-22), the portion of e_d at the difference frequency is:

$$e_d = \frac{d}{k_d} \beta_V \beta_{TM} \omega_V \omega_{TM} (\omega_{TM} - \omega_V) \sin (\omega_{TM} - \omega_V) t \qquad \text{(g-4-24)}$$

If the peak-to-peak television output signal is to be 1 volt, then

$$k_d = 2 \beta_{TV} \omega_{TV} \qquad \text{(g-4-25)}$$

$$= 12.57 \times 10^6 \left(\frac{r/s}{volt}\right)$$

---

[8] Members of Technical Staff of BTL, Transmission Systems for Communications, Vol. II., BTL, 463 West St., New York, N.Y., Section 22.

Since the distortion power due to this cause must be 33 percent of P_{TV} x 10^{-6}, and the television signal is 1 volt, the peak distortion voltage allowable is (see equation (g-4-19):

$$e_{dp} = \sqrt{.33} \times 10^{-3} \qquad \text{(g-4-26)}$$

and from equation (g-4-16)

$$e_{dp} = \frac{2 d \beta_V \beta_{TM} \omega_V \omega_{TM} (\omega_{TM} - \omega_V)}{2 \beta_{TV} \omega_{TV}} \qquad \text{(g-4-27)}$$

and

$$d = 4.61 \times 10^{-16} \qquad \text{(g-4-28)}$$

The relationship between linear delay in a bandpass channel (T_D) and phase deviation across the band is given[8] as:

$$T_D = 2d \, \omega_C \qquad \text{(g-4-29)}$$

For a carrier frequency of 50 mc, the allowable linear delay is:

$$T_D = 0.29 \text{ usec,} \qquad \text{(g-4-30)}$$

which is considered to be a reasonable requirement.

---

[8]
Members of Technical Staff of BTL, Op. Cit.

analysis of the am key demodulator

g-5.1 GENERAL.

The AM key demodulator is required to accept a 512-kc subcarrier which is keyed by a Morse-code signal (100 percent AM, on-off) from the PM carrier demodulator. Two types of output are required: a 1-kc tone, derived by hetrodyning a crystal oscillator signal with the input signal; and a dc signal, resulting from rectification of the 1-kc tone. The bandpass and lowpass filters were selected for optimum detection of the tone by human ear and for best compromise between S/N ratio and square-wave response for the dc signal. The uncertainty of the 512-kc subcarrier frequency is specified as ± 25 cps, due to all causes. A block diagram is given in figure g-5-1.

g-5.2 RELATIVE POWER OF THE SIGNAL COMPONENTS.

g-5.2.1 CARRIER POWER.

The AM key signal at the input to the carrier phase demodulator will have the form:

$$v(t) = A_C \sin \left[\omega_C t + \theta(t) \sin \omega_1 t \right] \qquad \text{(g-5-1)}$$

where A_C = peak amplitude, volts

ω_C = carrier angular frequency, radians per second (2π x 10 mc)

ω_1 = modulating angular frequency, radians per second (2π x 512 kc)

$\theta(t)$ = peak phase modulation index, two levels:

OFF (no information): 0.0

ON (Morse code type of keying): 1.25
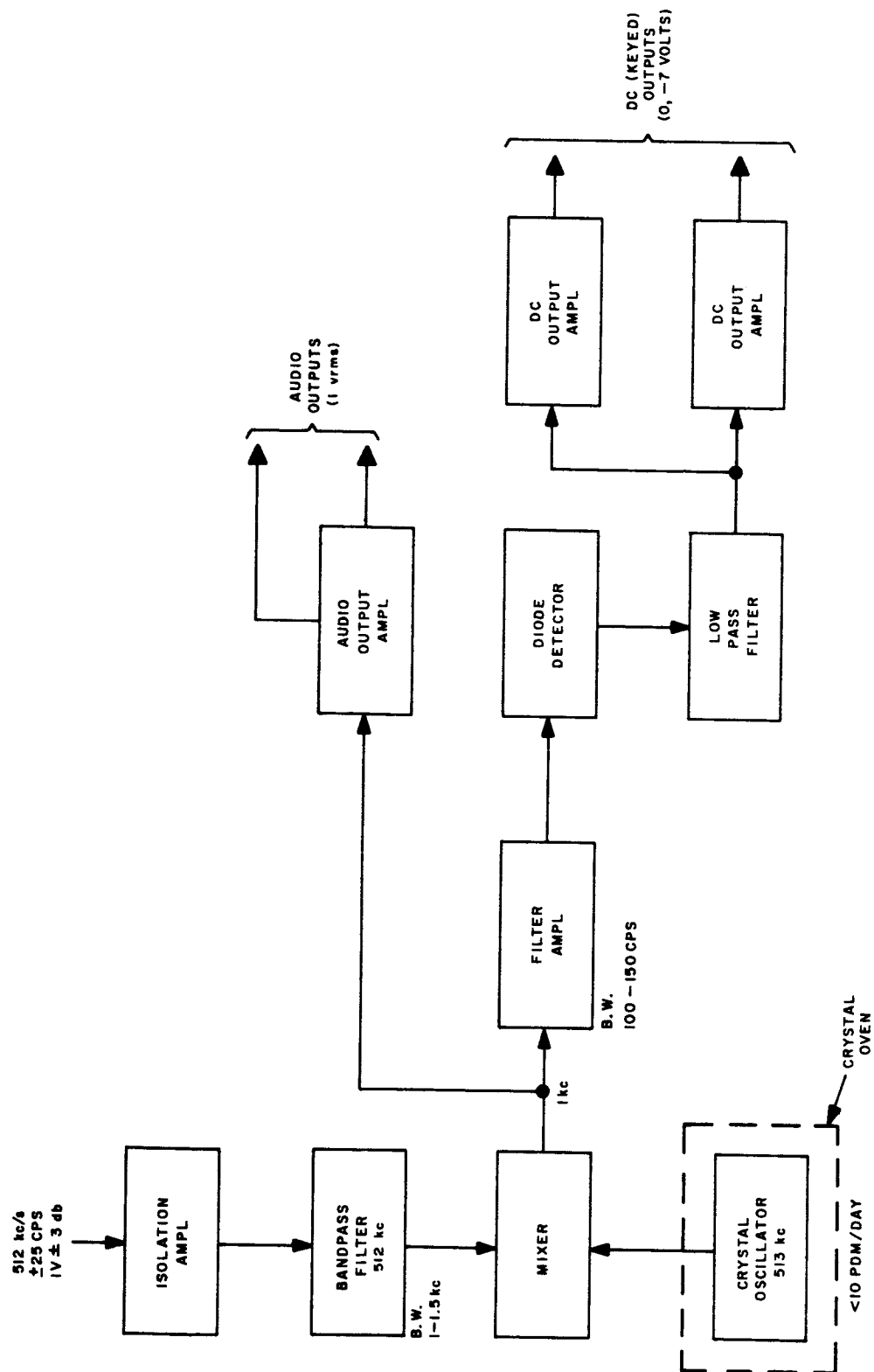
Figure g-5-1. AM Key Demodulator

When the subcarrier is off, equation (g-5-1) becomes:

$$v(t) = A_C \sin \omega_C t \qquad \text{(g-5-2)}$$

And total signal power becomes

$$P_T = \frac{A_C^2}{2} \qquad \text{(g-5-3)}$$

When the subcarrier is on, equation (g-5-1) becomes:

$$v(t) = A_C \left[\sin (\omega_C t + 1.25 \sin \omega_1 t) \right] \qquad \text{(g-5-4)}$$

or

$$v(t) = A \left[\sin \omega_C t \cos (1.25 \sin \omega_1 t) + \cos \omega_C t \sin (1.25 \sin \omega_1 t) \right] \qquad \text{(g-5-5)}$$

After substitution of Bessel function identities, v(t) becomes:

$$v(t) = A_C \left\{ (\sin \omega_C t) \left[J_0(1.25) + 2 \sum_{n=1}^{\infty} J_{2n}(1.25) \cos 2n\omega_1 t \right] \right.$$

$$\left. + (\cos \omega_C t) \left[2 \sum_{n=1}^{\infty} J_{2n-1}(1.25) \sin(2n-1)\omega_1 t \right] \right\} \qquad \text{(g-5-6)}$$

The voltage component at ω_C is, therefore:

$$v_C(t) = A_C \left[J_0(1.25) \sin \omega_C t \right] \qquad \text{(g-5-7)}$$

and the carrier power is

$$P_C = \frac{A_C^2}{2} J_0^2(1.25) \qquad \text{(g-5-8)}$$

From equation (g-5-3) and equation (g-5-8), the percentage of carrier power in the signal, with the subcarrier on, is:

$$\frac{P_C}{P_T} = J_0^2(1.25) = 0.471$$

or

$$P_C (db) = P_T(db) - 3.80 \qquad \text{(g-5-9)}$$

g-5.2.2 SUBCARRIER POWER.

From equation (g-5-5), the subcarrier component of the input signal is:

$$v_{SC}(t) = A_C \left\{ \cos\omega_C t \left[2 J_1(1.25)\sin\omega_1 t \right] \right\} \tag{g-5-10}$$

and

$$v_{SC}(t) = A_C J_1(1.25) \left[\sin(\omega_C + \omega_1)t - \sin(\omega_C - \omega_1)t \right] \tag{g-5-11}$$

The input modulating signal power to the PM carrier demodulator is, therefore:

$$P_{SC} = \frac{A_C^2}{2} J_1^2 (1.25) \tag{g-5-12}$$

From equation (g-5-3) and equation (g-5-12), the percentage of subcarrier power in the signal is:

$$\frac{P_{SC}}{P_T} = J_1^2 (1.25) = 0.260$$

or

$$P_{SC}(db) = P_T(db) - 2.84 \text{ db} \tag{g-5-13}$$

g-5.3 AM KEY DEMODULATOR PERFORMANCE.

g-5.3.1 THE HUMAN OPERATOR AS A DETECTOR.

It will be noted in figure g-5-1 that, after the mixer, no further bandpass filtering is applied to the tone which is to be monitored by ear.

Tests conducted by Craiglow [9] indicate that a trained operator, using isolated words, has a 98 percent word intelligibility measurement for a signal-to-noise ratio of minus 3 db in a 1-kc audio bandwidth, at a transmission rate of five words per minute. For a signal-to-noise ratio of -6 db and all other factors the same as above, word intelligibility was found to be 50 percent. The tests indicate that the human listener

---

(9) Craiglow, R. "Required S/N Ratio for CW Communications on Project Apollo," Collins Radio Company, Cedar Rapids Internal Memo, 19 December 1962.

has a bandwidth of from 50 cps to 100 cps and that threshold is not improved by narrow-band filtering prior to presentation. For this reason, narrow band filtering after conversion will not be used.

From the above information, an S/N of -3 db must be present in one sideband of the converted signal, with a bandwidth of 1 kc, for 98 percent intelligibility:

$$\left. P_{SC} \middle/ P_N \right|_{1kc} = -3.0 \text{ db} \tag{g-5-14}$$

from equations (g-5-9) and (g-5-13):

$$P_{SC}(db) - P_C(db) = 0.96 \text{ db} \tag{g-5-15}$$

From equations (g-5-14) and (g-5-15):

$$\left. \frac{P_C}{P_N} \right|_{1 \text{ kc}} (db) = -3.96 \text{ db,} \tag{g-5-16}$$

and since $10 \log \left(\dfrac{1 \text{ kc}}{60 \text{ cps}} \right) = 12.2,$

$$\tag{g-5-17}$$

The S/N required in the carrier loop bandwidth of 60 cps, for 98 percent intelligibility, will be:

$$\left. \frac{P_C}{P_N} \right|_{60 \text{ cps}} (db) = 8.24 \text{ db.} \tag{g-5-18}$$

In section g-8, it is shown that an S/N in the carrier phase demodulator loop of 6.3 db is required at threshold. When the 60-cps loop is being used, a trained operator will have approximately 98 percent intelligibility for an input S/N 1.94 db above this threshold, and better than 50 percent intelligibility at threshold.

g-5.3.2 SQUARE LAW DETECTOR.

Performance of the square law detector for the AM key signal depends primarily on the S/N in the bandwidth of the post-conversion filter, centered at 1 kc. Bandwidth of this filter depends on the required envelope response for step changes in the amplitude of the 1-kc input signal and on the frequency shift which may be expected from doppler and oscillator drift (±25 cps), of the 1-kc signal.

The pulse length of the shortest signaling element for American Morse code at 50 words per minute is 20 ms [10]. For a single-pole bandpass filter with a Q greater than 10, the envelope of the output signal after application of a unity-amplitude sine wave to the input at t = 0 is approximately [10]:

$$\text{Envelope} = 1 - e^{-\frac{\omega_n t}{2Q}} \qquad \text{(g-5-19)}$$

where ω_n is the natural center frequency of the bandpass filter and the frequency of the input excitation signal.

It will be assumed that, for satisfactory operation, the envelope of the filtered signal during application of the shortest signaling element must reach at least 90 percent of the steady state value. For this condition, it can be seen from equation (g-5-19) that:

$$\frac{\omega_n t}{2Q_{max}} = 2.3 \qquad \text{(g-5-20)}$$

And for f_n = 1kc,

$$Q_{max} = 1368t, \qquad \text{(g-5-21)}$$

and for the signal described above:

$$Q_{max} = 27.4 \qquad \text{(g-5-22)}$$

---

[10]   International Telephone and Telegraph Corporation, Reference Data for Radio Engineers, Stratford Press, Inc. 1957.

The minimum filter bandwidth for the 1-kc filter is, therefore:

$$f_{(3\ db\ BW)} = \frac{f_n}{Q_{max}} = 36.5\ cps. \tag{g-5-23}$$

This bandwidth is not sufficient to handle the ± 25 cps offset frequency which may exist. A bandwidth of 100 cps will be selected to accound for all frequency uncertainties. The wider bandwidth will improve envelope response time and will not deteriorate the S/N to the square-law detector an appreciable amount.

Davenport and Root [11] provide a detailed analysis of a full-wave square-law detector for which the output S/N, as a function of the input S/N, is:

$$\frac{S}{N}\bigg|_o = K_p \frac{(S/N)_{in}^2}{1 + 2\ (S/N)_{in}} \tag{g-5-24}$$

where

$$K_p = \frac{E\ (P^4)}{E^2\ (P^2)}. \tag{g-5-25}$$

$E(P^N)$ is the Nth moment of the modulating function (P). The modulating function for the AM key will be assumed to be as shown in figure g-5-2, with "on" amplitude of one, "off" amplitude of zero, and equal division of average time between the two states. The Nth moment is defined [11] as:

$$E(P^N) = \int_{-\infty}^{\infty} P^N p\ '(P)\ dP \tag{g-5-26}$$

$$P(t)$$
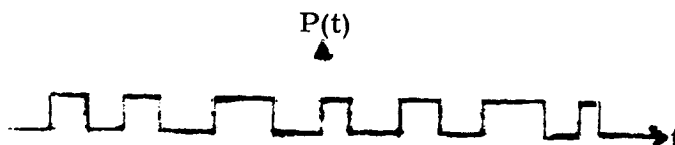
Figure g-5-2.   Assumed Modulating Signal for the AM Key Subcarrier

(11)   Davenport, W.B. and Root, W.L., Random Signals and Noise, McGraw-Hill Book Company, 1958.

where ʋ (P) is the probability density of P, which can be seen in figure g-5-2 to be:

$$(p) = \frac{1}{2} \delta \ (o) + \frac{1}{2} \delta \ (1) \qquad \text{(g-5-27)}$$

This distribution is shown in Figure g-5-3.
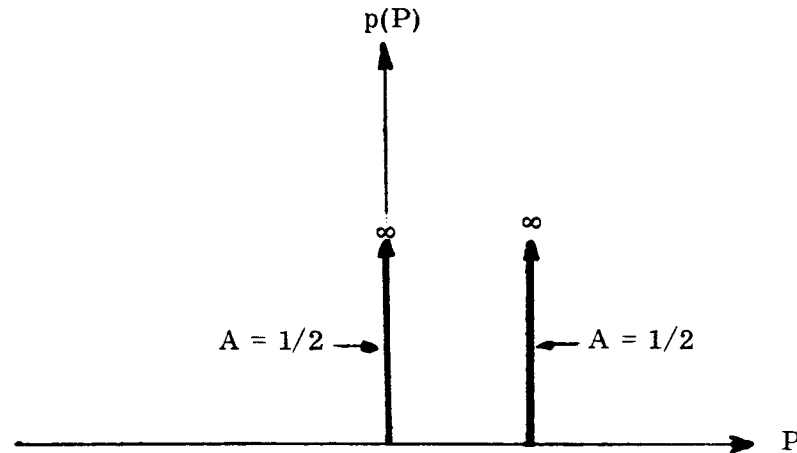
Figure g-5-3.   Probability Density, p (P), of AM key modulating signal, P.

The Nth moment for the signal of figure g-5-2 will therefore be:

$$E(P^N) = \frac{1}{2} \ P^N \bigg|_{P=O} + \frac{1}{2} \ P^N \bigg|_{P=1}$$

$$= \frac{1}{2} \text{ for all values of N.} \qquad \text{(g-5-28)}$$

Equation (g-5-25) then becomes:

$$K_p = 2 \qquad \text{(g-5-29)}$$

and equation (g-5-24) becomes

$$S/N \bigg|_o = \frac{2(S/N)^2_{in}}{1 + 2 \ (S/N)_{in}} \qquad \text{(g-5-30)}$$

_____

(11)   Davenport, W.B. and Root, W.L., Op. Cit.

As indicated previously, the S/N in the carrier phase demodulator loop will be 6.3 db at threshold, and since:

$$10 \log \left(\frac{100 \text{ cps}}{60 \text{ cps}} \right) = 2.22 \, , \tag{g-5-31}$$

the S/N in 100 cps into the square-law detector will be:

$$S/N \Big|_{in} (\text{db}) = 6.3 \text{ db} - 2.22 \text{ db} = 4.08 \text{ db}$$

or

$$S/N \Big|_{in} (\text{ratio}) = 2.56. \tag{g-5-32}$$

From equation (g-5-30):

$$S/N \Big|_{o} (\text{ratio}) = 2.14$$

or

$$S/N \Big|_{o} (\text{db}) = 3.3 \text{ db.} \tag{g-5-33}$$

It will be noted that the human operator would have about 50% intelligibility of random words at this input S/N.

analysis of telemetry subcarrier demodulator

g-6.1 GENERAL

The purpose of the telemetry subcarrier demodulator is to demodulate the PCM telemetry signal which has been modulated onto the 1.024-mc telemetry subcarrier by phase-reversal keying. The equipment must be designed to handle PCM bit rates between 1000 and 200,000 bits/sec*, although only two bit rates will be used for the Apollo program; 51.2 K bps and 1,600 bps. Two identical telemetry demodulators will be used in each system, one following the PM carrier demodulator and one following the FM carrier demodulator. A block diagram of the telemetry subcarrier demodulator is shown in figure g-6-1.

Preselection filters in the subcarrier telemetry demodulator provide rejection of other subcarrier signals, such as voice, and improve the input signal-to-noise ratio. The input signal-to-noise ratio for threshold is specified[1] as 8.5 db and the 1-db bandwidths of the required three preselection filters are given as 600 kc, 150 kc and 6 kc.

Synchronous demodulation must be used for binary PSK and several aspects and techniques involved in designing the telemetry subcarrier demodulator to provide this demodulation process will be discussed. The two major problem areas are: (1) the effects of noise in the synchronous detection process and (2) the generation of a reference signal for this type of demodulation. Circuit techniques and parameters will be selected for best overall performance.

---

* The minimum bit rate was originally 100 bps; See section g-10.

[1] GSFC-TDS-RFS-226, Op. cit.
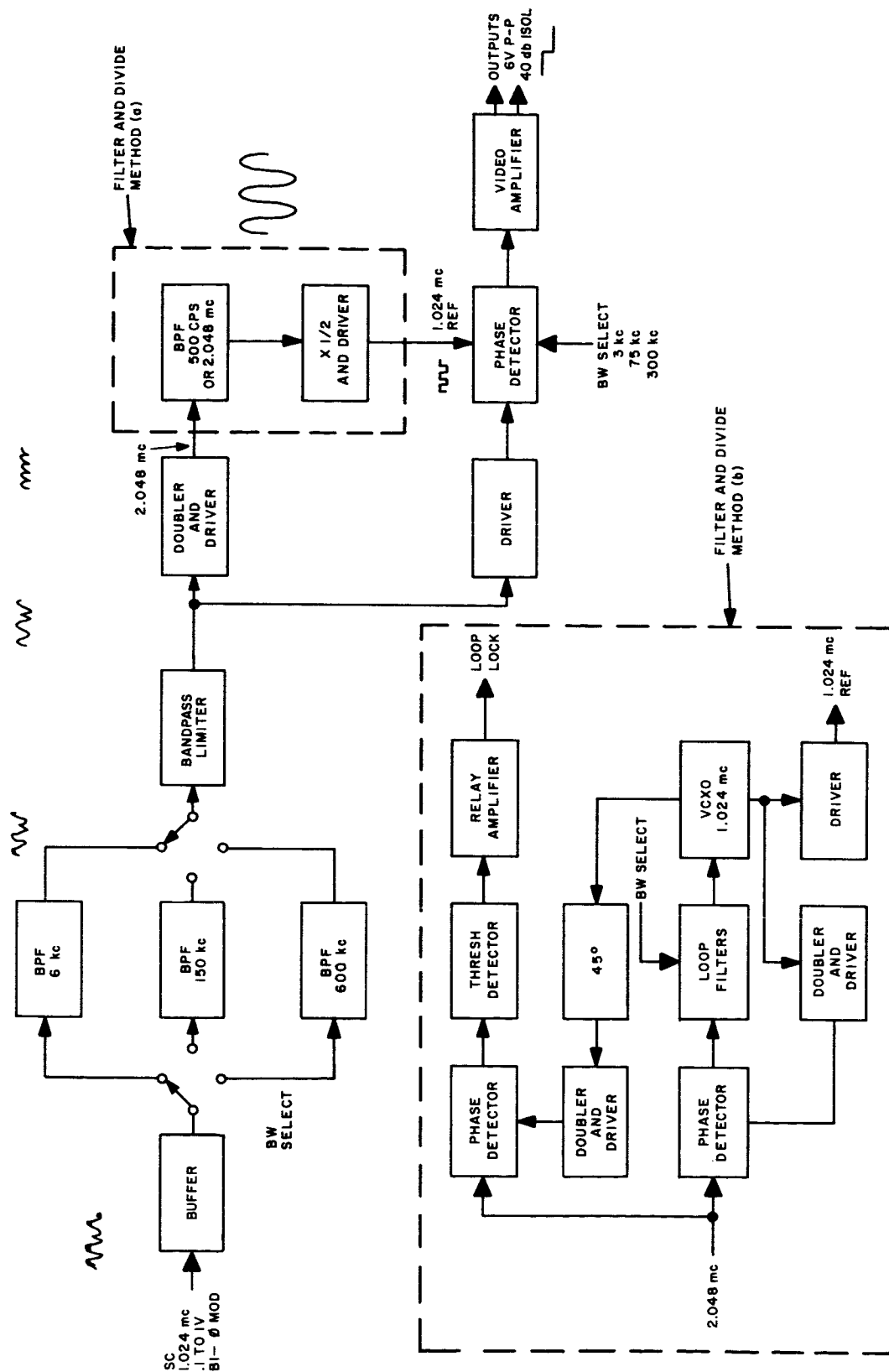
Figure g-6-1. Telemetry Subcarrier Demodulator

g-6.2 SYNCHRONOUS DEMODULATION OF PHASE-REVERSING BINARY SIGNALS IN GAUSSIAN NOISE, WITH PERFECT REFERENCE SIGNAL.

Assume for purposes of introduction that the unmodulated, noise-free carrier is available as the reference for a perfect phase detector as shown in figure g-6-2. The biphase modulated signal can be expressed in several different ways. Two are given by the following expressions:

$$s(t) = \sqrt{2} \ A \cos (\omega_0 t + m(t) \ \pi/2), \tag{g-6-1}$$

$$s(t) = \sqrt{2} \ A \ m(t) \sin \omega_0 t, \tag{g-6-2}$$

where m (t) = ±1, representing a random train of unit-amplitude pulses, with pulse widths of T_b.

The primary problem is to determine the probability of error in the binary decision, when the input signal is received under conditions of additive noise. That is, for a given signal-to-noise ratio, what is the probability that the output voltage will be positive when it should have been negative.* The phasor diagram in figure g-6-3 illustrates the effect of noise on the signal, distorting it in both amplitude and phase.

The output of a perfect sine detector can be written as:

$$V = A_0 A \sin \ m(t) \ \pi/2 \tag{g-6-3}$$

and if m(t) = ±1, then:

$$V = A_0 A \ m(t) \tag{g-6-4}$$

Notice that the output is a function of the input amplitude as well as the difference in phase. It can be shown[12] that, if there is a mis-synchronization between the

---

* This is not necessarily the bit error rate, but might be considered as a character error rate. The bit error rate will be a function of the type of coding and the operation of the PCM processor (bit synchronizer) which follows the telemetry demodulator.

[12] Jaffe, R. and Rechtin, R., "Design and Performance of Phase-Lock Circuits Capable of Near-Optimum Performance Over a Wide Range of Input Signal and Noise Levels," IRE Transactions on Information Theory, Volume IT-1 March 1955.

$s(t) + n(t)$ ──────▶ | PHASE DETECTOR | ──────▶ $V = A_0 A\ m(t)$

REFERENCE $\dfrac{A_0}{\sqrt{2}} \cos \omega_0 t$
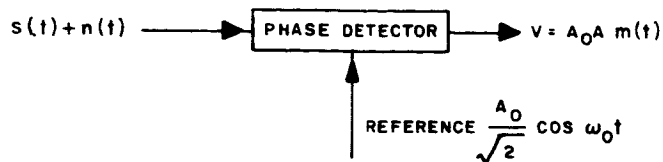
$s(t) = \sqrt{2}\ A\ \cos\left(\omega_0 t + m(t)\ \pi/2\right)$ WHERE $m(t) = \pm 1$

BIIO 563 R

Figure g-6-2.   Synchronous Detector For Binary PSK
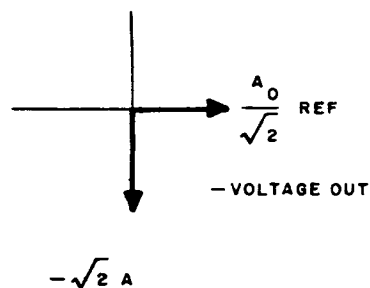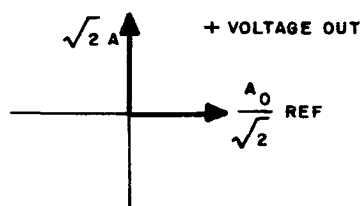
(A) PHASOR RELATIONSHIP ($+\pi/2$) WITH NO NOISE

(B) PHASOR RELATIONSHIP ($-\pi/2$) WITH NO NOISE
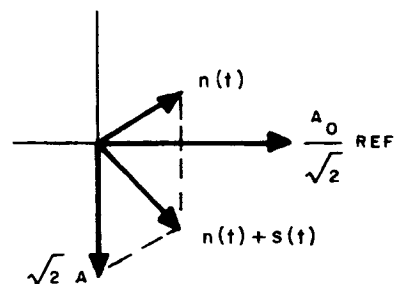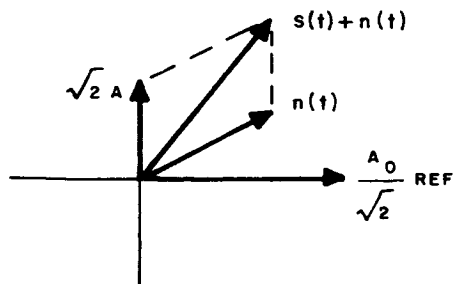
(C) PHASOR RELATIONSHIP ($+\pi/2$) WITH ADDITIVE NOISE   (D) PHASOR RELATIONSHIP ($-\pi/2$) WITH ADDITIVE NOISE

BIIO 562 R

Figure g-6-3.   Phasor Relationships Between Bi-Phase Modulated Signal,
Reference Signal and Noise

subcarrier and the reference of θ radians and if two successive pulses have the same sign, the output signal amplitude is effectively reduced by the factor cos θ. However, if the two successive pulses are of a different sign, then the amplitude reduction factor is slightly less and is given as:

$$\cos \theta + 2/\pi (\sin \theta - \theta \cos \theta). \tag{g-6-5}$$

If the phase of the reference is reversed exactly 180°, then the output voltage for +90° modulation will be negative instead of positive, as shown in figure g-6-3

Assuming a perfect phase detector, the probability of an error in the binary decision because of noise is the probability that the noise component will change the phase of the signal-plus-noise from that of the noise-free signal by more than 90°.

This probability can be calculated by integration of the probability density of the phase of a steady signal plus Gaussian noise. The probability density of phase can then be evaluated from the joint probability density of envelope and phase by integrating over all values of the envelope from 0 to ∞ and is found to be[13]:

$$P(\theta) = \frac{1}{2\pi} \left[1 + \sqrt{4\pi \ S/N} \ \cos \theta \cdot \Phi(X) \ \exp (S/N \cos^2 \theta) \right] \exp (-S/N), \tag{g-6-6}$$

where:

$$\Phi(X) = \frac{1}{\sqrt{2\pi}} \int_{-\infty}^{X} \exp \left(-\frac{X^2}{2}\right) \ dx,$$

and $x = \sqrt{2 \ S/N} \cos \theta.$

The probability density of phase is plotted in figure g-6-4 for several values of signal-to-noise ratio, S/N.

The probability of error (P_e) as a function of the signal to noise ratio, can be obtained by numerical or gaphical integration of the above equation, according to:

$$P_e = 1 - \int_{-\pi/2}^{\pi/2} p(\theta) \ d\theta \tag{g-6-7}$$

---

(13) Rice, S.O., "Mathematical Analysis of Random Noise" in "Noise and Stochastic Processes," Nelson Wax, Ed., Dover Publications, Inc. page 238, 1954
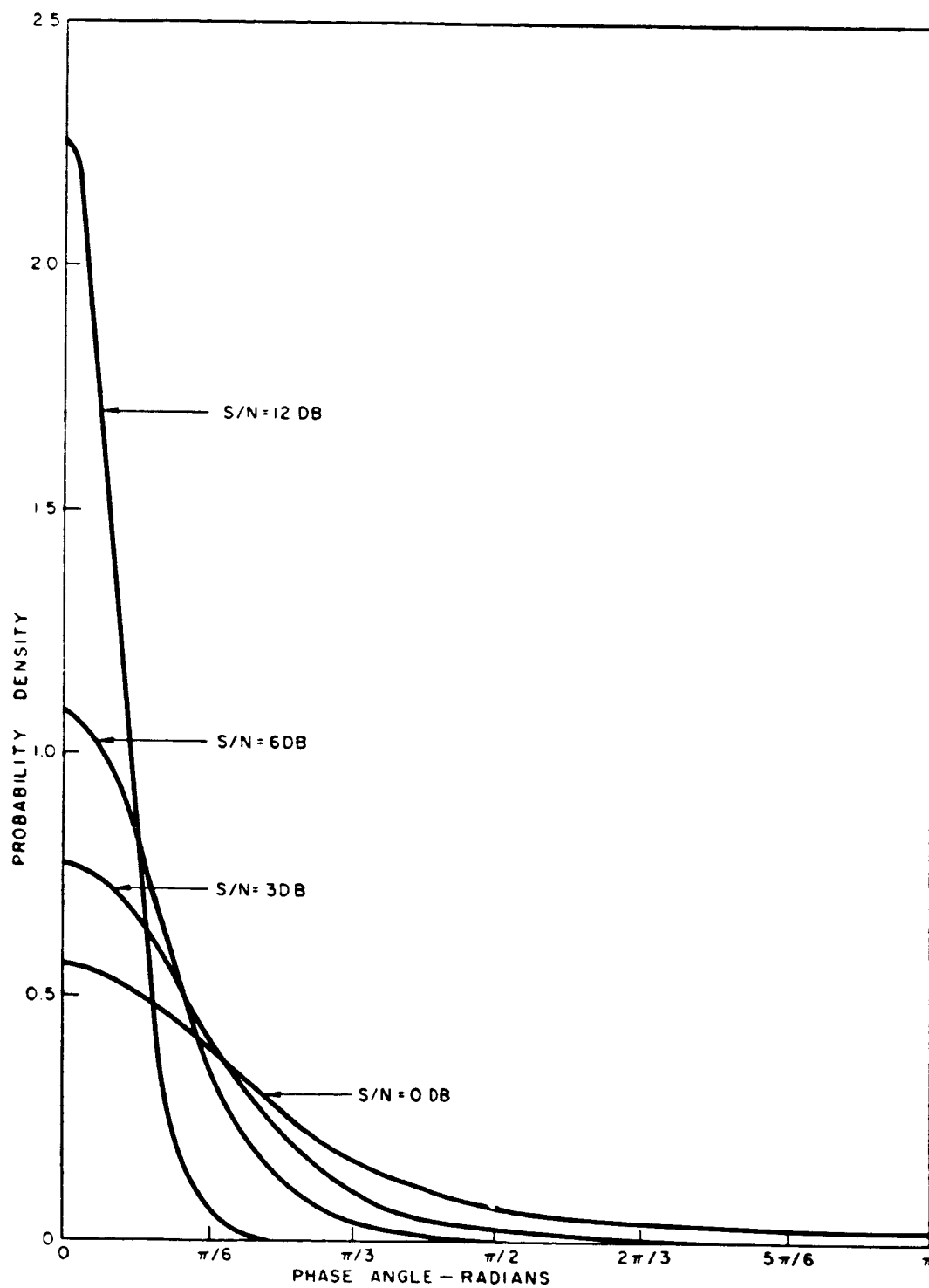
Figure g-6-4. Probability Density of Phase for
Sine Wave plus Gaussian Noise

where $\int_{-\pi/2}^{\pi/2} p(\theta) \, d\theta$ is the probability that $-90 \leq \theta \leq 90$ from the true value.

The results are shown in figure g-6-5, which shows the resulting probability of error for a perfect reference and perfect phase detector as calculated by C. Cahn[14]. This probability-of-error curve will provide a reference for evaluating the performance of the telemetry subcarrier demodulator, since figure g-6-5 represents the best performance that can be obtained.

Another source of mis-synchronization is the phase response of the input filters, which can cause the information in the sidebands to be shifted in phase relative to the center (subcarrier) frequency. With reasonable care in the design of the filters, however, this effect will be negligible compared to that caused by noise in the input signal.

g-6.3 SPECIFYING TELEMETRY SUBCARRIER DEMODULATOR THRESHOLD CONDITIONS.

Threshold for the telemetry subcarrier demodulator is difficult to specify in a manner which is easy to determine in the acceptance tests. The GSFC specifications only require that the threshold condition not occur for input signal-to-noise ratios greater than 8.5 db. A more meaningful specification would be "the bit error rate shall not exceed 10^{-5} bits/sec when the input signal-to-noise ratio is 8.5 db." When testing the demodulator without a bit synchronizer, however, the bit error rate is not easy to determine.

Even with the bit synchronizer, it is difficult to determine whether the demodulator has met the specification, because the bit error rate is a function of the PCM code and of bit synchronizer operation. Unfortunately, the bit error rate cannot even be simply related to the symbol error curve in figure g-6-5.

---

[14] Cahn, C.R., "Performance of Digital Phase-Modulation Communications System," IRE Transactions on Communications Systems, pp. 3-6, May 1959.
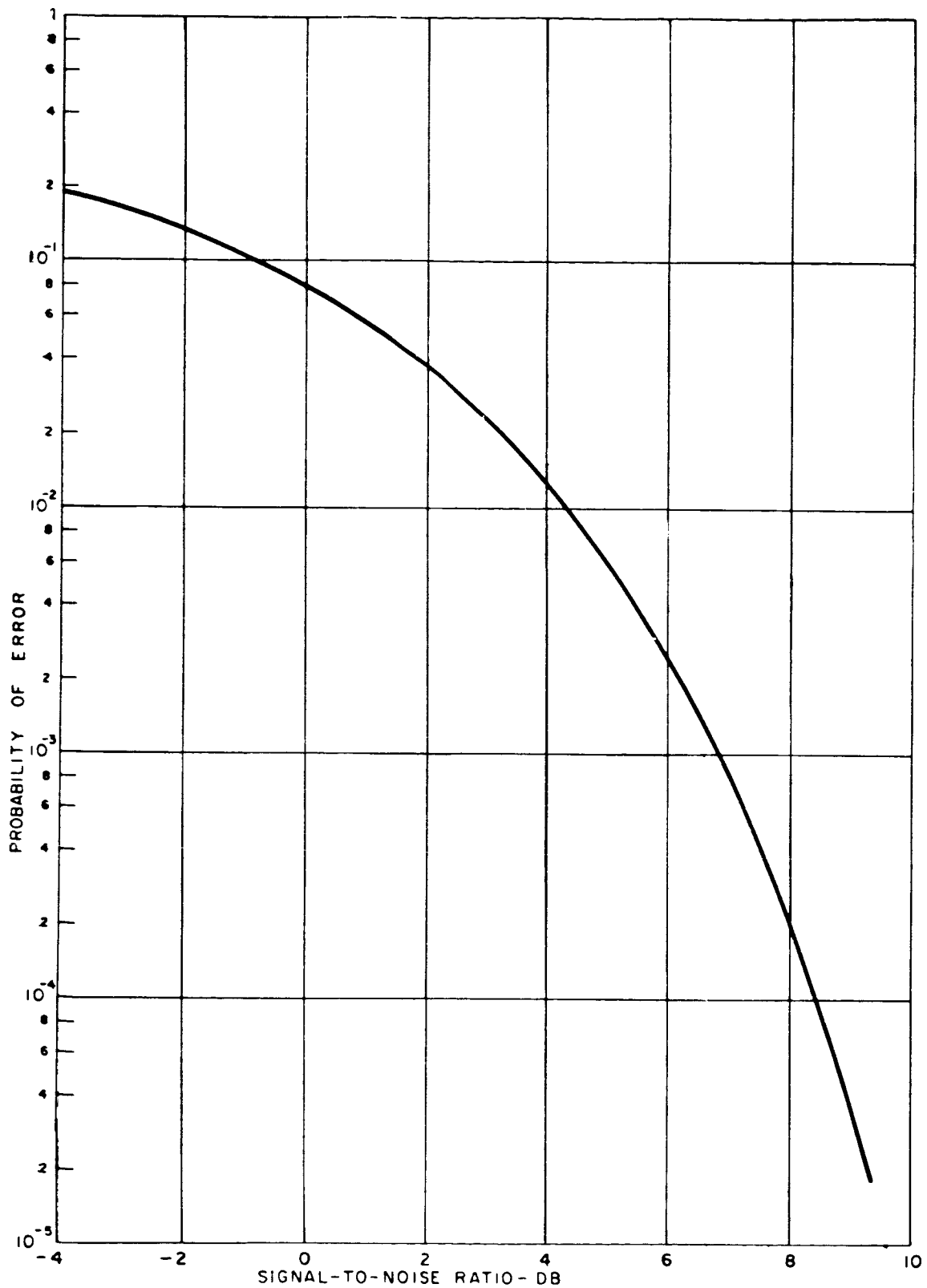
Figure g-6-5. Error Probability for Coherent
Detection of a Binary Signal

The bit error rate is a function of the output signal-to-noise ratio, which is determined by both the input signal-to-noise ratio and the phase jitter on the reference. In practice, the reference will also be derived from the input signal and it will, therefore, be contaminated by noise, which will reduce the output signal-to-noise. If the signal-to-noise ratio of the modulated signal is very high, the output signal-to-noise could be limited by the signal-to-noise ratio of the reference signal. For these reasons, a simple specification for threshold which can be easily measured on the demodulator is "the phase jitter on the derived reference signal at an input of 8.5 db shall not exceed $\overline{\theta}_o$ degrees rms." Usually, only the phase jitter noise need be treated, since most demodulators use some method of removing the amplitude variations from the reference signal before it is applied to the phase detector.

It remains to determine a suitable value for $\overline{\theta}_o$. Using equation (g-8-30) or figure g-8-9 (if the levels are within the usable range), an input rms signal-to-noise ratio of 8.5 db corresponds to an input phase jitter of 15° rms, which will be present in the signal input to the phase demodulator, independent of the reference signal. Since the effective rms input phase jitter will be the root-sum-square of the jitter of the signal and the reference, an effective input of 15.8° will result from a jitter on the reference of 5° and an effective input of 18° will result from a jitter on the reference of 10°. From equation (g-8-30) a signal-to-noise ratio of 18.2 db is required for 5° jitter and 12.2 db is required for a jitter of 10°. It was felt that additional phase jitter of 3° was unnecessarily large, particularly with the fact that, with a reference signal-to-noise ratio only 10 db greater than that of the input, the additional jitter would be 0.8°. Therefore, the value of $\overline{\theta}_o = 5°$ was chosen for the Collins specification.

g-6.4   SQUARING TECHNIQUE FOR BINARY PSK SYNCHRONIZATION.

Squaring equation (g-6-2) yields:

$$s^2(t) = A^2 \left[1 - \cos 2 (\omega_o t + \phi) \right] \; , \tag{g-6-8}$$

which contains an unmodulated frequency component at twice the subcarrier frequency. Filtering out the 2nd order component of the subcarrier frequency and dividing by 2 should, therefore, establish a coherent reference for the synchronous demodulator.

It should be pointed out that this squaring process leaves a 180° phase ambiguity, since both $\left[+ \sin(\omega_0 t + \phi)\right]^2$ and $\left[- \sin(\omega_0 t + \phi)\right]^2$ provide the same signal. This will be no problem in the Apollo program, however, since only PCM coding techniques which use a change in output polarity for information (rather than absolute polarity) will be used. Two of these PCM encoding techniques which may be used are: (1) non-return-to-zero-space (NRZ-S), in which a change in state represents a space (zero) and (2) non-return-to-zero-mark (NRZ-M), in which a change in state represents a mark (one).

It is of interest to first determine the signal-to-noise ratio which results from passing the data signal through a perfect squaring and filtering device, as shown in figure g-6-6.

Much of the analysis to follow has been presented in the literature in several places[11],[15]. However, because there are a considerable number of trade-offs in performance, complexity, cost and reliability according to the technique used to obtain synchronization for the telemetry demodulators, it was felt that the major steps of the analysis should be presented for completeness.
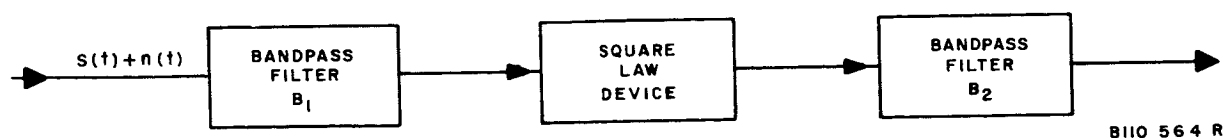
Figure g-6-6.   The Square-Law Network

(11)   W. Davenport, Jr., & W. Root, Op. cit

(15)   JPL Space Programs Summary No. 37-26, Vol. IV for the period 1 February
        1964 to 31 March 1964, dated 30 April 1964, pp. 240-246.

If the input to the bandpass filter B_1 is $x(t) = s(t) + n(t)$, the output will be:

$$x_1(t) = s(t) + n_1(t), \qquad \text{(g-6-9)}$$

Where $s(t)$ is the data signal defined in equations (g-6-1) and (g-6-2), $n(t)$ is white Gaussian noise and $n_1(t)$ has the noise spectrum:

$$S_{N_O}(f) \begin{cases} = N_B \text{ for } \dfrac{\omega_o}{2\pi} - \dfrac{B_1}{2} \leq f \leq \dfrac{\omega_o}{2} + \dfrac{B_1}{2} \\ = 0 \text{ Elsewhere.} \end{cases} \qquad \text{(g-6-10)}$$

The bandwidth B_1 of the input filter is often assumed to be wide enough so that the signal power in the output is essentially unchanged from that of the input. When a significant amount of the signal is lost in the filter, however, the loss must be considered in the signal calculations. The signal amplfied will be reduced by an amount which will be called r, where r^2 is the ratio of the filtered signal power to that of the unfiltered signal power.

In general, for a random sequence of unit-amplitude pulses with time duration T_b:

$$r^2 = \frac{\displaystyle\int_{-2\pi B_1}^{2\pi B_1} \frac{\sin^2(\omega T_b/2)}{(\omega T_b/2)^2} \, d\omega}{\displaystyle\int_{-\infty}^{\infty} \frac{\sin^2(\omega T_b/2)}{(\omega T_b/2)^2} \, d\omega} \qquad \text{(g-6-11)}$$

In practice, B_1 is made as narrow as possible in order to improve the signal-to-noise ratio into the square-law-device, at the expense of making r less than unity. With the specified[1] bandwidth of 6 kc for 1,600 bits per second, only the first sideband on each side of the subcarrier will be passed. For this condition[3] $r^2 = 0.65$, representing a loss of 2.5 db.

---

[1] GSFC-TDS-RFS-226, Op. cit.

[3] Stover, Op. cit.

When r is significant, equation (g-6-9) becomes:

$$x_1(t) = r\, s(t) + n_1(t) \tag{9-6-12}$$

A perfect square law device then produces the signal:

$$y(t) = r^2 A^2 \left[1 - \cos 2(\omega_o + \Phi)\right] + n_1^2(t) + 2\sqrt{2r}\, Am(t)\sin(\omega_o t + \Phi) \tag{g-6-13}$$

To determine the signal and noise power in the vicinity of $2\omega_o$, it is necessary to apply the auto-correlation function. The auto-correlation function in turn is transformed to obtain the spectral densities from the various terms. Since the expected value of the noise is zero and the signal and noise are independent, the spectral density of y(t) can be expressed as follows:

$$S_y(f) = S_{sxs}(f) + S_{sxm}(f) + S_{nxm}(f) \tag{g-6-14}$$

From pages 257 through 267 of the reference[11], the spectral densities of the above components in the vicinity of $2\omega_o$ have been calculated to be:

$$S_{sxs}\left(\frac{\omega_o}{\pi}\right) = \frac{r^4 A^4}{4}\, \delta\left(\frac{\omega_o}{\pi}\right) \tag{g-6-15}$$

where $\delta\left(\dfrac{\omega_o}{\pi}\right)$ is the unit impulse function:

$$S_{sxm}\left(\frac{\omega_o}{\pi} \pm \frac{B_1}{2}\right) = 2\, r^2 A^2 N_o \tag{g-6-16}$$

$$S_{mxm}\left(\frac{\omega_o}{\pi} \pm B_1\right) = 2N_o^2\left(B_1 - \left||f| - \frac{\omega_o}{\pi}\right|\right) \tag{g-6-17}$$

Figure g-6-7 illustrates the combined spectral density characteristics in the vicinity of $2\omega_o$.

----

(11) Davenport and Roote, Op. cit.
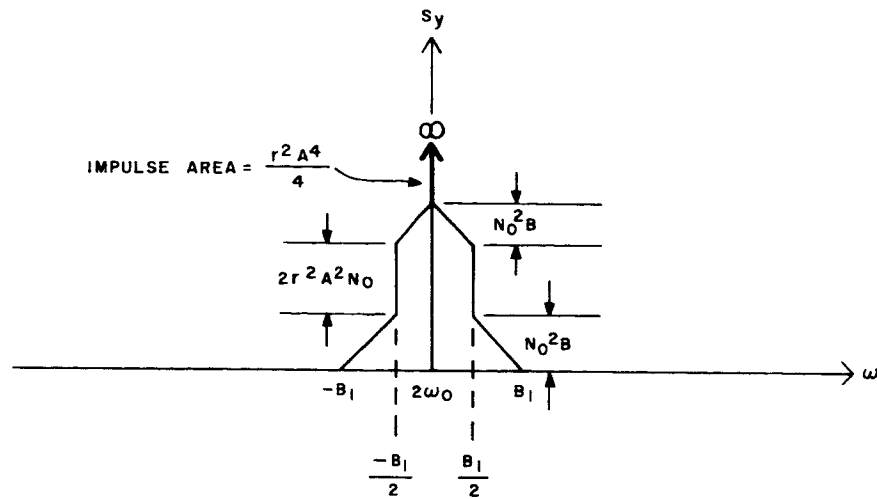
Figure g-6-7.   Spectral Density in the Vicinity of $2\omega_o$ for a Full-Wave Squaring Device, In Response to a Sine-Wave Plus Gaussian-Noise Input

It will be noted that the output of the square law device is not white (flat) and it can be shown[13] that the output noise is not Gaussian, but that the statistics of the output approach Gaussian statistics as $\dfrac{B_1}{B_2} \to \infty$.   Thus, under the assumption that $B_1 \gg B_2$, the output may be treated as flat and Gaussian for first order calculations.

The signal-to-noise ratio into the square law device will be:

$$S/N_i \; = \; \frac{r^2 A^2}{2N_o B_1} \qquad\qquad (g\text{-}6\text{-}18)$$

<hr>

(13)   Rice, Op. cit.
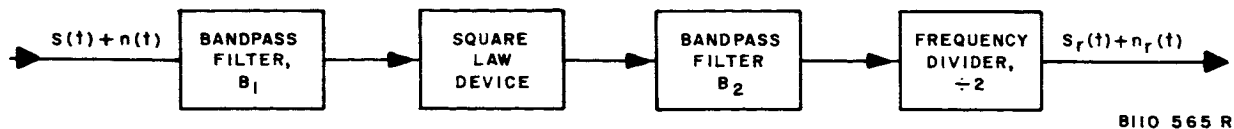
Figure g-6-8.   Coherent Reference Generator for ±90° PSK Demodulation

The output signal-to-noise of the square law device in the immediate vicinity of $2\omega_o$ is given as:

$$S/N_s = \frac{r^4 A^4}{4} \cdot \frac{1}{2 r^2 A^2 N_o B_1 + 2 N_o^2 B_1^2} \cdot \frac{B_1}{B_2} \qquad \text{(g-6-19)}$$

or:

$$S/N_s = \frac{1}{2} \frac{(S/N_i)^2}{(1 + 2 S/N_i)} \cdot \frac{B_1}{B_2} \qquad \text{(g-6-20)}$$

g-6.5   FILTER BANDWIDTH SELECTION.

A simple approach to obtaining the reference signal for the phase detector would be to pass the output of the squaring network of figure g-6-6 through a perfect frequency divider which divides by two. The resulting network is shown in figure g-6-8.

If the maximum allowable rms phase jitter on the reference signal is specified as θ_o, then from equation (g-8-30), the lowest allowable output signal-to-noise ratio of the above generator chain will be:

$$S/N_{r_1} = \frac{1}{2 \overline{\theta}^2} \qquad \text{(g-6-21)}$$

Assuming that the frequency divider contributes no additional phase jitter, the maximum allowable rms phase jitter at the input to the frequency divider can be twice

g-6-14

that at the output. Therefore, the lowest allowable output signal-to-noise ratio from the filter B_2 can be calculated from the expression:

$$S/N_{2_L} = \frac{1}{8 \ \overline{\theta}_o^2} \qquad \text{(g-6-22)}$$

Combining equation (g-6-22) with equation (g-6-20), the maximum allowable bandwidth of filter B_2 can be determined when both the output phase jitter θ_o and the input signal-to-noise into filter B_1 are known. The resulting expression is:

$$B_2 = 4B_1 \ \overline{\theta}_o^2 \ \frac{(S/N_i)^2}{1 + 2 \ (S/N_i)} \qquad \text{(g-6-23)}$$

For example, using the value of 5° (0.087 radians) for θ_o, 7.25 kc for B_1*, and 8.5 db (7.08 numerical) for S/N_i, the maximum allowable bandwidth for B_2 is 725 cps. Since the telemetry subcarrier frequency is 1.024 mc, the center frequency of the bandpass filter is 2.048 mc. Thus, a narrow-band filter of 0.035 percent or less would be required. Such a narrow bandwidth is possible only with a crystal filter or, as indicated in paragraph g-6.6, a phase-lock loop. A crystal filter of this width is within (but barely within) the present state-of-the-art, as shown by figure g-6-9.

It may be of interest to determine the minimum value which the bandwidth B_2 may have, aside from the practical problem of constructing it. Making B_2 smaller improves the signal-to-noise ratio into the frequency divider, as well as making the assumption of Gaussian noise into the frequency divider more valid. However there is a minimum for B_2, which is determined by the frequency uncertainty of the telemetry subcarrier. This uncertainty is due to frequency drift of the subcarrier oscillator in the spacecraft and the difference in doppler shift between the subcarrier signals and the rf carrier. In the case of the Apollo Spacecraft, the stability of the 1.024-mc subcarrier oscillator is in the order of one part in 10^5 or ±10 cps. The maximum

---

* This is the noise bandwidth for a four-pole, 0.1-db ripple, (Chebyshev) filter whose 1-db bandwidth is 6 kc. Six kc is the lowest bandwidth specified for the input to the telemetry subcarrier demodulator.

Figure g-6-9. Range of Available (State-of-the-Art) Crystal Filters

doppler under acceleration conditions in the near-earth orbit is in the order of 150 kc at S-band, resulting in a shift of the telemetry subcarrier frequency of about 70 cps. Thus the maximum uncertainty in the received subcarrier frequency is ±80 cps and the minimum value for B_2 is 160 cps. All of the above considerations are true for a passive (crystal) filter. The use of a phase-lock loop as a filter will now be discussed and it will be found that the minimum bandwidth may be considerably less than 160 cps.

g-6.6   USE OF A PHASE LOCK LOOP AS A FREQUENCY DIVIDER AND FILTER.

Figure g-6-10 illustrates how a phase lock loop can be utilized as a frequency divider.

The phase lock loop is essenitally a narrow filter and thus it could serve as both the filter B_2 and the frequency divider of figure g-6-8. Equation (g-6-23) and the related discussion can be essentially applied directly to the case where the phase lock loop is used, in which case, the loop noise bandwidth is used in place of B_2.

One advantage of using the phase lock loop instead of the crystal filter is that the noise bandwidth of the loop can be made much smaller than that achievable with crystal filters. The loop automatically tracks the incoming signal and there would appear to be no lower limit to the filter bandwidth which could be used, since the doppler and subcarrier frequency drift in the spacecraft would not restrict the selection of a bandwidth as they do for the crystal filter. However, there is a practical limit when one considers the acquisition problem and herein lies one of the disadvantages of the phase lock loop. It is likely that some of the data would be lost while the

BIIO 566 R
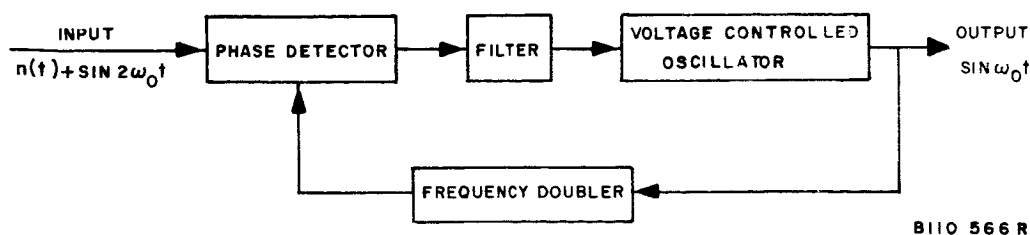
Figure g-6-10.   Phase Lock Loop as a Filter and ($\div$2) Frequency Divider

loop is locking up at the beginning of a transmission or while it is reacquiring after momentary loss of lock. The amount of data lost will be a function of the bit rate, the loop bandwidth and the loop gain.

Frequency acquisition by phase lock loops is discussed in section g-8. It would be informative at this point to calculate the acquisition time for typical loop parameters. A loop noise bandwidth of 100 cps with an unlocked vco stability in the order of a part in 10^5 would provide an essentially noise-free signal, while providing enough range to insure that the probability of loss of lock after initial acquisition would be extremely small. To provide the best acquisition time, the damping factor should be 0.5. Using equation (g-8-45), the acquisition time for a strong-signal condition can be found. Assuming an initial offset of 80 cps and a bandwidth of 200 cps, the acquisition time would be approximately 27 milliseconds. At a bit rate of 200,000 bits/sec this represents a loss of 5400 bits, which would probably not be serious. The acquisition time for lower signal-to-noise ratios would, of course, be somewhat longer. To provide more nearly optimum trade-off between noise bandwidth and acquisition time, several loop bandwidths could be provided, to reduce the noise bandwidth when lower bit rates permit and to reduce acquisition time for the higher bit rates.

g-6.7   THE USE OF LIMITERS IN PHASE DEMODULATION.

The use of a limiter as a signal suppression device and, hence, as a means of automatically controlling the loop gain for optimum filtering is discussed in section g-8. The discussion there is based upon a perfect limiter; that is, one in which the total output power is a constant, regardless of the input. Equations (g-8-22) and (g-8-23) imply that the use of a limiter affords an improvement of up to 3 db in the signal-to-noise ratio for a high input signal-to-noise ratio (S/N_{in}) and causes no more than 1 db of degradation for low values of S/N_{in}. The output S/N for a given input S/N for a perfect limiter is[16] is:

$$S/N_{out} = \gamma \, r^2 \, S/N_{in} \qquad (g-6-24)$$

[16] Chadima, George E., Jr., "Phase Noise Theory Applied to Detection," Collins Research Report No. 272, Cedar Rapids, Iowa, Collins Radio Company, March 1963

Values of γ may be found from the curve in figure g-6-11.

For example, suppose a perfect bandpass limiter precedes the phase demodulator in the telemetry subcarrier demodulator. At the specified threshold input S/N of 8.5 db (7.08 numerical ratio), with r^2 = .91, γ will be 1.72 and the effective S/N input will be 10.4 db, an improvement of 1.9 db.

It is also of interest to determine the effect that such a limiter will have if it precedes the square-law device in the coherent reference generator as shown in figure 9-6-1. Using equation (g-6-23), with the S/N_{in} of 10.4-db, and using the values of 5° for $\bar{\theta}_{o}$ and 7.25 kc for the noise bandwidth, the maximum allowable bandwidth for filter B_r becomes 1164 cps.

g-6.8   EFFECT OF USING A SQUARE WAVE REFERENCE SIGNAL FOR DEMODU-
         LATION.

If a digital type of divider is used, it is usually more convenient to furnish the reference signal to the detector in the form of a square wave, which switches the phase detector from one state to another. The error due to mis-synchronization is greater using square pulses for the reference than it is when using a sinusoidal
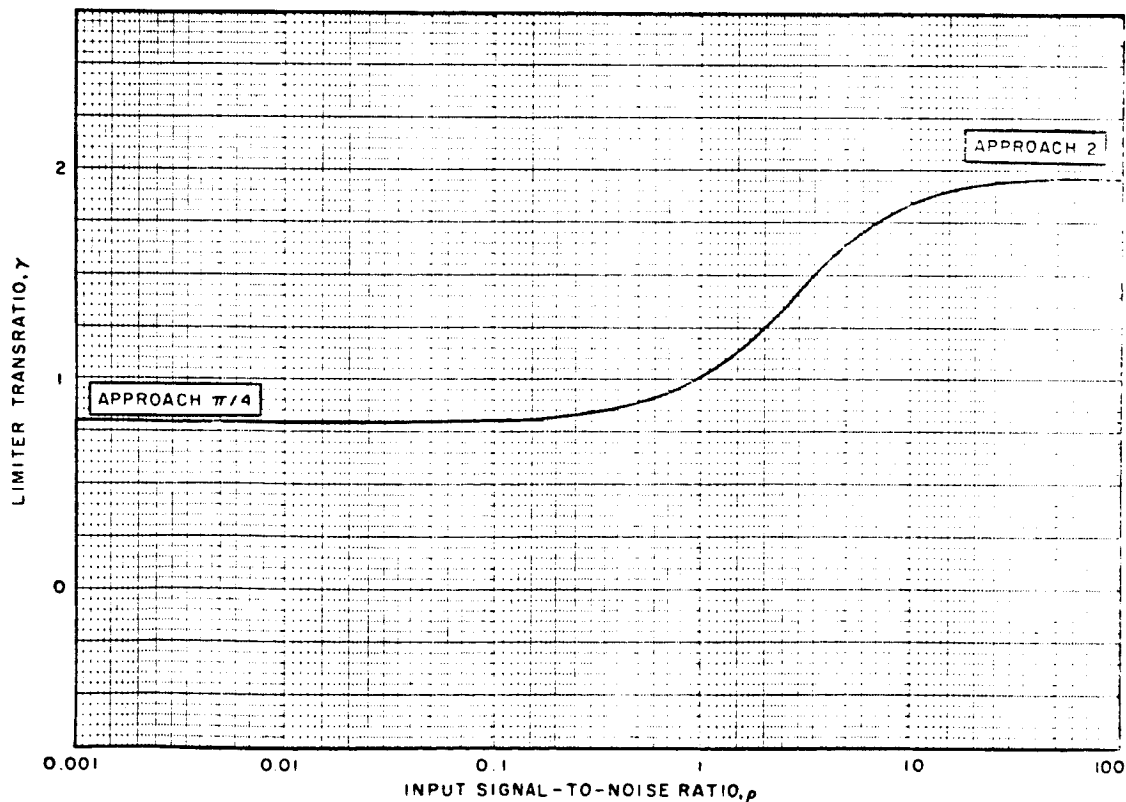
Figure g-6-11.   Bandpass Limiter Transratio, γ

reference[16]. Since the allowable mis-synchronization for the telemetry demodulator has been specified to be 15° rms, it is doubtful that it would be worth the effort to generate a sinusoidal reference signal just to reduce the effect of such mis-synchronization.

The characteristics of the phase detector change, however, according to the type of reference signal which is used. The shape of the phase detector transfer function, combined with the statistics of the phase noise, will determine the output signal-to-noise ratio. Equation (g-6-3) describes the sinusoidal characteristics of a phase detector with a sinusoidal reference. A rectangular reference signal can be used to obtain a triangular or linear phase detector function, which would have the following output:

$$V = A_o A m(t) \; \pi/2, \qquad\qquad (g-6-25)$$

which is essentially the same as that given in equation (g-6-4). Thus, one concludes that, for binary ±90° PSK, the square wave reference signal would perform essentially the same as for the sinusoidal reference.

It should be noted that a linear transfer function for a phase detector can only be maintained in a noise-free condition. Just as the characteristics of the reference signal shape the transfer function of the phase detector, so does the phase noise. In particular, it can be shown[16] that the statistics of the phase noise tend to suppress the relative phase angle between the modulated signal and the reference, and, as the signal-to-noise ratio decreases, the transfer function of the phase detector will become essentially sinusoidal. This is illustrated in figure g-6-12.

Although all phase detectors approach sinusoidal shapes under poor signal-to-noise ratios, the variance of the noise will be quite different depending upon the strong signal transfer function. Chatima[16] has performed a detailed analysis of the output signal-to-noise characteristics of different types of phase detectors and concludes that,

[16] Chatima, Op. cit.
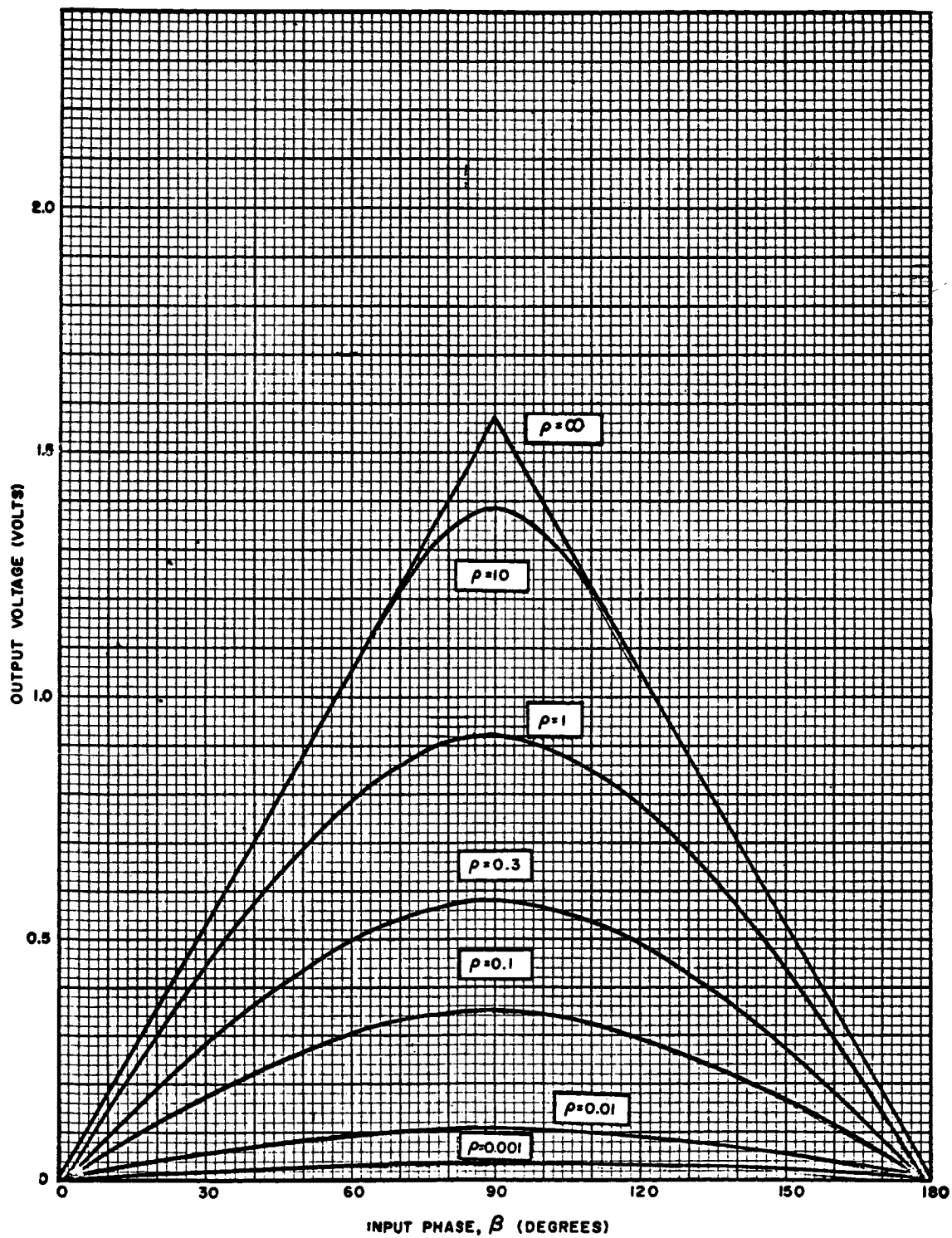
Figure g-6-12.   Triangular Detector Characteristics

if the input signal-to-noise ratio is much greater than unity, the sinusoidal transfer function suppresses the noise more for binary ±90° PSK than the linear detector. However, as the input signal-to-noise ratio approaches unity, the output signal-to-noise characteristic becomes essentially the same.

g-6.9 CONCLUSIONS.

The next step in the analysis would be to investigate the output signal-to-noise characteristics of digital types of frequency dividers for input signal-to-noise ratios in the order of 18 db (in 725-cps bandwidth). Unfortunately, information was not available on the performance of present state-of-the-art digital dividers with noisy input signals. It seems reasonable to assume, however, that with 18 db of input signal-to-noise, the reference signal can be generated properly with a squarer, a filter (either crystal or phase-lock loop), and a digital frequency divider. If the digital divider requires a significantly higher input signal-to-noise ratio in order to keep the output phase jitter to no more than 5° rms, it may not be possible to obtain a crystal filter with narrow enough bandwidth. If such is found to be the case, the alternative would be to use the phase lock loop. As pointed out in the preceding sections, the acquisition time is not insignificant with the phase lock loop, not to mention the additional complexity in equipment but, because of its added flexibility and more nearly optimum filtering, it is preferred over the crystal-filter-and-digital-divider technique. It was also pointed out that some signal-to-noise improvement is obtained with the use of a bandpass limiter preceding the demodulator but a significantly large improvement in the overall bit error rate will not be seen because of the non-linearity of the overall demodulation process. Furthermore, it was concluded that, from a practical standpoint, it would not be worth the trouble to convert the square wave out of the digital divider into a sinusoidal reference, although theoretically some improvement could be obtained.

analysis of voice subcarrier and biomedical demodulators

g-7.1 GENERAL.

Figure g-7-1 is a block diagram of the voice subcarrier demodulator. The unit receives a 1.25-mc subcarrier from either the carrier phase demodulator or the carrier frequency demodulator. The subcarrier is frequency modulated by either voice alone or by a composite of voice and seven biomedical subcarriers. These biomedical subcarriers have been frequency-modulated by physiological data from the astronauts. After filtering and hard limiting, the signal is fed into a phase-lock loop fm demodulator. Three wideband outputs are provided for the baseband signal taken from the loop filter. (One for the tape recorder, one for the output selector and biomedical channels, and one spare.) A bandpass filter is provided for voice signal extraction. A 90° phase shifter and quadrature detector are used for in-lock indication.

In this section, optimum bandwidths for the 1.25-mc phase lock loop are computed for the different types of modulation and the required threshold input signal-to-noise ratios. As a result of these computations, it is possible to determine optimum modulation indices for the biomedical subcarriers on the 1.25-mc signal. The biomedical subcarrier demodulators are analyzed in this section because of the interaction between the characteristics of the voice subcarrier and the biomedical subcarriers.

It can be seen from table g-1-2 that biomedical subcarrier number one has a frequency of 4.0 kc, which is well within the audible range. To prevent the subcarrier from being distributed in the station audio system, with the associated annoyance and reduction of intelligibility, an audio output filter was specified with 20 db of attenuation at 4 kc. This results in a -3-db response of 3.4 kc for the audio channel.
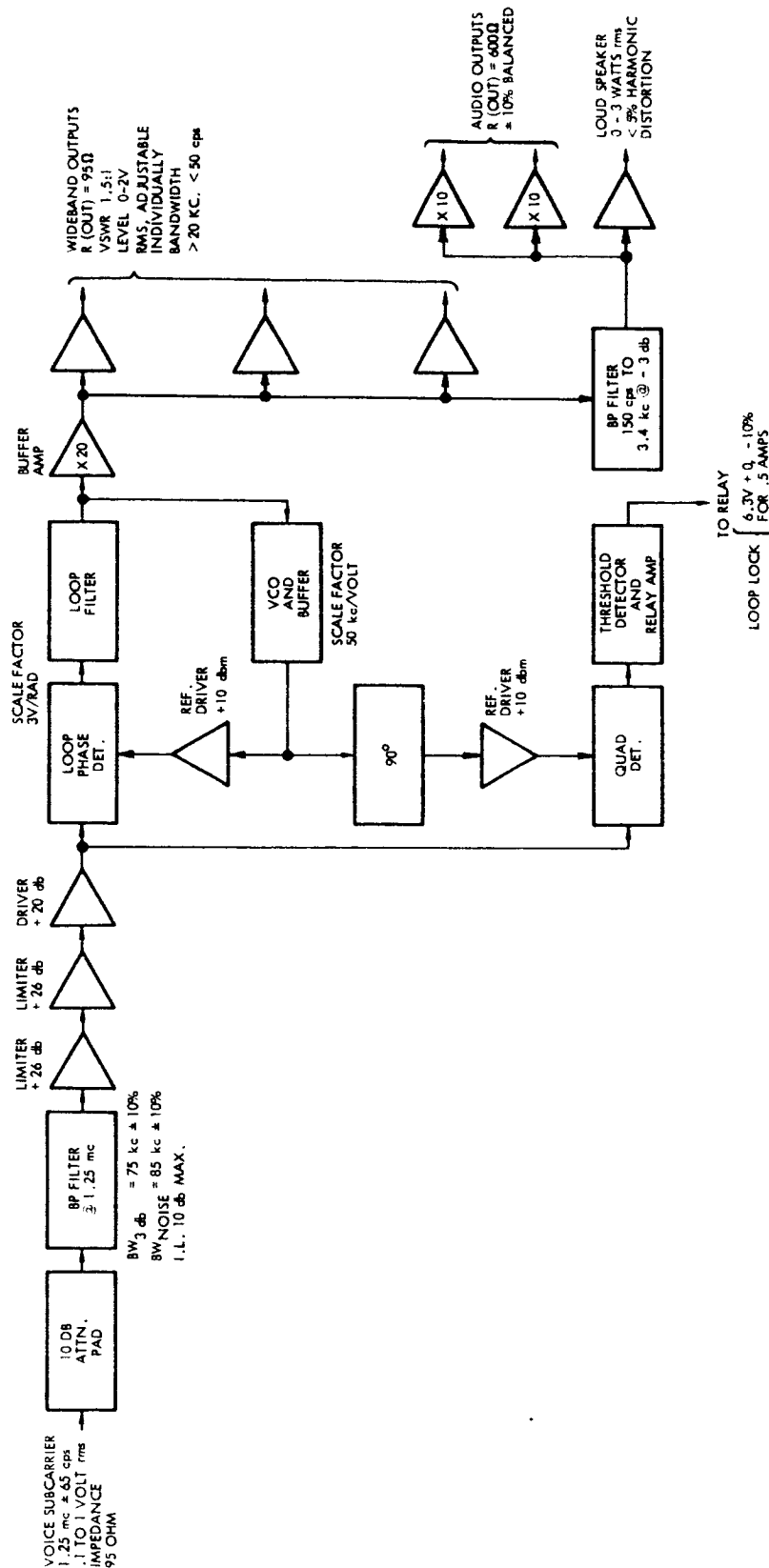
Figure g-7-1. Voice Subcarrier Demodulator

g-7.2 CRITERION FOR OPTIMUM PERFORMANCE.

The criteria used for selection of optimum bandwidths for the 1.25 mc fm demodulator will be the same as that used for the fm carrier demodulator. That is, for a given carrier modulation and white gaussian noise at the loop input, the loop threshold should occur at the minimum possible ratio of total signal power to noise spectral density, at the phase detector input. The bandwidths obtained for these conditions are optimum for the modulation characteristics used.

The design procedure here is, however, somewhat different than that for the main carrier fm demodulator, in that the seven biomedical channels at the output of the 1.25-mc subcarrier demodulator must be detected in separate fm demodulators. It seems reasonable to require simultaneous threshold of both the biomedical subcarrier demodulators and the 1.25-mc subcarrier demodulator. This being the case, the design should be such that all of the demodulators (1.25 mc and biomedical subcarriers) have the lowest possible thresholds. Of the currently available fm demodulators, the phase lock discriminators exhibit the lowest threshold characteristics. For this reason, phase lock demodulators were chosen for detection of the biomedical sub-carrier.

The total peak phase error in the wideband 1.25-mc phase-lock demodulator is the sum of errors due to modulation and noise, as follows:

$$\epsilon_T = \epsilon_m + \rho_N \sigma_N \qquad \text{(g-7-1)}$$

where:

ϵ_T = total loop peak phase error in radians

ϵ_m = total modulation tracking error in radians

σ_N = rms noise error in radians

ρ_N = weighting factor for noise error (equal to 3 for

ρ_N = peak to rms noise ratio)

The loop peak phase errors for the 1.25-mc subcarrier, modulated by voice only and by voice plus the seven biomedical subcarriers, will be discussed. In the case of the latter, the design is for simultaneous threshold of the detectors in the voice and biomedical channels, at the minimum possible signal-to-noise-spectral-density ratio for the input to the voice subcarrier demodulator. The analysis results in optimum values for:

    (1)   Bandwidths the voice subcarrier demodulators

    (2)   Bandwidths of each of the biomedical subcarrier demodulators

    (3)   Threshold signal-to-noise levels

    (4)   Modulation indices for the biomedical subcarriers on the 1.25-mc carrier.

g-7.3   SELECTION OF OPTIMUM BANDWIDTHS AND CORRESPONDING THRESHOLD SIGNAL-TO-NOISE RATIOS FOR BIOMEDICAL SUBCARRIER DEMODULATORS.

The characteristics and modulation of the biomedical subcarriers as specified[1] are described in table g-1-2 of this report. The total peak phase error of the kth subcarrier demodulator may be expressed[5] as:

$$\epsilon_T = \frac{\beta_k}{\sqrt{1 + \left(\frac{\omega_n}{\omega_k}\right)^4}} + 0.729\rho \left(\frac{\Phi_N}{P_k}\right)^{1/2} \omega_n^{1/2} \qquad \text{(g-7-2)}$$

where:

    ϵ_T = total loop peak phase error in radians

    β_k = FM modulation index of information on subcarrier (peak frequency deviation divided by peak modulating frequency)

    Φ_N = noise spectral density at loop input (watts/cps)

    ω_n = phase lock loop natural frequency

    P_k = k^{th} subcarrier power

---

[1]   GSFC-TDS-RFS-226, Op. cit

[5]   Martin, Op. cit.

TABLE g-7-1.   MODULATION PARAMETERS FOR BIOMEDICAL SUBCARRIERS

I BIOMEDICAL CHANNEL NO.	II FREQUENCY (kc)	III BIOMEDICAL SUBCARRIER MODULATION INDEX, β_k	IV LOOP NOISE BANDWIDTH (cps)	V REQUIRED S/N IN LOOP NOISE BANDWIDTH (db)	IV 1.25-MC SUBCARRIER MODULATION INDEX
1	4	100	250	4.3	0.0815
2	5.4	135	280	4.5	0.088
3	6.8	170	290	4.8	0.093
4	8.2	205	370	4.1	0.0964
5	9.6	192	370	4.1	0.0955
6	11.0	175	290	4.9	0.094
7	12.4	8.3	980	4.7	0.1697

and the other symbols are as defined above. β_k can be determined from table g-2-1 (example: $\beta_1 = 200/2 = 100$), as can ω_k (example: $\omega_1 = 2\pi$ (2 cps) = 12.56 radians/sec). The peak error due to noise can be obtained by setting $\rho = 3$ (peak-to-rms ratio for gaussian noise). As discussed in section g-4, a reasonable choice for ϵ_T at loop threshold is $\pi/2$. Using these values reduces equation (g-7-2) to P_T/Φ_N as a function of ω_n. Thus, the optimum loop bandwidth can be obtained as that value of ω_n which results in a minimum P_T/Φ_N for $\epsilon_T = \pi/2$, $\rho = 3$. A graphical procedure was used, as in section g-4.2, for each of the biomedical subcarriers. The results are listed in columns 4 and 5 of table g-7-1. Column 3 lists β_k. The values for the last column will be computed in a following section.

g-7.4 EVALUATION OF SPECIFIED LOOP NOISE BANDWIDTH AND SIGNAL-TO-NOISE RATIO.

The loop noise bandwidth of the 1.25-mc subcarrier demodulator was specified[1] as 50 kc, with a required signal-to-noise ratio in that bandwidth of 4.7 db and a modulation index for the voice signal on the subcarrier of 2.5. The following analysis substantiates the choice of a 50-kc bandwidth and yields threshold signal-to-noise ratios in this bandwidth for test tones of 800, 1000, and 3400 cps, simulating a voice signal. The biomedical data subchannels will not be considered.

The peak phase error for the 1.25-mc subcarrier demodulator for voice-only modulation and white gaussian noise at the input will be[5]:

$$\epsilon_T = \frac{\beta_V}{\sqrt{1 + \left(\dfrac{\omega_n}{\omega_V}\right)^4}} + 0.729 \, \rho_N \, (\Phi_N/P_V)^{1/2} \, \omega_n^{1/2} \qquad \text{(g-7-3)}$$

where:

β_V = FM modulation index of voice signal on the 1.25-mc subcarrier

ω_V = modulating frequency (radians/sec)

P_V = 1.25 mc subcarrier power

---

[1] GSFC-TDS-RFS-226, Op. cit.

[5] Martin, Op. cit.

and the other symbols are as defined previously.

From equation (g-8-10), the loop noise bandwidth is equal to $1.06\,\omega_n = 50$ kc. Therefore, $\omega_n = 4.71 \times 10^4$ and, using $\epsilon_T = \pi/2$ and $\rho = 3$, as in the previous section, it is found from equation (g-7-3),

$$\Phi_N/P_V = 4.44 \times 10^{-6} \left[\frac{\pi}{2} - \frac{2.5}{\sqrt{1 + (\frac{4.71 \times 10^4}{\omega_t})^4}} \right]^2 \qquad \text{(g-7-4)}$$

Using equation (g-7-4), the threshold signal-to-noise ratio in 50 kc can be computed for various sine wave test tones which might be representative of the voice signal. Using 800, 1000 and 3000-cps tones yields the following results:

ω_t	P_V/Φ_N (db)	P_V/N
2π (800)	49.8	2.8
2π (1000)	49.2	2.2
2π (3400)	52.8	4.8

An input signal-to-noise ratio of 4.7 db was specified[1]. As can be seen from the above, this value will be satisfactory.

It should be noted that, when no biomedical subcarriers are present on the 1.25-mc subcarrier, the voice signal is originating from the Apollo Command Module. In this case, it is processed by peak clipping of 12 db and then passing it through a 2.5-kc filter with a 12 db-per-octave rolloff. A test tone of any frequency between 1 kc and 3.4 kc would therefore provide a satisfactory representation of the voice signal.

g-7.5   ANALYSIS OF 1.25-MC SUBCARRIER DEMODULATOR FOR VOICE AND SEVEN BIOMEDICAL SUBCARRIERS.

In this section, the optimum bandwidth for the 1.25-mc subcarrier demodulator will be determined for the case where the modulating signal consists of the voice

---

[1]   GSFC-TDS-RFS-226, Op. cit.

signal and the seven biomedical subcarrier channels. The modulation indices for the biomedical subcarriers which will result in simultaneous threshold of the 1.25-mc subcarrier demodulator and the biomedical subcarrier demodulators will also be determined. Finally, the 1.25-mc subcarrier demodulator input signal-to-noise in 50-kc bandwidth at threshold will be computed for this mode.

Biomedical subcarriers combined with unsuppressed speech (no clipping or narrowband filtering), are transmitted only from an extra-vehicular astronaut, via the VHF-AM communications link. In the command module, this signal is modulated onto the 1.25-mc subcarrier for transmission to earth via the S-Band link. For this reason, the voice will be assumed to be unprocessed when it is combined with the biomedical subcarriers.

The total peak phase error in the 1.25-mc demodulator loop is the sum of the errors due to modulation and noise and may be written as [5]:

$$\epsilon_T = \frac{\beta_V}{\sqrt{1 + \left(\dfrac{\omega_n}{\omega_V}\right)^4}} + \sum_{m=1}^{7} \frac{\beta_m}{\sqrt{1 + \left(\dfrac{\omega_n}{\omega_m}\right)^4}}$$

$$+ 0.729 \, \rho_N \, (\Phi_N/P_V)^{1/2} \, \omega_n^{1/2} \qquad\qquad \text{(g-7-5)}$$

where:

β_m = modulation index of mth biomedical subcarrier on the 1.25-mc subcarrier.

ω_m = frequency (radians/sec) of mth biomedical subcarrier and the other quantities are as described in section g-7.4.

The output S/N of a discriminator (assuming the input S/N to be above threshold) may be expressed, in terms of an equivalent AM input S/N, as [3]:

$$(S/N)_o = 3 \beta^2 \, (P/2 \, \Phi_N \, f_m) \qquad\qquad \text{(g-7-6)}$$

[3] Stover, Op. cit.

[5] Martin, Op. cit.

where:

f_m = modulating frequency and $(S/N)_o$ -- measurement bandwidth

β = FM modulation index ($\Delta f/f_m$)

P_S = Input signal power

Φ_N = Input noise spectral density

Equation (g-7-6) may be rewritten as:

$$\beta = \left[\frac{2f_m}{3} (S/N)_o \right]^{1/2} \left[\Phi_N/P_S \right]^{1/2} \qquad (g-7-7)$$

From section g-7-1, f_m = 3.4 kc. It has been shown[9] that the peak-to-average ratio for unprocessed speech is approximately 14.7 db. If an output rms-signal to rms-noise ratio of 15 db is required for the voice signal, the peak-output-signal to rms noise ratio will be 29.7 db. The peak-to-average ratio for a sine wave is 3 db. Consequently, an equivalent (same peak-signal to rms-noise ratio) sine wave modulation will have an rms-signal-power to rms-noise-power ratio of 26.7 db (4.68×10^2 numerical). Hence, equation (g-7-7) may be written as:

$$\beta_v = \left[2 \frac{(3.4 \times 10^3)(4.68 \times 10^2)}{3} \right]^{1/2} \left[\Phi_N/P_S \right]^{1/2} \qquad (g-7-8)$$

$$\beta_v = 1.03 \times 10^3 (\Phi_N/P_S)^{1/2} \qquad (g-7-9)$$

Expression (g-7-9) will be used in optimizing equation (g-7-5). Having found the optimum bandwidth, then $\beta_v = 2.5$ will be used to compute the threshold value of P_V/Φ_N.

Also from reference (3), the output signal-to-noise ratio of a discriminator for a bandpass subcarrier modulating the carrier can be written in terms of the input P_V/Φ_N ratio as:

$$(S/N)_o = \frac{\beta^2}{2B} \left[P_S/\Phi_N \right] \qquad (g-7-10)$$

---

[9] Craiglow, Op. cit.

[3] Stover, Op. cit.

where B is the detection bandwidth for the subcarrier at the output of the demodulator. It must be much less than the frequency separation between the subcarrier and the carrier. Equation (g-7-10) may be rewritten as:

$$\beta = \left[2B \ (S/N)_o^{1/2} \right] \left[\Phi_N/P \right]^{1/2} \tag{g-7-11}$$

The optimum loop noise bandwidths and the corresponding threshold signal-to-noise ratios for the seven biomedical subcarriers were derived in section g-7.5 and are listed in columns 4 and 5 of table g-7-1. These may be used in equation (g-7-11) to express the deviation ratios for each of the subcarriers in terms of Φ_N/P_V at the input to the 1.25-mc subcarrier demodulator. The resulting seven expressions may be used in optimization of equation (g-7-5). Having found the minimum threshold value of Φ_N/P_V, equation (g-7-11) may be used to find the β_m which will ensure simultaneous threshold of the biomedical subcarriers and the 1.25-mc subcarrier demodulator. Carrying out the above substitutions and setting $\epsilon_T = \frac{\pi}{2}$ and $\rho_N = 3$ reduces equation g-7-5) to:

$$
\frac{\pi}{2} = \left\{ \frac{1.03 \times 10^3}{\sqrt{1 + \left(\dfrac{\omega_n}{6.28 \times 10^3} \right)^4}} + \frac{36.7}{\sqrt{1 + \left(\dfrac{\omega_n}{2.51 \times 10^4} \right)^4}} \right.
$$

$$
+ \frac{39.6}{\sqrt{1 + \left(\dfrac{\omega_n}{3.39 \times 10^4} \right)^4}} + \frac{41.85}{\sqrt{1 + \left(\dfrac{\omega_n}{4.27 \times 10^4} \right)^4}}
$$

$$
+ \frac{43.4}{\sqrt{1 + \left(\dfrac{\omega_n}{5.15 \times 10^4} \right)^4}} + \frac{43.0}{\sqrt{1 + \left(\dfrac{\omega_n}{6.03 \times 10^4} \right)^4}}
$$

$$
+ \frac{42.35}{\sqrt{1 + \left(\dfrac{\omega_n}{6.81 \times 10^4} \right)^4}} + \frac{76.4}{\sqrt{1 + \left(\dfrac{\omega_n}{7.67 \times 10^4} \right)^4}}
$$

$$
\left. + \ 2.187 \sqrt{\omega_n} \right\} \left[\Phi_N/P_V \right]^{1/2} \tag{g-7-12}
$$

Equation (g-7-12) expresses (P_V/Φ_N) as a function of ω_n. This relationship is plotted in figure g-7-2. As can be seen from the figure, the minimum threshold level occurs at $\omega_n = 2.5 \times 10^4$ radians/sec. However, there is only about 0.3 db difference between that value of P_V/Φ_N and the value at $\omega_n = 4.7 \times 10^4$ ($B_N = 50$ kc). Consequently, the 50-kc loop noise bandwidth, as specified in GSFC-TDS-RFS-226, will be satisfactory.

As can be seen from figure g-7-2, the threshold value of (P_V/Φ_N) for $\omega_n = 4.7 \times 10^4$ is approximately 53.4 db. Using this value in equation (g-7-11), along with the loop noise bandwidths and signal-to-noise ratios as described in table g-7-1, will allow the evaluation of β_m for simultaneous threshold of the biomedical subcarriers with the 1.25-mc subcarrier demodulator. This procedure was used to obtain the values given in the last column of table g-7-1.

The value of β_V given by using $P_V/\Phi_N = 53.4$ db in equation (g-7-11) is 2.18. If, however, $\beta = 2.5$[1] is used with the biomedical indices found above, the threshold is found to be at $P_V/\Phi_N = 53.46$ db.

The threshold signal-to-noise level for the 1.25-mc subcarrier demodulator then becomes 53.46 db 10 log $(50 \times 10^3) = 6.46$ db. Hence, when the biomedical subcarriers are present, the required signal-to-noise ratio becomes about 6.5 db, compared to the value of 4.7 db required for voice only.

g-7.6 CALCULATION OF TEST CONDITIONS FOR THE VOICE SUBCARRIER DEMODULATOR.

g-7.6.1 PURPOSE AND PROCEDURE.

Simulation parameters will be calculated for tests to verify that the input and output signal-to-noise conditions of the voice subcarrier demodulator are within acceptable limits. The derivations will be in three steps:

(1) An equivalent sine wave tone will be calculated which will give the same threshold level as the voice-plus-biomedical-subcarrier modulation of the 1.25-mc subcarrier would yield.

---

[1] GSFC-TDS-RFS-226, Op. cit.
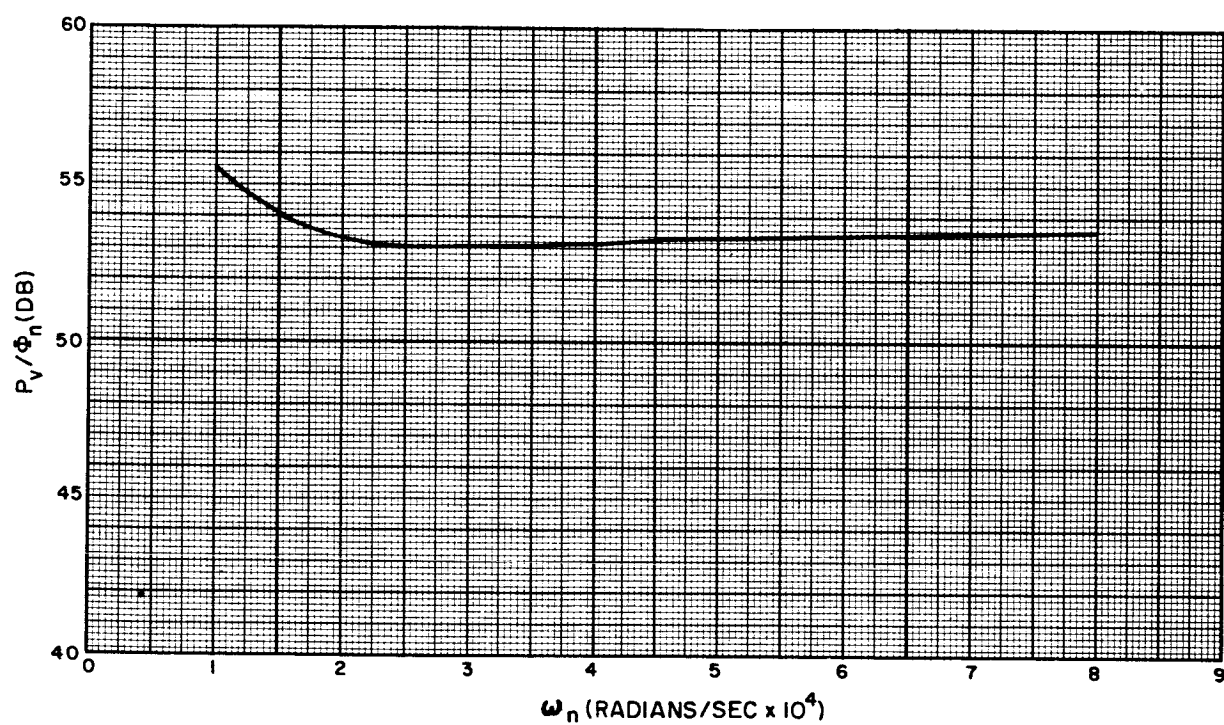
Figure g-7-2.   Voice Subcarrier Demodulator Loop Optimization and Variation in
Loop Threshold Level Versus ω_n (Voice Plus Seven Biomedical Subcarriers)

(2) Using this "full-load" test tone, the relationship between the input and output signal-to-noise ratios of the voice subcarrier demodulator will be determined.

(3) The required output signal-to-noise ratio will be determined for an input to the voice subcarrier demodulator from the fm carrier demodulator, with the carrier demodulator at threshold and with the full-load test tone modulating the subcarrier.

g-7.6.2 CALCULATION OF TEST TONE FOR VOICE SUBCARRIER DEMODULATOR.

As indicated in section g-7-5, the threshold level for the voice subcarrier demodulator with voice and the seven biomedical subcarriers modulating the subcarrier is about 6.5 db. The total peak phase error for the voice subcarrier demodulator for sine wave modulation and white gaussian noise may be written as[5]:

$$
\epsilon_T = \frac{\beta_V}{\sqrt{1 + \left(\dfrac{\omega_n}{\omega_t}\right)^4}} + 0.729\, \rho_N \left(\frac{N}{P_V}\right)^{1/2} \left(\frac{1}{1.06}\right)^{1/2}, \qquad \text{(g-7-13)}
$$

where all quantities are as previously defined. For $\epsilon_T = \pi/2$, $\beta_V = 2.5$, $\rho_N = 3$ and $P_V/N = 4.38$ (6.5 db), equation (g-7-13) becomes:

$$
\frac{1}{\sqrt{1 + \left(\dfrac{\omega_n}{\omega_t}\right)^4}} = 0.228 \qquad \text{(g-7-14)}
$$

From figure g-4-4, $K_2 = \dfrac{\omega_n}{\omega_t} = 2.06$.

$$
f_t = \frac{\omega_t}{2\pi} = \frac{50 \times 10^3}{(1.06)\,(2.06)\,(2\pi)} = 3.66 \text{ kc} \qquad \text{(g-7-15)}
$$

Thus, a sine wave tone of 3.66 kc, with a modulation index of 2.5, will produce the same threshold level as would a composite signal consisting of the seven biomedical subcarriers and the 3.4-kc, voice-simulating tone.

---

[5] Martin, Op. cit.

g-7.6.3   CALCULATION OF OUTPUT SIGNAL-TO-NOISE RATIO FOR VOICE SUB-
          CARRIER DEMODULATOR.

The output signal-to-noise ratio for an fm discriminator operating above threshold,
with sine wave modulation and white gaussian noise, can be written as[17]:

$$(S/N)_o = \frac{3}{2\pi}(\Delta f)^2 \frac{1}{a^3} \left[P_V / \Phi_N \right] \quad , \qquad \text{(g-7-16)}$$

where a is the post-filter noise bandwidth at the demodulator output and Δf is the
peak frequency deviation of the signal.

From section g-7.5, the threshold signal-to-noise level for the voice subcarrier
demodulator is 6.5 db in 50 kc. Therefore,

$$P_V / \Phi_N = 6.5 + 47 = 53.5 \text{ db}$$

For a modulation index of 2.5 and f_m = 3.66 kc as calculated in section g-7.6.2,

$$\Delta f = (2.5)(3.66) \text{ kc} = 9.15 \text{ kc}.$$

Then equation (g-7-14) can be written as:

$$(S/N)_o(\text{db}) = 129.4 - 30 \log a \qquad \text{(g-7-17)}$$

This expression is plotted in figure g-7-3. From the figure, the output signal-
to-noise ratio from the voice subcarrier demodulator, in a bandwidth a, can be read
for the values of β_1, f_m, and input signal-to-noise noted on the graph.

g-7.6.4   SIGNAL-TO-NOISE RATIO OUT OF THE VOICE SUBCARRIER DEMODU-
          LATOR WHEN THE MAIN CARRIER FM DEMODULATOR IS AT THRESHOLD.

The relationship between the output signal-to-noise ratio in a baseband, one-
sided noise bandwidth (a) and the input signal-to-noise ratio for the voice subcarrier
demodulator was given in equation (g-7-16). The actual output noise from the carrier
FM demodulator will be triangular but may be reasonably approximated as a flat
spectrum over the narrow (relative to the total carrier demodulator output) voice

_____

[17]   Schuartz, Mischa, "Information Transmission, Modulation and Noise,"
       McGraw-Hill Book Co., Inc., 1959.
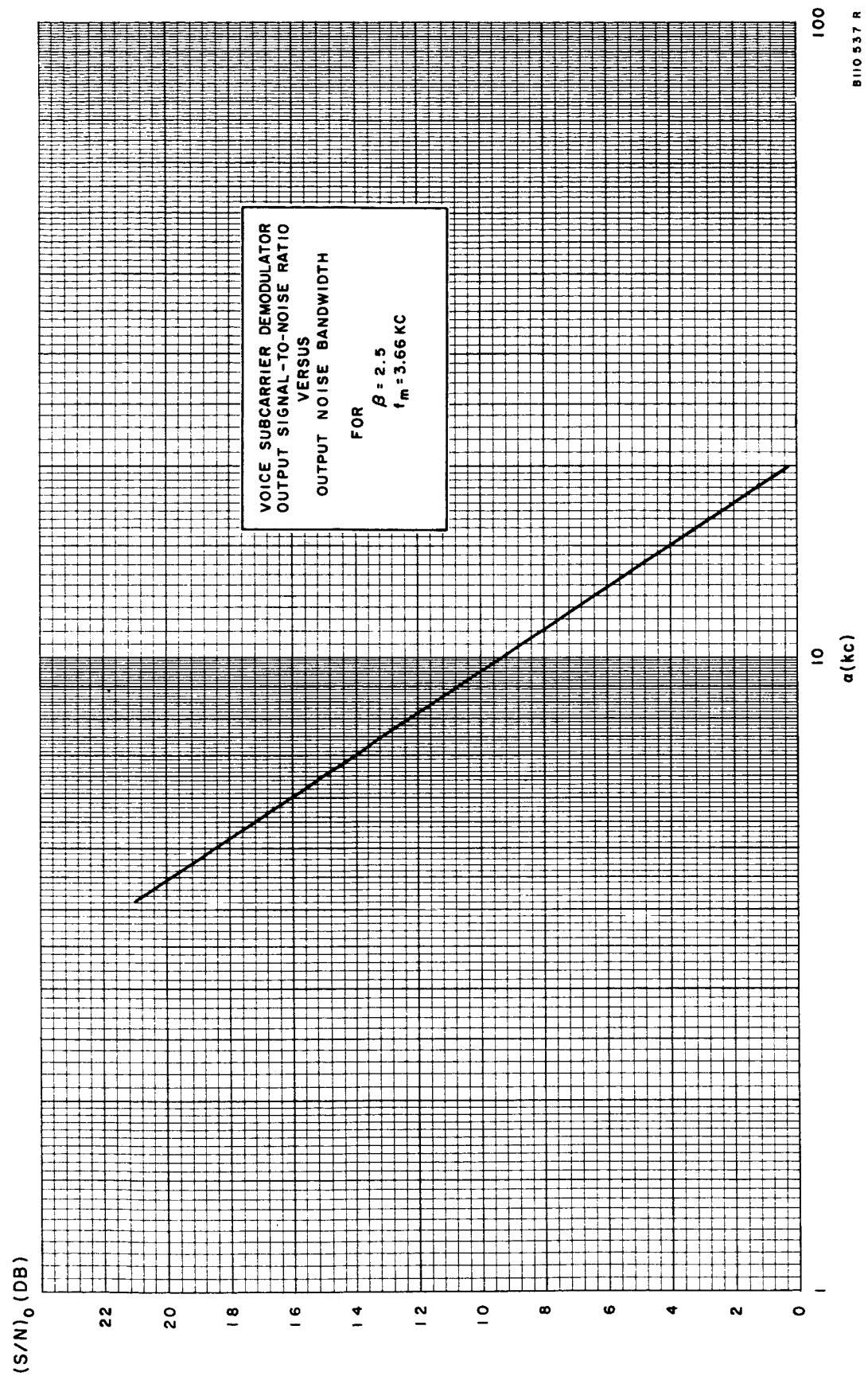
Figure g-7-3.   Voice Subcarrier Demodulator Output Signal-to-Noise Ratio
Versus Output Noise Bandwidth

demodulator input bandwidth. Using the above relationship and the test tone of the previous section:

$$S/N_o \text{ (db)} = 76.03 - 30 \log a + P/\Phi_N \text{ (db)} \qquad \text{(g-7-18)}$$

It was found in section g-2.3 that, for mode E modulation, the input signal-to-noise ratio of the voice subcarrier demodulator will be 15.8 db in 50 kc at the threshold of the FM carrier loop and, therefore:

$$P/\Phi_N \text{ (db)} = 15.8 + 10 \log 50 \times 10^3 = 62.8 \qquad \text{(g-7-19)}$$

An output frequency response for the voice demodulator of -1 db at 20 kc has been assumed and the noise bandwidth for this test will be assumed to also be -20 kc (an additional output filter may be required for the test). Since $30 \log (2 \times 10^4) = 129$ (db), equation (g-7-18) becomes:

$$(S/N)_o \text{ (db)} = 76.03 = 129 + 62.8 = 9.83 \text{ db} \qquad \text{(g-7-20)}$$

Therefore, for mode E modulation, with the fm carrier demodulator operating at the specified threshold and with a 3.66-kc test tone modulating the voice subcarrier, the output signal-to-noise ratio from the voice subcarrier demodulator would theoretically be 9.83 db, measured in a 20-kc noise bandwidth. To allow for actual equipment operation, a value of 7.0 db was specified[2].

---

(2) Collins Radio 126-0429-001, Op. cit.

phase lock loop fundamentals

g-8.1 INTRODUCTION.

There are many techniques that are employed for the detection of narrow-band signals in the presence of wideband noise. Perhaps one of the more versatile techniques, one which is often used in space communication and artificial satellite tracking, is the phase-lock loop technique. Basically, the phase-lock loop technique is an active filtering technique and the loop optimization is based upon optimum filter theory as developed by N. Weiner [18]. One of the earliest comprehensive reports on phase-lock loop principles was authored by R. Jaffe and E. Rechtin in March 1955 [12]. In this report, Jaffe and Rechtin were concerned mostly with the phase-lock loop which is designed for optimum operation with a frequency step signal input (i.e., a second-order loop)*. The second-order loop is the most widely used type and, therefore, most of the design considerations of this report will be for a second-order loop.

Jaffe and Rechtin state that to implement a phase-loop, which would be optimum (in accordance with optimum filter theory) over a wide range of loop input signal and

---

* Other types of phase-lock loops are first-order loops (optimum operation with a phase step input) and third-order loops (optimum operation with a frequency ramp input). Third-order loops are generally used where rapid signal acquisition is required for high doppler tracking situations.

[18] Wiener, N., "Extrapolation, Interpolation and Smoothing of Stationary Time Series," The Technology Press and John Wiley Sons, Inc. 1949

[12] Jaffe and Rechtin, Op. cit.

noise levels, would require the use of auxiliary servos to adjust the loop parameters. However, they have developed and experimentally verified the idea that a fixed-component phase loop, preceded by a bandpass limiter, offers nearly optimum performance over a wide range of input signal and noise levels. This latter form of the phase loop is implemented more easily than the variable parameter form and is the most widely used technique of phase lock loop design.

Jaffe and Rechtin developed a linear model of the phase-lock loop, which yields predictable results in system design. A simple phase-lock loop and its linear model are shown in figure g-8-1. This linear model is used as the basis for most of the loop analysis in this report.

g-8.2   PHASE LOOP TRANSFER FUNCTION

The general form of the optimum transfer function for a phase loop having minimum mean-square noise error (σ_N^2) under the constraint that the transient error power equivalent (E_T^2) within the loop cannot exceed a specified amount, may be determined by minimizing the total mean-square error (Σ^2). This statement is written in mathematical notation as:

$$\Sigma^2 = \sigma_N^2 + \lambda^2 E_T^2 = \text{minimum,} \qquad \text{(g-8-1)}$$

where λ is a Langrangian multiplier [19] to be determined from phase loop noise bandwidth considerations and where:

$$\sigma_N^2 = \frac{1}{2\pi j} \int_{-j\infty}^{j\infty} \left| H(s) \right|^2 \Phi_N(s)\, ds \qquad \text{(g-8-2)}$$

$$E_T^2 = \frac{1}{2\pi j} \int_{-j\infty}^{j\infty} \left| \theta_1(s) \right|^2 \left| 1-H(s) \right|^2 ds \qquad \text{(9-8-3)}$$

$\Phi_N(s)$ is the input phase noise spectral density which is assumed to be constant over the loop input bandwidth. $\Phi_N(s)$ is, therefore, equal to $\Phi_N(0)$.

---

[19]   Courent, R. and Hilbert D. "Methods of Mathematical Physics." Vol. 1 Interscience Publishers, New York - London, 1953.

A SIN(ωt + Θ_1) → **PHASE DETECTOR** → **LOOP FILTER**

B COS (ωt+Θ_2)

VOLTAGE CONTROLLED OSCILLATOR

A. SIMPLE PHASE-LOCK LOOP

Θ_1(S) → [—] → K_M → F(S)

Θ_2(S)

$\dfrac{K_V}{S}$
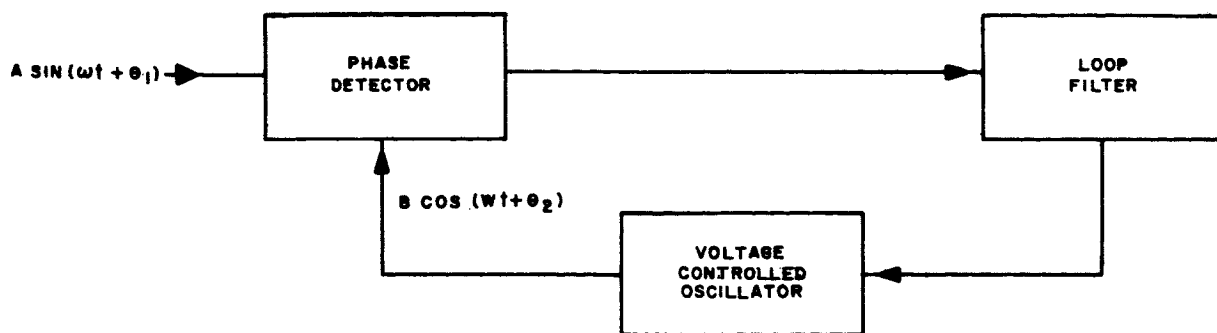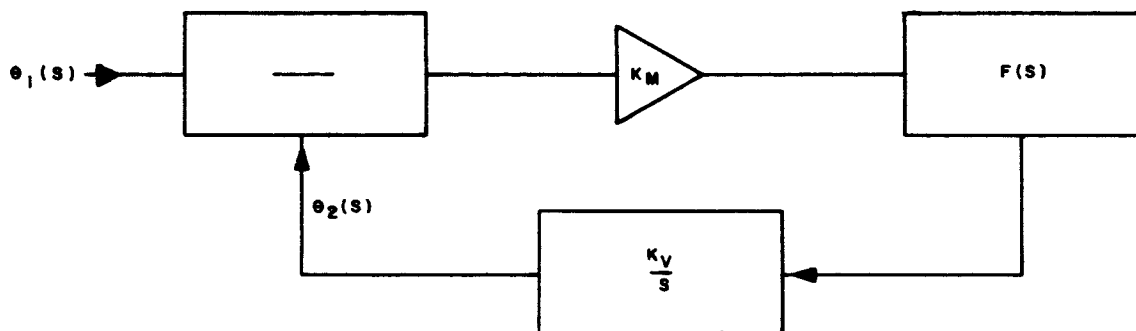
B. LINEAR MODEL

BIIO 568 R

Where:

K_M = Phase Detector Constant, volts per degree.

K_V/s = Voltage controlled oscillator (vco) transfer function, where K_V has dimensions of degrees per second per volt.

$F(s)$ = Loop filter transfer function.

$H(s)$ = Phase loop transfer function.

$$H(s) = \frac{K_M K_V F(s)}{s + K_M K_V F(s)} = \frac{G\, F(s)}{s + G\, F(s)}$$

Figure g-8-1.   A Simple Phase-Lock Loop and Linear Model

After (g-8-1) is minimized, [12] the general form of the optimum phase loop transfer functions is:

$$H(s) = \frac{\lambda^2}{\psi(s)} \left[\frac{|\Theta_1(s)|^2}{\psi(-s)} \right]_+ \qquad\qquad (g\text{-}8\text{-}4)$$

where:

$$|\psi(s)|^2 = \psi(s)\,\psi(-s) = \Phi_N(0) + \lambda^2 |\Theta_1(s)|^2 , \qquad (g\text{-}8\text{-}5)$$

with $\psi(s)$ being the factor of $|\psi(s)|^2$ having poles only in the left-half s-plane, and $\psi(-s)$ being the factor having poles only in the right-half s-plane. The "+" subscript following the bracketed terms of (g-8-4) indicates that only those poles of the bracketed terms which are in the left-half s-plane are to be retained. The bracketed terms must be expanded into their partial fraction form before selection of the left-half s-plane poles.

The optimum physically realizable second-order loop transfer function, optimized for a frequency step input, has also been developed [2]. Only the results are given here. For a frequency step input:

$$\Theta_1(s) = \frac{K}{s^2} , \qquad\qquad (g\text{-}8\text{-}6)$$

where K is a constant with dimensions of degrees per second, the optimum second-order loop transfer function is:

$$H(s) = \frac{\sqrt{2}B_2 s + B_2^2}{s^2 + \sqrt{2}B_2 s + B_2^2} , \qquad\qquad (g\text{-}8\text{-}7)$$

where:

$$B_2^4 = (\lambda^2 K^2)/\Phi_N(0) , \qquad\qquad (g\text{-}8\text{-}8)$$

with λ and $\Phi_N(0)$ as previously defined.

---

(12)   Jaffe and Rechtin, Op. cit.

(2)   Collins Radio Company, Op. cit.

g-8.3   LOOP NOISE BANDWIDTH

The loop noise bandwidth of the loop is defined as follows:

$$2B_L = \frac{1}{2\pi j} \int_{-j\infty}^{j\infty} \left| H(s) \right|^2 ds \qquad \text{(g-8-9)}$$

Using this definition, the total noise power (σ_N^2) in the loop is equal conveniently to $2B_L \Phi_N(0)$. The second-order threshold loop noise bandwidth can be determined from (g-8-9) by using the method outlined in page 371 of reference (20). The result is:

$$2B_{L_O} = \frac{3B_2}{2\sqrt{2}} \quad \text{cycles per second} \qquad \text{(g-8-10)}$$

g-8.4   OPTIMUM LOOP FILTER TRANSFER FUNCTION

From Figure g-8-1, it is seen that the phase-lock loop will have a transfer function of the form:

$$H(s) = \frac{\Theta_2(s)}{\Theta_1(s)} = \frac{GF(s)}{s + GF(s)} , \qquad \text{(g-8-11)}$$

where G is the open-loop gain equal to $K_M K_V$. Solving for F(s) from (g-8-11):

$$F(s) = \frac{s}{\left[G \frac{1}{H(s)} - 1 \right]} \qquad \text{(g-8-12)}$$

Substituting (g-8-7) into (g-8-12), the optimum second-order loop filter transfer function is given as:

$$F(s) = \frac{\sqrt{2} B_2 S + B_2^2}{Gs} \qquad \text{(g-8-13)}$$

(20)   Newton, G.G. Jr., Gould, L.A., and Kaiser, J.F., "Analytical Design of Linear Feedback Controls", John Wiley and Sons, Inc., 1957.

g-8.5 SECOND-ORDER LOOP FILTER APPROXIMATION

In practice, an RC filter approximation is usually used in place of the active filter required in equation (g-8-13). It has been shown [12] that the optimum filter can be approximated by the circuit shown in figure g-8-2.
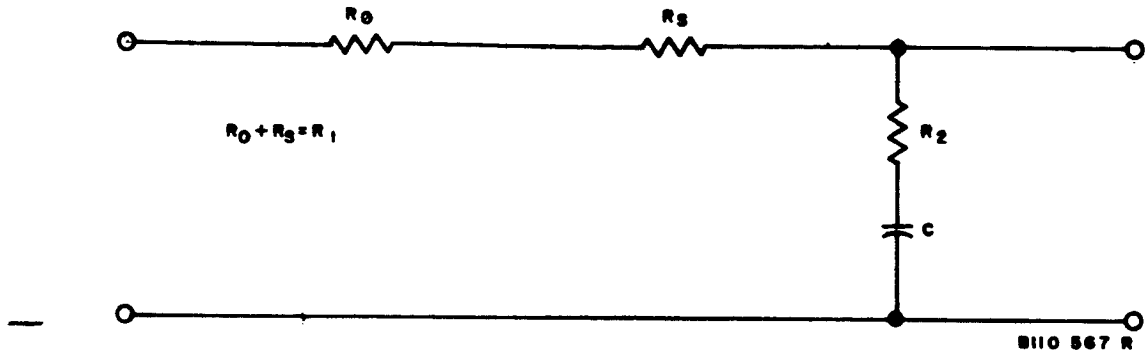
Figure g-8-2. Approximation to Optimum Loop Filter

R_o is the output impedance of the driving source. It has been shown [12] that the values of the time constants should be:

$$T_1 = R_1 C = G_o / B_2^2 \tag{g-8-14}$$

$$T_2 = R_2 C = \sqrt{2/B_2} \tag{g-8-15}$$

Substituting for B_2^2 from equation (g-8-10)

$$T_1 = \frac{9}{32} \left(\frac{G_o}{B_{L_o}^2} \right) \tag{g-8-16}$$

$$T_2 = \frac{3}{4B_{L_o}} \tag{g-8-17}$$

Equations (g-8-16) and (g-8-17) give the filter time constants in terms of the threshold loop noise bandwidth and the open loop gain. The above relationships are

---

[12] Jaffe and Rechtin, Op. cit.

REQUIRED LOOP TIME CONSTANT, T_1
FOR SECOND ORDER PHASE - LOCK LOOP

$2B_{L_o} = 200$ CPS

$2B_{L_o} = 60$ CPS

$$T_1 = \frac{9\,G_o}{8\,(2B_{L_o})^2}$$

$$G_o = 360\ K_M\,K_V\,\alpha_o$$

$$T_1 = R_1\,C$$

T_1, SECONDS

G_o, GAIN - OPEN LOOP
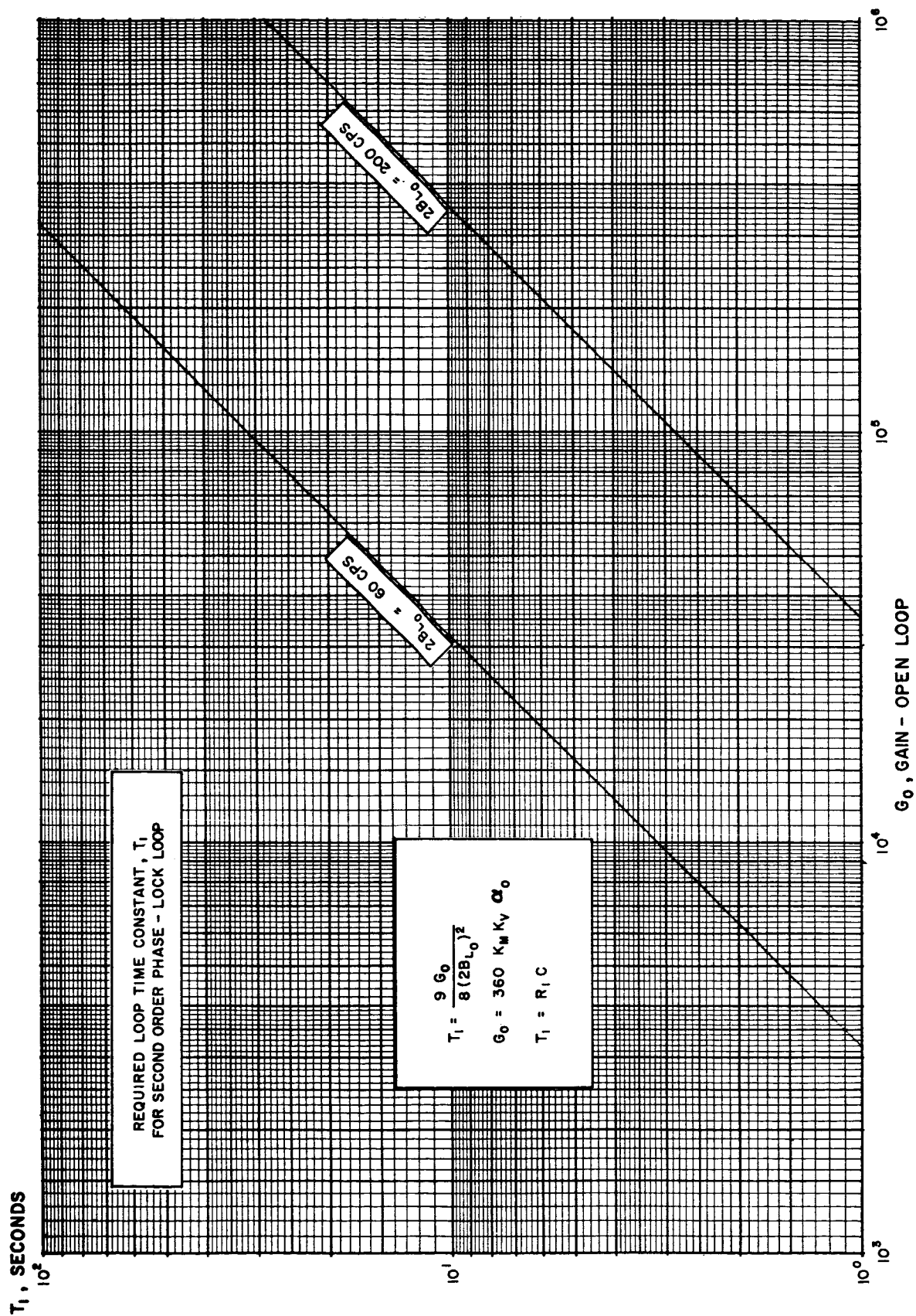
Figure g-8-3. Required Loop Time Constant (T_1) for Second-Order Phase-Lock Loop
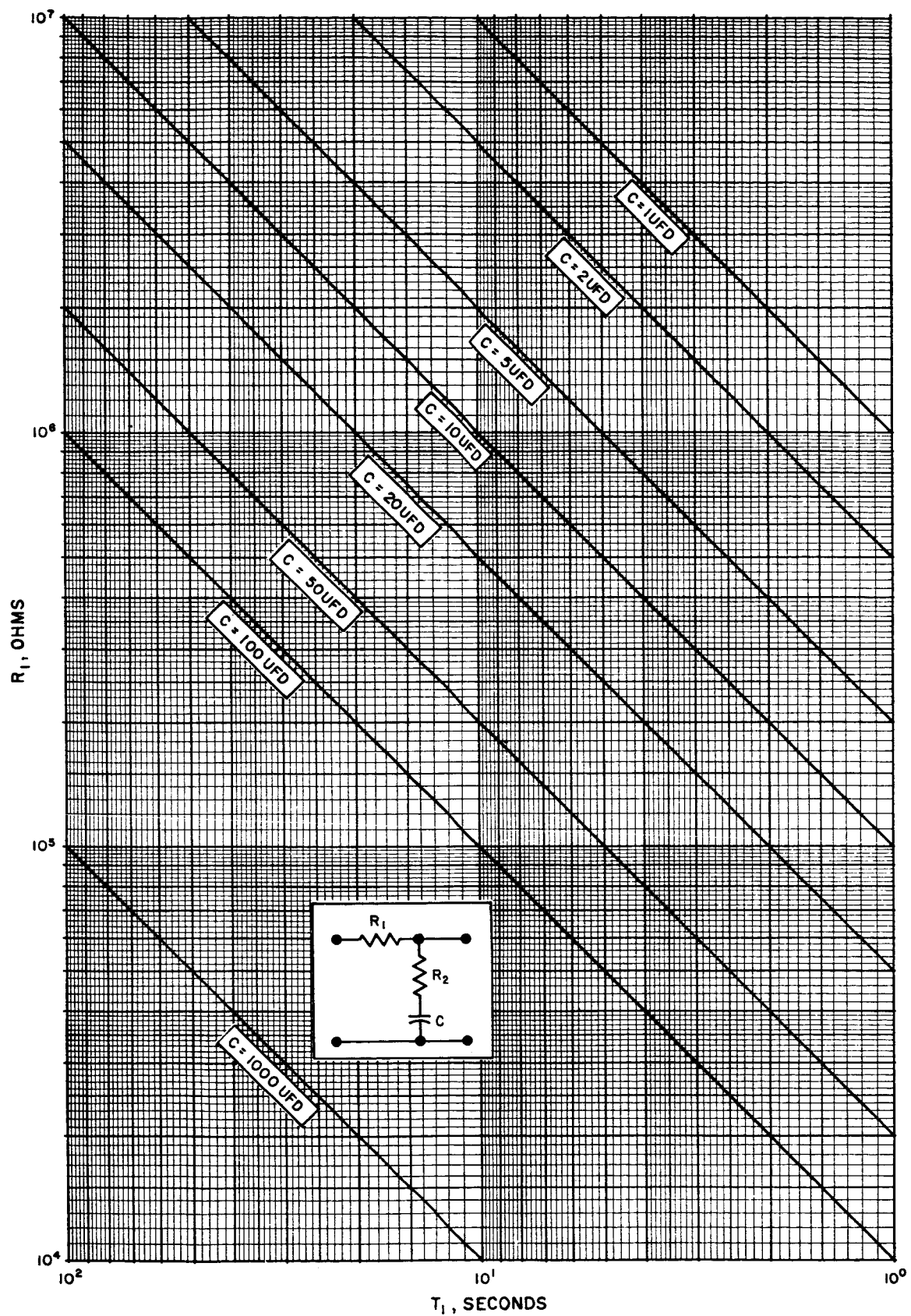
Figure g-8-4. Tracking Filter Series Resistance (R_1) Versus Loop Time Constant (T_1)
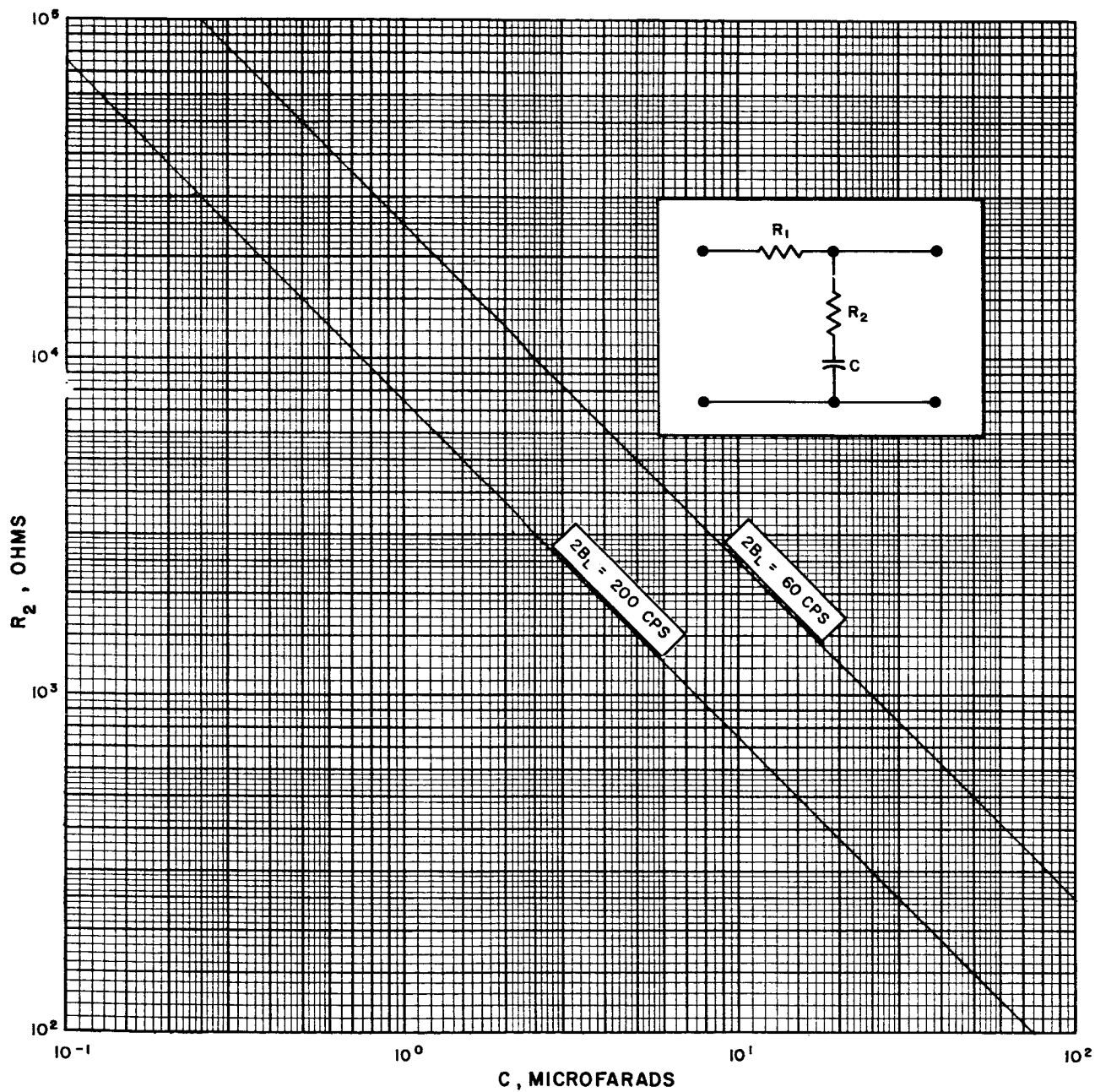
Figure g-8-5. Tracking Filter Shunt Resistance (R_2) Versus Tracking
Filter Shunt Capacitance (C)
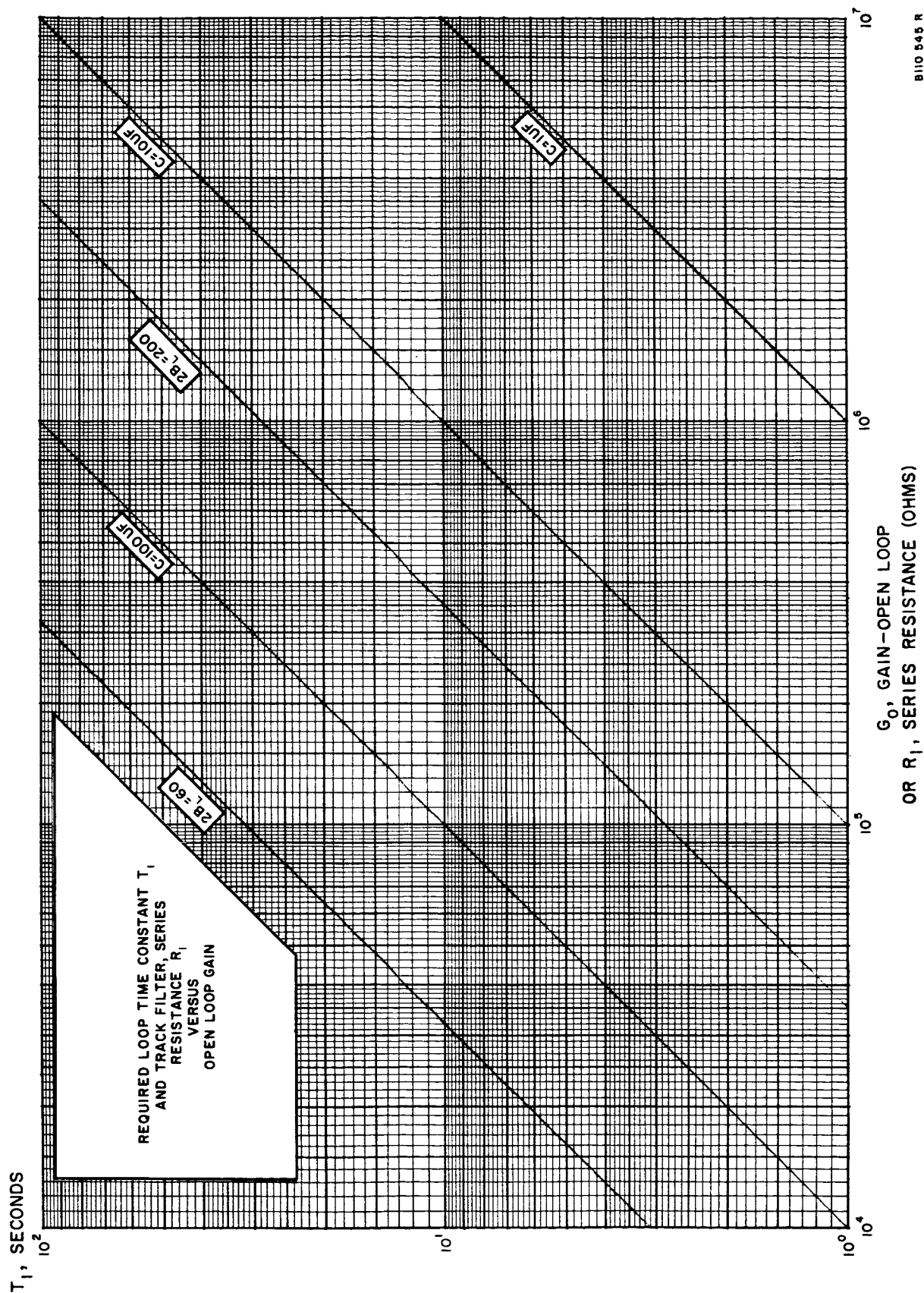
Figure g-8-6. Required Loop Time Constant (T_1) and Tracking Filter Series

Resistance (R_1) Versus Open Loop Gain

plotted in figures g-8-3 through g-8-6. The transfer function for the above filter can be written as:

$$F(s) = \frac{T_2 s + 1}{(T_1 + T_2)s + 1} \qquad (g\text{-}8\text{-}18)$$

Substituting equation (g-8-18) into equation (g-8-9),

$$H(s) = \frac{G(T_2 s + 1)}{s^2(T_1 + T_2) + s(1 + GT_2) + G} \qquad (g\text{-}8\text{-}19)$$

where T_1 and T_2 are derived for operation at threshold and G is the open-loop gain at the particular operating point.

g-8.6   EFFECT OF SIGNAL-TO-NOISE CHANGES ON FILTER DESIGN

If the value of $2B_{L_o}$ is specified, then B_2 can be determined from equation (g-8-10) and substituted into equation (g-8-13). Notice from equation (g-8-8) that, if the values of K and $\Phi_N(0)$ are also specified, the Lagrangian multiplier λ to minimize the total mean-square error is also determined. If, after the loop is designed accordingly, the value of $\Phi_N(0)$ changes, the loop transfer function (g-8-7) is no longer optimum for minimizing the total mean-square error for the step frequency input given in (g-8-6). It can be shown [16] that the input phase noise spectral density is:

$$\Phi_N(0) = \left(\frac{P_N}{P_S}\right)\frac{1}{4 B_C} \quad \frac{(\text{radians})^2}{\text{cps}} \quad , \qquad (g\text{-}8\text{-}20)$$

where P_N/P_S is the noise-to-signal power ratio at the phase detector input and $2 B_C$ is the if. noise bandwidth. Thus, it can be seen that providing an optimum loop over a range of signal-to-noise ratios will require some means of changing the loop as the signal-to-noise ratio changes.

---

[16]   Chadima, Op. cit.

One possible solution is to use an agc based upon the signal only. Such an agc voltage may be obtained if the signal is multiplied in a phase detector by a 90°, phase-shifted version of the vco output. The inputs to the multiplier (phase detector) will then be in phase and the dc multiplier output will be proportional to the signal level. This technique works reasonably well and has been used successfully for several phase-locked tracking receivers under the GSFC four-stations contract. It has been shown [12], however, that the use of a narrow-band limiter preceding the phase detector provides loop performance which is closer to the theoretical, optimum loop.

g-8.7 THE EFFECT OF LIMITER ACTION

The effect that the bandpass limiter preceding the phase detector has on the loop is to change the open-loop gain (G) in conjunction with the limiter input noise-to-signal power ratio, when the noise-to-signal power ratio at the limiter input is large. This change in the open-loop gain is due entirely to the limiter-caused signal suppression, which follows the approximate relationship [12, 18]:

$$\alpha \approx \sqrt{\frac{1}{1 + \frac{4}{\pi}\frac{P_N}{P_S}}} , \qquad \text{(g-8-21)}$$

where α is the signal suppression factor and P_N/P_S is the noise-to-signal power ratio at the limiter input. Equation (g-8-21) is based upon the fact that the output signal-to-noise ratio of a bandpass limiter is approximately the same as the input ratio, varying between the following limits:

$$S/N_{out} \text{ (limiter)} = \frac{\pi}{4} S/N_{in}, \text{ as } S/N_{in} \rightarrow 0 \qquad \text{(g-8-22)}$$

$$S/N_{out} \text{ (limiter)} = 2 S/N_{in}, \text{ as } S/N_{in} \rightarrow \infty \qquad \text{(g-8-23)}$$

---

[12] Jaffe and Rechtin, Op. cit.

[18] Wiener, Op. Cit.

In one case the signal suppresses the noise and in the other case the noise suppresses the signal. Theoretical work at Collins Radio Company [16] has resulted in a more exact expression for α for intermediate values of P_N/P_S. A plot of equation (g-8-21) and the more exact function, as evaluated by a computer program, is shown in figure g-8-7.

The open-loop gain, for $\alpha = 1$, is equal to $K_M K_V$, a constant. The effect of $\alpha \leq 1$ is to vary the open-loop gain and, therefore the proper definition of open-loop gain with a bandpass limiter is,

$$G = \alpha \, K_M K_V. \tag{g-8-24}$$

Following standard design procedure, the loop filter transfer functions are determined using the lowest operable open loop gain (G_O). For practical purposes, this occurs at the point where the loop loses synchronism, which has been determined experimentally [12] to be approximately where the rms phase noise at the output of the voltage-controlled oscillator (vco) is equal to one radian. The input signal level for which G_O is determined is usually called the threshold signal level. Some designers prefer to define the threshold condition as being at some signal level where the rms phase noise at the output of the vco is less than one radian such as 0.35 radians rms.

The optimum loop filter transfer function for the second-order loop, F(s), can be modified to:

$$F_2(s) = \frac{\sqrt{2} \, B_2 \, s + B_2^2}{G_O \, s} \tag{g-8-25}$$

For a loop with a variable open-loop gain, the second-order loop transfer function can be expressed as:

$$H(s) = \frac{\dfrac{G}{G_O} \, (2 \, B_2 S + B_2^2)}{s^2 + \dfrac{G}{G_O} \, (\sqrt{2} \, B_2 \, s + B_2^2)} \tag{g-8-26}$$

---

(16)   Chadima, George E., Jr. Op. Cit.

(12)   Jaffe, R. and Rechtin, R. Op. Cit.
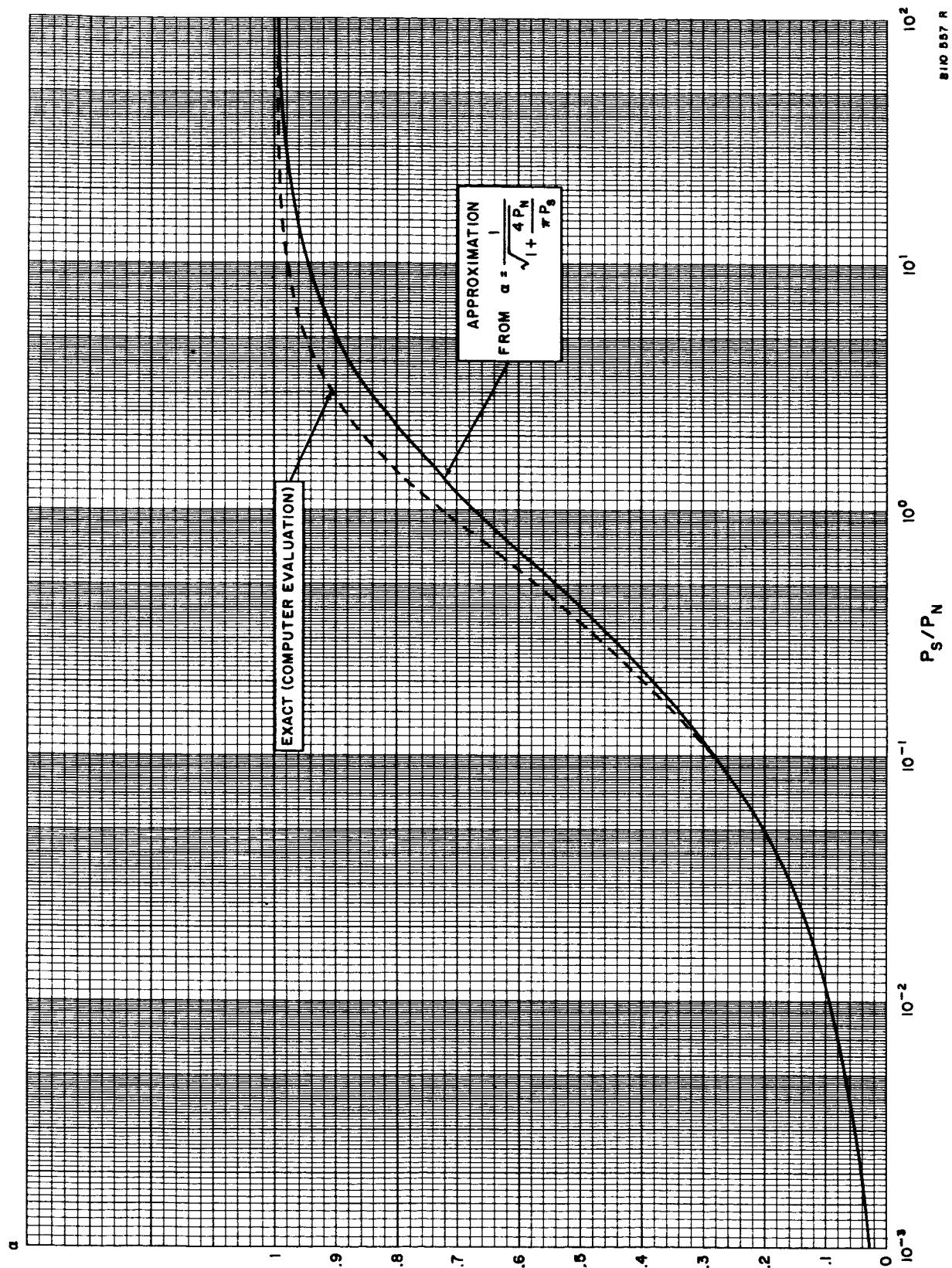
Figure g-8-7.   Signal Suppression Factor as a Function of Limiter Input
Signal-to-Noise Ratio

Notice that, as G approaches G_0, the form of the transfer function approaches that of equation (g-8-7).

For clarity it should be stated that, since the gain (G) is directly proportional to the signal suppression factor (α), the ratio G/G_0 is equal to the ratio α/α_0. The relationship between threshold loop noise bandwidth and the loop noise bandwidth at an input signal level other than threshold may be determined by substituting (g-8-26) into (g-8-9), integrating, and then substituting B_2 from equation (g-8-10) into the result.

For the second-order loop[12],

$$\frac{2B_L}{2B_{L_O}} = \frac{1}{3}\left[2\,(\frac{\alpha}{\alpha_o}) + 1\right] \,, \tag{g-8-27}$$

where $2B_L$ is the loop noise bandwidth at other than the threshold condition. The relationship in equation (g-8-27) is plotted in figure g-8-8.

g-8.8 LOOP PHASE NOISE POWER.

Assuming a noiseless loop input signal, a noiseless vco output signal, and a flat input phase noise spectral density, the noise power appearing at the vco input due to front-end noise is:

$$\sigma_N^2 = \left[\Phi_N\,(0)\right]\frac{1}{2\pi j}\int_{-j\infty}^{j\infty}|H\,(s)\,|^2\,ds = 2\,B_L\Phi_N\,(0) \,, \tag{g-8-28}$$

where $2B_L$ is the loop noise bandwidth. Using the approximation in equation (g-8-20) for $\Phi_N(0)$, the phase noise power or, using the more common designation, "phase jitter" in the loop is then:

$$\sigma_N^2 \approx \frac{2B_L}{4B_C}\frac{P_N}{P_S}\,(\text{radians})^2 = \frac{B_L}{2B_C} \tag{g-8-29}$$

where $\rho = P_S/P_N$. Or if $\frac{B_L}{B_C} = 1$, $\sigma_N^2 = \frac{1}{2\rho}$, $\tag{g-8-30}$

(12) Jaffe, R. and Rechtin, R., Op. Cit.
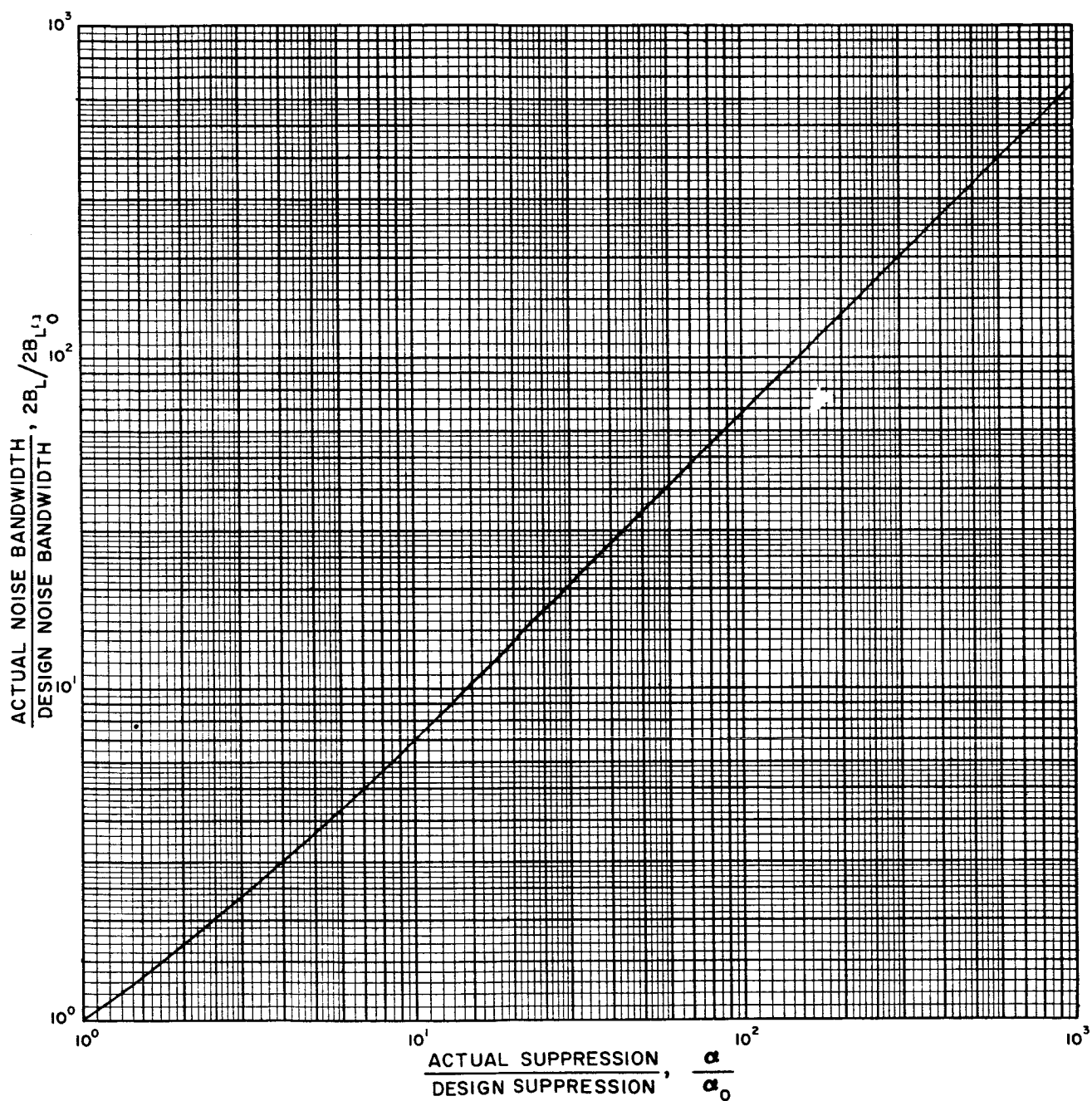
Figure g-8-8. Loop Noise Bandwidth Ratio versus Limiter Signal
Suppression Ratio

where ρ is the signal-to-noise ratio in the loop bandwidth. Thus, the rms phase jitter is approximately:

$$\sigma_N = 40.5 \sqrt{\frac{P_N B_L}{P_S B_C}} \quad \text{degrees rms.} \tag{g-8-31}$$

Theoretical investigation [16] has shown that equation (g-8-31) is a good approximation for $\rho > 10$. The approximation of equation (g-8-30) is 13 percent too low when $\rho = 1$. The theoretical plot by Chadima for σ_N^2 is given in Figure (g-8-9) for $B_L/B_C = 1$. Frazier and Paige [23] have shown experimentally that the phase-lock loop jitter lies between the form given by Chadima in figure g-8-9 and that described by equation (g-8-30). Also shown in figure g-8-9 for comparison is the expression $\sigma_N^2 \approx \frac{1}{\rho}$, which is an approximation which is often used erroneously by design engineers.

g-8.9 PHASE LOOP THRESHOLD SIGNAL LEVEL.

The threshold signal level of a phase loop is usually defined in one of two ways: (1) that loop input signal level at which the phase loop loses synchronism or (2) that loop input signal level at which the phase loop noise jitter becomes 0.35 radians rms.

The loss of synchronism occurs when the rms phase jitter at the vco output is approximately equal to one radian. For convenience, many design engineers assume that the rms phase jitter is exactly one radian at an input signal-to-noise ratio of unity. However, from figure (g-8-9) it can be seen that this occurs when the input signal-to-noise ratio is 0.7. Therefore, the threshold signal level for unity rms phase jitter is given as:

$$P_{S_{th}}\bigg|_{\sigma_N = 1} = 0.7 \; K T_S \, (2 \, B_{L_O}). \tag{g-8-32}$$

where k is Boltzmann's constant = 1.38×10^{-23} joules/degree Kelvin and T_S is the system noise temperature in degrees Kelvin.

---

(16) Chadima, George E., Jr., Op. Cit.

(23) Frazier, J.P. and Page, J., "Phase-Lock Loop Frequency Acquisition Study," IRE Transactions on Space Electronics and Telemetry, SET-8, pp. 210-226, September 1962.

From figure g-8-9, it can also be seen that the rms phase jitter reaches 0.35 radians at a signal-to-noise ratio of 4.6. Therefore, the threshold signal level for the 0.35 rms phase jitter is given as:

$$P_{Sth} \Big|_{\sigma_N = 0.35} = 4.6 K T_s (2B_{L_O}) \qquad (g\text{-}8\text{-}33)$$

The difference in signal level between the two definitions is 8.2 db.

g-8.10   LOOP TRANSIENT PHASE ERROR.

Although the phase loop is optimized with the constraint that the transient error power-equivalent may not exceed a prescribed amount, the concept of bounded transient error power-equivalent is lost in actual design practices. Therefore, it is of more value to observe the phase error $(\Delta\theta)$ within the loop. The loop phase error is an indication of how well the loop is following a prescribed signal, and it is not difficult, by using equation (g-8-3), to obtain the transient error power-equivalent. Rewriting (g-8-3) in the form:

$$E_T^2 = \int_0^\infty \left[\Delta\theta(t)\right]^2 dt \qquad (g\text{-}8\text{-}34)$$

shows the relationship between loop phase error and transient error power-equivalent.

The loop phase error, $\Delta\theta(s)$, due to an input function, $\theta(s)$, is of the form:

$$\Delta\theta(s) = \theta_1(s) - \theta_2(s) = \theta_1(s)\left[1-H(s)\right] \qquad (g\text{-}8\text{-}35)$$

The phase error, as a function of time, is determined by taking the inverse Laplace transform of (g-8-35).

The (transient) input functions of interest in this report are the frequency step:

$$\theta_1(s) = \frac{360\Delta f}{s^2} \qquad (g\text{-}8\text{-}36)$$

and the frequency ramp:

$$\theta_1(s) = \frac{360\Delta f}{s^3}, \qquad (g\text{-}8\text{-}37)$$

where Δf is in cps per second.
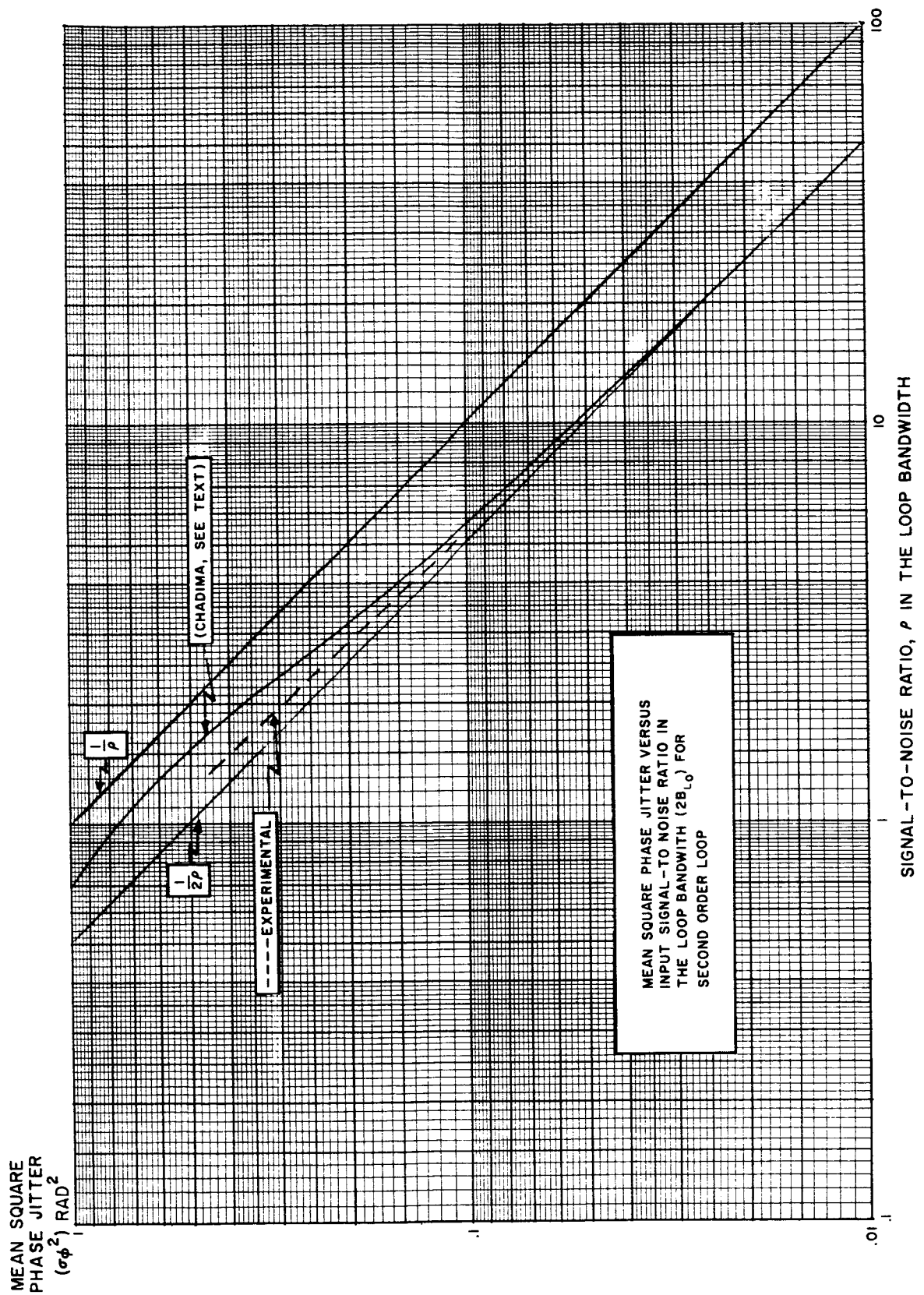
Figure g-8-9. Mean Square Phase Jetter versus Input Signal-to-Noise Ratio in the Loop Bandwidth $(2B_{L_0})$ for Second Order Loop

For the optimum second-order loop, the phase error for the frequency step input is:

$$\Delta\theta(t) = \frac{510(\Delta f)}{B_2} e^{-\frac{B_2 t}{\sqrt{2}}} \sin \frac{B_2 t}{\sqrt{2}} \text{ degrees}$$ (g-8-38)

and for the frequency ramp input:

$$\Delta\theta(t) = \frac{360}{B_2^2} (\Delta f)_{1-2} e^{-\frac{B_2 t}{\sqrt{2}}} \cos \frac{B_2 t}{\sqrt{2}} - 0.785 \text{ degrees}$$ (g-8-39)

Notice that, for the frequency ramp input, the loop phase error of the second-order loop has a steady-state value of:

$$\Delta\theta(t)_{ss} = \frac{360(\dot{\Delta} f)}{B_2^2}$$ (g-8-40)

In paragraph g-8.5 an approximation to the optimum loop filter was given. It is of interest to determine what the phase error for the frequency step and frequency ramp, using the approximate filter, should be. Substituting (g-8-18) and (g-8-36) into (g-8-35) gives:

$$\theta(s) = \frac{360}{s^2} f \left[\frac{s^2 + \left(\frac{1}{T_1 + T_2}\right)s}{s^2 + \left(\frac{1 + GT_2}{T_1 + T_2}\right)s + \frac{G}{T_1 + T_2}} \right]$$ (g-8-41)

Applying the final value theorem to (g-8-41), it can be shown that the steady-state phase error for a frequency step is:

$$\Delta\theta(t)_{ss} = \frac{360\Delta f}{G} \text{ degrees}$$ (g-8-42)

Values for equation (g-8-42) are plotted in figure g-8-10.

g-8.11   PHASE-LOCK LOOP FREQUENCY ACQUISITION.

Usually the loop oscillator differs initially in frequency (or at least in phase) from the input signal, and the loop will be "out of lock."   The presence of the input signal will be indicated by a beat note out of the phase detector which is equal to the frequency difference. If the loop bandwidth is sufficiently wide and the loop gain sufficiently large, the loop will eventually come into synchronism and will be "in lock." In many
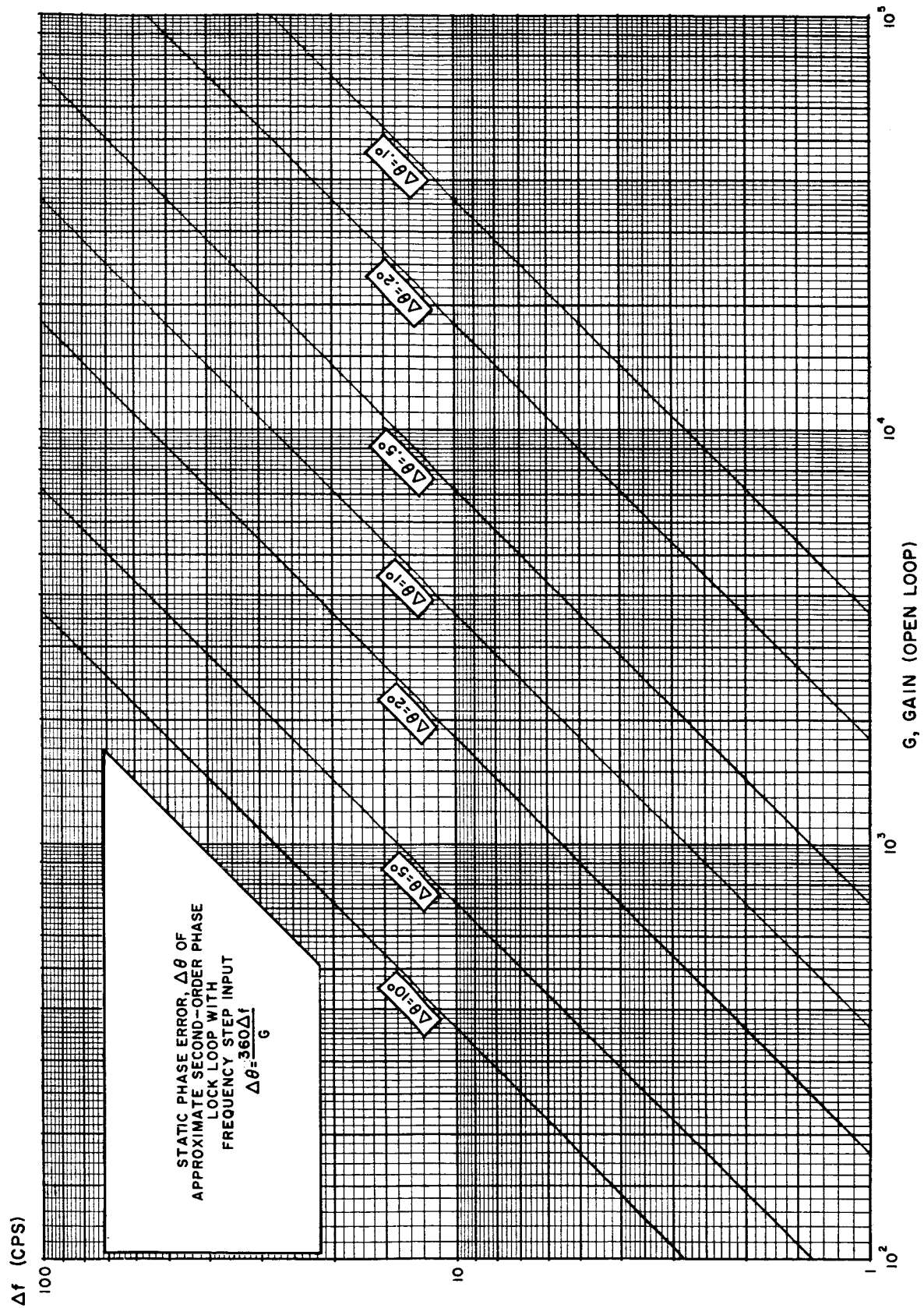
Figure g-8-10. Static Phase Error (Δθ) of Approximate Second-Order Phase Lock Loop With Frequency Step Input

cases it is necessary to provide an external means of manually or automatically changing the loop oscillator frequency so as to acquire the input signal.

Theoretical analysis of the frequency acquisition characteristics of phase lock loops is difficult because of the non-linear nature of the loops in an unlocked condition. Viterbi [22] has made one of the more comprehensive theoretical attempts to analyze the acquisition characteristics of phase lock loops. The initial assumption is that, prior to application of the signal, the loop oscillator is at some stationary point and that the oscillator is free to move, upon application of the signal, except for the constraints of the loop itself.

Viterbi shows that, for a second-order loop with a perfect integrator and with a damping factor of ζ , the pull-in time for a large initial frequency error of Ω is given by the approximate expression:

$$ t \simeq \frac{(\Omega)^2}{2 \zeta \omega_n^3} \quad \text{sec} \tag{g-8-43} $$

For a small initial frequency error, with $\zeta = 0.707$, the pull-in time is approximately:

$$ t \simeq \frac{27(\Omega)^2}{256 \, B_L^3} \quad \text{sec} \tag{g-8-44} $$

or:

$$ t \simeq 4.16 \frac{(\Delta f)^2}{(B_L)^3} \text{sec} \tag{g-8-45} $$

Viterbi also gives the pull-in range for a second-order loop with an RC tracking filter and with a damping factor of ζ as:

$$ |\Delta f| = \frac{\omega_n}{\pi} \sqrt{\frac{\zeta \omega_n}{RC} + 1} \text{ cps} \tag{g-8-46} $$

---

[22] Viterbi, A.J., "Acquisition and Tracking Behavior of Phase-Locked Loops," JPL External Publication No. 673, 14 July 1959.

For $\zeta = .707$ the pull-in range is given as:

$$\left| \Delta f \right| = \frac{4}{3} \frac{\sqrt{2}}{\pi} B_L \sqrt{\frac{4 B_L}{3 RC} + 1} \quad cps \qquad (g\text{-}8\text{-}47)$$

For the case where the initial frequency error is greater than the pull-in range, the loop oscillator must be swept to achieve acquisition. It is felt that the theoretical results which have been performed to date are not completely adequate and that the best information which is available on the acquisition characteristics of phase lock loops in which the loop oscillator is being swept comes from experimental investigations.

In particular, one of the more comprehensive experimental investigations into the subject matter has been conducted by Frazier and Paige [23] of General Electric Company. These investigations consisted of a series of experiments on a low-frequency, electronic scale model, using GEESE* model principles. Curves and empirical formulation were compiled from the experimental data which can be used in predicting acquisition characteristics of phase lock loops in general. The only questionable aspect of the Frazier and Paige experiments is that the sweeping voltage was not removed from the loop oscillator when synchronization occurred as would be the case with an automatic acquisition scheme.

From the experimental results, the following formulation was developed, which predicts the maximum sweep rate for 90 percent probability of acquisition, as a function of the input signal-to-noise ratio:

$$R_{90} \ (cps/sec) = \frac{\left[\frac{\pi}{2} - \frac{1.1}{S/N_i} \right] \left[0.9 \frac{\alpha}{\alpha_0} \right] \omega_{n_0}^2}{2 \pi (1 + \delta)} \qquad (g\text{-}8\text{-}48)$$

where S/N_i = input signal-to-noise ratio into the closed-loop noise bandwidth.

ω_{n_0} = natural frequency of loop at threshold, i.e., when the limiter suppression factor for $\alpha = \alpha_0$.

δ is the over-shoot factor, which depends upon the damping factor and which can be obtained from the curve in figure g-8-11.

_____

(23)   Frazier, J.P. and Paige, J., "Phase-Lock Loop Frequency Acquisition Study," JRE Transactions on Space Electronics and Telemetry, SET-8, pp. 210-226, September 1962.

*   General Electric Electronic System Evaluator.

The optimum range of damping factors is from 0.5 to 0.85, with the best results occurring for a damping factor of 0.5 when the loop oscillator is being swept. When the loop oscillator is not being swept, the best acquisition results occur for a damping factor of 0.707. In general, the best phase lock loop performance for other than acquisition occurs for a damping ratio of 0.707, which is the damping ratio assumed in all other discussions in this report concerning the second order phase-lock loop.
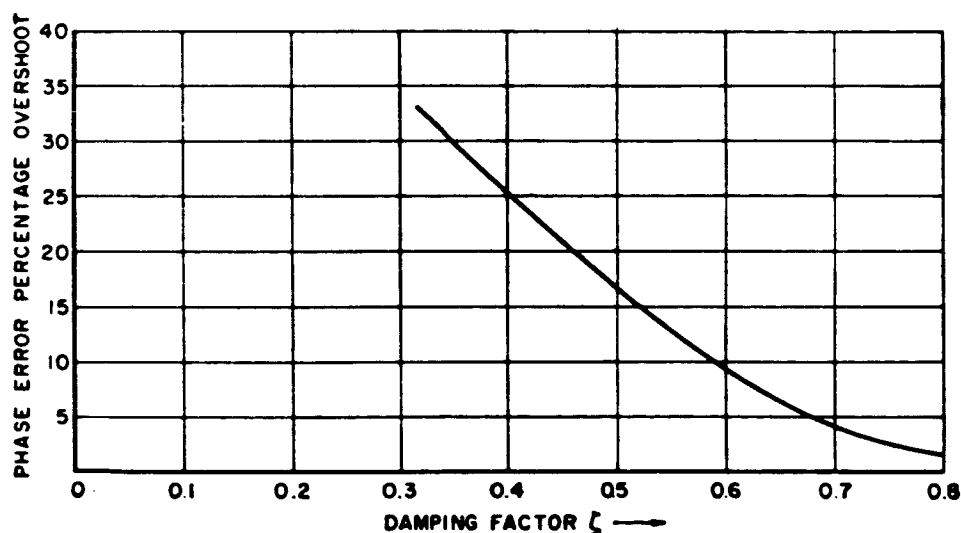
Figure g-8-11.   Phase Error Percentage Overshoot as a Function of Damping
Factor for a Linearly Changing Input Frequency

section g-9

---

fm emergency voice demodulation

g-9.1 GENERAL.

The original requirement[1] was for the emergency voice demodulator to operate on a signal from the 50-mc if. amplifier in the fm carrier loop and to demodulate emergency voice signals that were to be frequency modulated directly onto the carrier. After this study was started, the specification for emergency voice was changed to agree with the Block II vehicular equipment. Emergency voice signals will now be demodulated directly from the PM carrier. As discussed in section g-3, the demodulation process may be accomplished in the carrier loop of the PM demodulator. It is felt that it will be worthwhile to include a summary of the problems associated with the fm emergency voice mode, however, since the Block I equipment will transmit emergency voice on the fm carrier, as originally specified (see section g-10).

g-9.2 FM EMERGENCY VOICE DEMODULATOR.

The fm emergency voice demodulator was to contain a conventional fm discriminator and a phase-lock loop (fm feedback) type of discriminator. Both discriminators were to simultaneously receive their inputs from the if. amplifier in the fm carrier loop. The output of the conventional discriminator would be connected to the emergency voice monitors, except when the phase-lock loop demodulator was in lock. At such times, the in-lock signal from the coherent detector would switch the inputs of the emergency voice monitors to the output of the loop. The loop noise bandwidth was specified as 33 kc, with a maximum modulation rate of 3 kc.

---

[1]GSFC-TDS-RFS-226, Op. Cit.

The designs of the loop and the conventional discriminator present no problems in themselves. The fm feedback loop will provide a threshold improvement of 5 to 7 db over the conventional fm discriminator. The two primary purposes for including the conventional discriminator were:

(1) For backup

(2) To permit reception of signals while the loop was in the process of acquiring the signal.

g-9.3 FM EMERGENCY VOICE PROBLEMS.

Acquisition of the signal would be one of the major problem areas, particularly since the range and range rate tracking receivers will not remove the doppler from the fm signals. As indicated in paragraph g-1.4.1.1, the frequency uncertainty of the received carrier could be as high as ±150 kc. This, combined with the possible frequency uncertainty of the tracking receiver oscillator, requires a conservative design having an acquisition range of ±300 kc.

Another major problem would be to provide control of the gain of the 50-mc if. amplifier that precedes the emergency voice demodulator. The gain of the amplifier is normally controlled by coherent agc, which is derived from the fm carrier loop. If the emergency voice signal had a fairly strong signal-to-noise ratio (refer to section g-4 for fm loop thresholds), the main fm carrier loop would rapidly acquire the signal because of its wider bandwidth and, thus, would provide coherent agc to the 50-mc if. amplifier. However, once the emergency voice phase-lock loop has acquired the signal, it would be desirable to have the agc transferred to the emergency voice demodulator, because of its significantly lower bandwidth and, consequently, lower threshold (as much as 10 to 18 db).

Having the main fm carrier demodulator loop acquire lock prior to the emergency voice loop is only an advantage if the conventional fm discriminator has been designed to operate with the if. signal levels normally provided by the main fm carrier loop agc. Otherwise, a third agc system to operate when only the conventional fm discriminator output is being utilized, would have to be provided. It should be noted that the thresholds of the conventional fm discriminator and the main fm carrier loop are about the same, because the fm feedback threshold improvement offsets the effect of a narrower bandwidth on the conventional discriminator.

Normally, a conventional fm discriminator uses a noncoherent agc, but there may be some improvement in performance by using coherent agc from the main fm carrier loop. Prior to the change from fm to PM for emergency voice, it was tentatively decided to provide a noncoherent agc mode for the conventional fm discriminator, to be selected by the operator instead of the coherent agc from the carrier loop. In any case, once the emergency voice loop acquired the signal, the gain would be automatically controlled by its associated coherent detector. Thus, the fm emergency voice demodulator, when combined with the main fm carrier loop, would have included three agc systems for a common amplifier.

It will be noted that automatic switching to noncoherent agc upon reception of the emergency voice signal by the conventional discriminator would not have been provided. In addition to the fact that coherent agc may be better, there would be considerable difficulty in distinguishing the emergency voice signal from the tv and other baseband signals. During normal fm reception of tv, for example, the emergency voice conventional discriminator would have provided an output (meaningless, perhaps, but a definite output) and the emergency voice loop would have been continually trying to lock to the tv signal appearing at its output. A simple time delay may have been sufficient to prevent the emergency voice loop from capturing control of the 50-mc if. amplifier in the presence of such signals, but a simple diode-type of agc detector would not have allowed the conventional discriminator to distinguish between voice and tv signals. If the demodulator had been required to automatically switch to noncoherent agc upon initial reception of emergency voice signals, it would have been necessary to provide a logic network, based upon presence or absence of the subcarriers or perhaps the tv sync subcarrier. This appeared to be a rather formidable problem. Perhaps if more time had been spent on the fm emergency voice demodulator, a simple solution would have been found.

It is significant to note that, at the initial meeting with the equipment manufacturer (STL), they considered "automatic determination of the received mode" to be one of the most significant problems of the demodulator design.

g-9-3

CM-LEM tracking station interference

g-10.1 GENERAL.

Comparison between the Apollo S-band parameters described by the data demodulator specification (GSFC-TDS-RFS-226) and existing and possible future specifications to which Collins Radio Company will furnish command module and lunar excursion module communication equipment indicates that some discrepancies exist between them. The possible problem areas are of three types:

(1) Incompatibilities between the RFS-226 specification and present spacecraft equipment specification, for both the command module and the lunar excursion module.

(2) Indicated future alterations of the spacecraft equipment, which would influence the design and operation of the Unified S-Band tracking station equipment. The Cedar Rapids Division of Collins has been advised of several possible future changes in equipment requirements for the Apollo command module that would require corresponding changes in the ground tracking station equipment. While these changes have not to date been contractually incorporated into the equipment specifications, they will be noted here because of their potential influence on the ground system.

(3) Changes in the specified interference between the data demodulator and other station equipment, primarily the R&RR receivers.

These remarks are not the result of an extensive compatibility study, but are discussions of the more obvious areas of conflict that have become evident during the data demodulator analysis.

g-10.2   INCOMPATIBILITIES BETWEEN EXISTING SPECIFICATIONS.

g-10.2.1   FM MODULATION INDICES.

For fm modes A through C, RFS-226 lists the peak carrier phase deviation by the telemetry and voice subcarriers as 1.25 and 0.91 radians, respectively (see table g-1.1 of this analysis).

Present equipment specifications for the command module call for a peak phase deviation of 1 radian for 1-volt peak input voltage to the carrier phase modulator of the S-band transponder. The carrier phase modulator receives its input from the PM mixing network of the premodulation processor, the output of which is specified as 1.1 volts peak for the telemetry subcarrier and 0.84 volt peak for the voice subcarrier. Modulation with this signal will result in 1.1 radians peak carrier phase deviation (instead of 1.25 radians) for the telemetry channel and 0.84 radian (instead of 0.93 radian) for the voice.

On the other hand, present specifications for the lunar excursion module (LEM) call for a 1.1 peak voltage out of the LEM premodulation processor for the telemetry subcarrier and 0.5 volt peak for the voice subcarrier. Assuming the same transponder phase modulation characteristic as for the CM (1 radian/volt), this signal will produce 1.1 peak radians and 0.5 peak radian carrier phase deviation by the telemetry and voice subcarriers, respectively.

These numbers are different from those listed in RFS-226 (the 0.5 radian is also different from the command module specification) and the differences will, of course, affect circuit margin calculations for the ranging code, the voice subcarrier, and the telemetry subcarrier.

In like manner, the peak carrier phase deviations listed for PRN ranging are higher than the actual values. This is because the wideband modulation phase detector of the S-band transponder has a sine wave response rather than the assumed linear response, so that for large carrier phase deviations the voltage out of the detector is proportional to the sine of the deviation. This voltage is used to modulate the down-link carrier, and for an up-link deviation due to ranging of 1.12 radians, the down-link carrier will not be deviated 1.12 radians as indicated in table g-1-1, but instead will be deviated by $\sin(1.12) = 0.90$ radian.

It should be noted that the entire up-link baseband spectrum is remodulated onto the down-link, including the 30- and 70-kc subcarriers and all their beat frequencies and harmonics. This, of course, changes the relative distribution of power in the down-link spectrum, causing additional variation of the actual circuit margins from those calculated in any analysis based on values taken from table g-1-1.

g-10. 2. 2   LUNAR EXCURSION MODULE (LEM) TRANSMISSIONS.

Transmission equipment specifications for the LEM presently call for an fm lunar stay mode, consisting of the voice signal, the seven biomedical subcarriers, a 14. 5-kc subcarrier (all at baseband), and a 512-kc, low bit-rate (1. 6 kb) telemetry subcarrier. This mode of operation is, of course, incompatible with the specified ground system data demodulation equipment and, if such a composite signal were received, none of the information could be demodulated with the specified data demodulator.

g-10. 2. 3   MUTUAL INTERFERENCE BETWEEN CM AND LEM DOWN-LINKS.

GSFC personnel have indicated* that the probable arrangement of radio frequencies for space-to-ground links for the Apollo program will be:

  (1)   2282. 5 mc — PM transmission from the CM

  (2)   2287. 5 mc — PM or fm transmission from the LEM

  (3)   2297. 5 mc — FM transmission from the CM.

With the specified if. bandwidth of 10 mc for the fm demodulator channel, interference will exist between the 2282. 5-mc and the 2287. 5-mc signals, which are only 5 mc apart, if they are used simultaneously and if the LEM is transmitting fm.

g-10. 2. 4   BIOMEDICAL SUBCARRIERS.

The demodulator specification indicates that the biomedical subcarriers are to be combined with the voice and the resulting signal frequency modulated on the 1. 250-mc subcarrier. The specification to which the Block II spacecraft equipment is presently being built is in agreement with this, but in the Block I equipment, the biomedical subcarriers are modulated directly onto the baseband.

---

*GSFC-Collins Radio Company Meeting on USB Signal Data Demodulators,
    15 July 1964, at GSFC.

g-10.2.5   MODE D-1 (IRIG STORED-DATA SUBCARRIERS).

In the original specification,[1] there was to be a mode D-1, in which nine fm telemetry subcarriers, with center frequencies between 14.5 and 165 kc, were to be multiplexed onto the fm baseband with the other signals. Contractually, the requirement to demodulate these subcarriers has been deleted. These subcarriers will be transmitted from the Block I vehicular equipment presently being built and use of three of them has been considered for the Block II equipment.

g-10.2.6   FM EMERGENCY VOICE.

The data demodulator is being built, as indicated in this report, to demodulate baseband emergency voice signals on the PM carrier. This agrees with the signal transmitted by the Block II vehicular equipment. The Block I equipment, however, will transmit emergency voice signals on the fm carrier, as originally specified.[1]

g-10.3   EXPECTED CHANGES IN SPACECRAFT EQUIPMENT SPECIFICATIONS.

g-10.3.1   SIMULTANEOUS TRANSMISSION OF STORED AND REAL-TIME DATA.

The question of the best method of transmitting recorded data simultaneously with real-time information is a very involved one. At least two methods are presently being considered:

   (1)   Use of a separate fm transmitter in addition to the specified PM transmitter

   (2)   Addition of a third subcarrier to the composite signal modulating the PM carrier.

Either of these approaches would require that the data demodulators for the ground tracking system be different from those presently specified.

Transmission of telemetry and television on an fm carrier 15 mc removed from the PM carrier is being considered.* The PM signal would be as described in this report. Such an approach will place an additional multiplexing requirement on the spacecraft (preliminary investigation indicates it can be handled) and may require modification of the ground station.

---

(1)   GSFC-TDS-RFS-226, Op. cit.

*   No documentation available on this subject.

A preliminary investigation of the third-subcarrier approach has been made at Collins Cedar Rapids.[24] The investigation indicates that a subcarrier at 1.408 mc could be used with the two existing subcarriers. The calculations were based on three unmodulated sine-wave subcarriers (similar to the analysis in paragraph g-2.4) and modulation indices were based on simultaneous threshold with minimum signal level. The analysis did not consider the ranging signal nor the turnaround of the up-link subcarriers and the intermodulation products they would generate when combined with the three down-link subcarriers.

The analysis indicated that little over 2 db would be lost for the telemetry sub-carrier and a little over 7 db would be lost for the voice subcarrier when the third subcarrier is added. There is an intermodulation product only 9.6 db down from the voice subcarrier, which would contain modulation from both telemetry subcarriers and the voice subcarrier and that is removed 68 kc from the voice subcarrier. The system may work but such a conclusion would require more proof than this preliminary analytical investigation.

There is a possibility* that this approach will be used on the Block II equipment.

g-10.3.2   MODULATION INDICES.

It has been indicated[25] that the modulation indices for the Apollo program may be changed so that the various signal components will threshold simultaneously. As indicated in paragraph g-10.2.1, changes of modulation index will change circuit margin calculations and possibly affect the choice of the best bandwidths.

g-10.3.3   MODE D-2.

In connection with the elimination of mode D-1, it has been indicated that mode D-2 (telemetry and voice only, on fm) is to be eliminated. This possibility will not affect the equipment design or operation, however, and is only included here for reference.

---

[24] Collins Radio Company EMS-404, 23 June 1964.

[25] North American Aviation, "Apollo CMS Communications System, Block I and II Change Review," 24 August 1964

* No documentation is available on this subject.

g-10.4   RECEIVER INTERFACE SPECIFICATION CHANGES.

After this study was essentially completed, the following contractual changes were made in the specification of the R&RR receiver output levels:

(1) The 10-mc signal out of the receiver, for use by the demodulator, will be held to a level of -22 dbm ±1 db. This level was originally specified as -70 dbm ±1 db. Assuming that a receiver output could be (statically) 5 db low (-27 dbm), the threshold noise power may be recalculated (as in paragraph g-3.2):

	100 cps	30 cps
Loop Bandwidth (B_{LO}):	100 cps	30 cps
Input Signal Level (Constant):	-27 dbm	-27 dbm
Approximate Signal-to-Noise Ratio for $\sigma_N = 0.35$ Radian rms:	6 db	6 db
Noise Power for $\sigma_N = 0.35$ Radian rms:	-33 db	-33 db
$10 \log_{10} (2B_{LO})$:	23	17.6
Noise Density per Cycle of Bandwidth:	-56 dbm	-50.6 dbm
Allowable Margin:	2 db	2 db
Threshold Noise Density:	-58 dbm/cps	-52.6 dbm/cps
$10 \log_{10} (3 \text{ mc})$:	64.8	64.8
Noise Power at Threshold (in 3 mc):	+6.8 dbm	+12.2 dbm

It is possible that the receiver output will limit at 0 dbm, as the 50-mc output does (see discussion below).

(2) The 50-mc output of the R&RR receiver was originally unspecified, but was calculatable (section g-4.3) as +15 dbm. The maximum output level for this signal is now specified to be limited to 0 dbm. This does not affect any of the threshold conditions of this channel.

g-10.5   MINIMUM BIT RATE FOR PCM.

The original specification [1] indicated a requirement for a minimum PCM bit rate of 100 bps. Because of the design problems involved with low bit rates into the

---

[1]GSFC-TDS-RFS-226, Op. Cit.

telemetry subcarrier demodulator (see section g-6) and since the lowest expected bit rate for the Apollo program is 1,600 bps, a joint (GSFC/Collins/STL*) agreement was made at the STL design revision meeting that the minimum bit rate for equipped design will be 1,000 bps.

* Space Technology Laboratories (STL) will manufacture the signal data demodulator hardware.

bibliography

1. National Aeronautics and Space Administration, Goddard Space Flight Center, Greenbelt, Maryland, "Specification for Signal Data Demodulator System," Specification No. GSFC-TDS-RFS-226, Revision I, December 1963.

2. Collins Radio Company, Dallas Division, Richardson, Texas, "Subsystem Specification, Unified S-Band Signal Data Demodulator", Specification No. 126-0429-001, Revision C, 4 September 1964.

3. Stover, Harris A., "Second Interim Report on the Modulation Techniques Study for the Apollo C and D Subsystem", Report No. AR-151-2, Cedar Rapids, Iowa, Collins Radio Company, October 1962.

4. National Aeronautics and Space Administration, Goddard Space Flight Center, Greenbelt, Maryland, "2300-Mc Parametric Amplifier Performance Specification", Specification No. GSFC-553-PAR-1 (No date).

5. Martin, Benn D., "The Pioneer IV Lunar Probe: A Minimum-Power FM/PM System Design," Technical Report No. 32-215, Jet Propulsion Laboratory, Cal. Tech., Pasadena, California, March 1962.

6. Termin, F.E., "Electronic and Radio Engineering," 4th Edition, McGraw-Hill Book Company, 1955

7. Brockman, M. and Victor, W., "The Application of Linear Servo Theory to the Design of AGC Loops," JPL External Publication No. 586, 22 December 1958.

8. Members of the Technical Staff of BTL, "Transmission System for Communications," Volume II, Section 22.

9. Craiglow, R., "Required S/N Ratio for CW Communications on Project Apollo," Collins Radio Company, Cedar Rapids Internal Memo, 19 December 1962.